

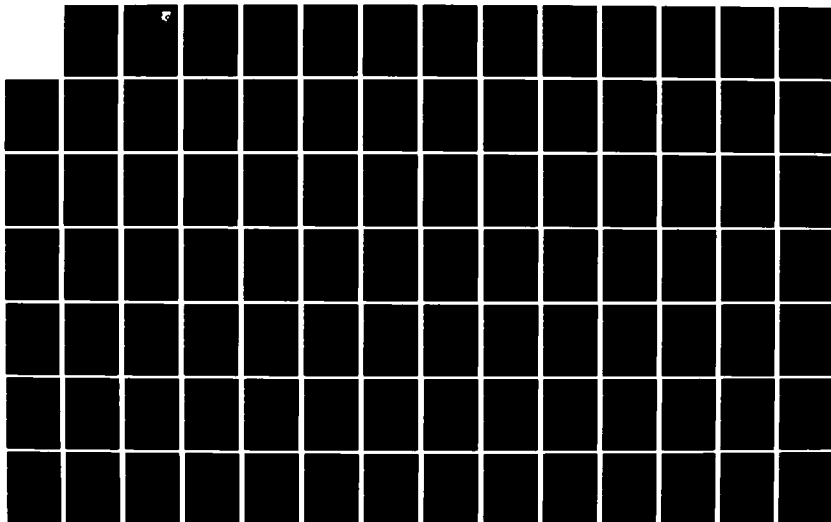
AD-A122 317

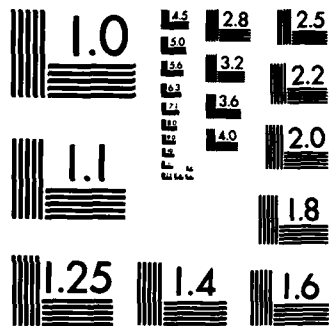
DYNAMIC STABILITY OF STRUCTURES: IMPERFECTION SENSITIVE
SYSTEMS ACTED UPON. (U) GEORGIA INST OF TECH ATLANTA
SCHOOL OF ENGINEERING SCIENCE AN. G J SIMITSES ET AL.
MAY 81 AFWAL-TR-81-3040 F33615-79-C-3221 F/G 20/11

1/2

UNCLASSIFIED

NL





MICROCOPY RESOLUTION TEST CHART
NATIONAL BUREAU OF STANDARDS-1963-A

AD A 122317

AFWAL-TR-81-3040

DYNAMIC STABILITY OF STRUCTURES: IMPERFECTION
SENSITIVE SYSTEMS, ACTED UPON BY STEP-LOADS



George J. Simitzes
Georgia Institute of Technology
Atlanta, Georgia 30338

May 1981

Interim Report for Period October 1979 - April 1980

Approved for public release; distribution unlimited.

FLIGHT DYNAMICS LABORATORY
AIR FORCE WRIGHT AERONAUTICAL LABORATORIES
AIR FORCE SYSTEMS COMMAND
WRIGHT-PATTERSON AIR FORCE BASE, OHIO 45433

DEC 13 1982

A

82 12 13 113

NOTICE

When Government drawings, specifications, or other data are used for any purpose other than in connection with a definitely related Government procurement operation, the United States Government thereby incurs no responsibility nor any obligation whatsoever; and the fact that the government may have formulated, furnished, or in any way supplied the said drawings, specifications, or other data, is not to be regarded by implication or otherwise as in any manner licensing the holder or any other person or corporation, or conveying any rights or permission to manufacture use, or sell any patented invention that may in any way be related thereto.

This report has been reviewed by the Office of Public Affairs (ASD/PA) and is releasable to the National Technical Information Service (NTIS). At NTIS, it will be available to the general public, including foreign nations.

This technical report has been reviewed and is approved for publication.



VIPPERLA B. VENKAYYA
Project Engineer



FREDERICK A. PICCHIONI, Lt Col, USAF
Chief, Analysis & Optimization Branch

FOR THE COMMANDER



RALPH L. KUSTER, JR., Col, USAF
Chief, Structures & Dynamics Division

"If your address has changed, if you wish to be removed from our mailing list, or if the addressee is no longer employed by your organization please notify AFWAL/FIBR, W-PAFB, OH 45433 to help us maintain a current mailing list".

Copies of this report should not be returned unless return is required by security considerations, contractual obligations, or notice on a specific document.

UNCLASSIFIED

SECURITY CLASSIFICATION OF THIS PAGE (When Data Entered)

REPORT DOCUMENTATION PAGE		READ INSTRUCTIONS BEFORE COMPLETING FORM
1. REPORT NUMBER AFWAL-TR-81-3040	2. GOVT ACCESSION NO. AD-A122 317	3. RECIPIENT'S CATALOG NUMBER
4. TITLE (and Subtitle) Dynamic Stability of Structures: Imperfection Sensitive Systems, Acted Upon By Step-Loads		5. TYPE OF REPORT & PERIOD COVERED Interim Report Oct 1979 - April 1980
		6. PERFORMING ORG. REPORT NUMBER
7. AUTHOR(s) George J. Simitzes Costas Lazopoulos		8. CONTRACT OR GRANT NUMBER(s) F33615-79-C-3221
9. PERFORMING ORGANIZATION NAME AND ADDRESS Georgia Institute of Technology Atlanta, Georgia 30338		10. PROGRAM ELEMENT, PROJECT, TASK AREA & WORK UNIT NUMBERS Projects 2304, 2401 Tasks 2304N1, 240102 Wk Units 2304N114, 24010244
11. CONTROLLING OFFICE NAME AND ADDRESS Flight Dynamics Laboratory (FIBRA) AF Wright Aeronautical Laboratories (AFSC) Wright-Patterson Air Force Base OH 45433		12. REPORT DATE June 1980
		13. NUMBER OF PAGES 117
14. MONITORING AGENCY NAME & ADDRESS (if different from Controlling Office)		15. SECURITY CLASS. (of this report) Unclassified
		15a. DECLASSIFICATION/DOWNGRADING SCHEDULE
16. DISTRIBUTION STATEMENT (of this Report) Approved for public release; distribution unlimited.		
17. DISTRIBUTION STATEMENT (of the abstract entered in Block 20, if different from Report)		
18. SUPPLEMENTARY NOTES		
19. KEY WORDS (Continue on reverse side if necessary and identify by block number) Dynamic Stability Buckling Analysis Imperfection Sensitive Damping Step Loads Preloading Ideal Impulse		
20. ABSTRACT (Continue on reverse side if necessary and identify by block number) Structural configurations subjected to loads that fall under the category of an ideal impulse are considered. Emphasis is placed on systems that exhibit either limit point instability or an unstable bifurcational branch in the post-buckling region. The purpose of the present work is to investigate the concept of dynamic stability of structural elements subjected to step-loads and develop the related criteria and estimates for finding critical conditions. The step load consists		

DD FORM 1473

JAN 73

EDITION OF 1 NOV 65 IS OBSOLETE

UNCLASSIFIED

SECURITY CLASSIFICATION OF THIS PAGE (When Data Entered)

UNCLASSIFIED

SECURITY CLASSIFICATION OF THIS PAGE(When Data Entered)

of a suddenly applied load of constant magnitude and finite duration t_0 , and the investigation will include the two extreme cases of $t_0 \rightarrow \infty$ and $t_0 \rightarrow 0$ (ideal impulse). Moreover, the effect of various parameters (small damping and preloading) on the critical conditions is studied. The developed solution methodology is demonstrated through a geometrically imperfect model and a load eccentricity model of one degree of freedom and a snap-through model of two degrees of freedom.

UNCLASSIFIED

SECURITY CLASSIFICATION OF THIS PAGE(When Data Entered)

Forward

This report was prepared by Professor George J. Simitzes and Mr. Costas Lazopoulos both of the School of Engineering Science and Mechanics, at the Georgia Institute of Technology, Atlanta, Georgia. The work was performed under Contract No. F33615-79-C-3221 with the U.S.A.F. Aeronautical Systems Division (AFSC), Wright-Patterson Air Force Base, Ohio 45433. This interim technical report was released by the authors in June, 1980. The report covers work conducted, under contract, from October, 1979 through April, 1980 (end of Phase I).



A

TABLE OF CONTENTS

SECTION	PAGE NO.
I. INTRODUCTION	1
II. GEOMETRY AND STATIC ANALYSIS OF THREE MECHANICAL MODELS	4
Model A. Geometrically Imperfect Model	4
Model B. Load Eccentricity Model	7
Model C. A Snap-Through Model	9
III. IDEAL IMPULSE	15
Statement of the Problem	15
Model A	16
Model B	20
Model C	21
IV. CONSTANT LOAD OF INFINITE DURATION	26
Model A	26
Model B	27
Model C	27
V. CONSTANT LOAD OF FINITE DURATION	37
Statement of the Problem	37
General Procedure	37
Model A	39
Model B	43
Model C	44
VI. THE INFLUENCE OF PRELOADING - CONSTANT LOAD OF FINITE DURATION	52
Statement of the Problem	52
Model A	58
Model B	69
Model C	81

TABLE OF CONTENTS
(Continued)

SECTION	PAGE NO.
VII. THE INFLUENCE OF SMALL DAMPING, CONSTANT LOAD OF FINITE DURATION	92
Statement of the Problem	92
General Approach	92
Model A	95
Model B	100
Model C	106
REFERENCES	112
APPENDIX A THE BRACHISTOCHRONE PROBLEM	114

LIST OF ILLUSTRATIONS

<u>Figure</u>		<u>Page</u>
1	Geometry and Sign Convention for Model A	5
2	Load-Displacement Curves for Model A	6
3	Geometry and Sign Convention for Model B	8
4	Geometry and Sign Convention for Model C	9
5	Locus of Static Equilibrium Positions for Model C	13
6	Load-Displacement Curve for Model C	14
7	"Zero-Load" Total Potential versus $\theta - \theta_0$ (Model A)	19
8	Phase Plane Curves for Model B	22
9	Upper and Lower Bounds for the Critical Ideal Impulse (Model C)	25
10	Total Potential versus Displacement for Various Loads (Model A)	28
11	Static and Dynamic Critical Loads (Model A)	29
12	Static and Dynamic Critical Loads (Model B)	30
13	Critical Conditions for Model B. Constant Load of Infinite Duration	31
14	Upper and Lower Bounds for the Critical Load (Infinite Duration) (Model C)	36
15	Constant Load, p , versus Critical Duration Time, $\tau_{o\ cr}$, (Model A)	41
16	Impulse, $(p\tau_o)$, versus Critical Duration Time, $\tau_{o\ cr}$, (Model A)	42
17	Constant Load, p_{cr} , versus Critical Duration Time, $\tau_{o\ cr}$, (Model B)	45
18	Impulse, $(p\tau_o)$, versus Critical Duration Time, $\tau_{o\ cr}$, (Model B)	46
19	Load, p , versus Critical Duration Time, $\tau_{o\ cr}$, (Model C)	50

LIST OF ILLUSTRATIONS (CONT'D)

<u>Figure</u>		<u>Page</u>
20	Impulse, $(p\tau_o)$, versus Critical Duration Time, $\tau_{o_{cr}}$, (Model C)	51
21	Definitions of Total Potentials (One-Degree-of-Freedom System)	54
22	Superimposed Load, p , versus Critical Finite Time Duration, $\tau_{o_{cr}}$, Preloaded Model A, $\theta_o = 0.005$	63
23	Superimposed Load, p , versus Critical Finite Time Duration, $\tau_{o_{cr}}$, Preloaded Model A, $\theta_o = 0.01$	64
24	Superimposed Load, p , versus Critical Finite Time Duration, $\tau_{o_{cr}}$, Preloaded Model A, $\theta_o = 0.02$	65
25	Superimposed Impulse, $(p\tau_o)$, versus Critical Duration Time, $\tau_{o_{cr}}$, Preloaded Model A, $\theta_o = .005$	66
26	Superimposed Impulse, $(p\tau_o)$, versus Critical Time Duration, $\tau_{o_{cr}}$, Preloaded Model A, $\theta_o = 0.01$	67
27	Superimposed Impulse, $(p\tau_o)$, versus Critical Duration Time, $\tau_{o_{cr}}$, Preloaded Model A, $\theta_o = 0.02$	68
28	Superimposed Load, p , versus Critical Duration Time, $\tau_{o_{cr}}$, Preloaded Model B, $\bar{e} = 0.005$	75
29	Superimposed Load, p , versus Critical Duration Time, $\tau_{o_{cr}}$, Preloaded Model B, $\bar{e} = 0.01$	76
30	Superimposed Load, p , versus Critical Duration Time, $\tau_{o_{cr}}$, Preloaded Model B, $\bar{e} = 0.02$	77
31	Superimposed Impulse, $(p\tau_o)$, versus Critical Duration Time, $\tau_{o_{cr}}$, Preloaded Model B, $\bar{e} = 0.005$	78
32	Superimposed Impulse, $(p\tau_o)$, versus Critical Duration Time, $\tau_{o_{cr}}$, Preloaded Model B, $\bar{e} = 0.01$	79

LIST OF ILLUSTRATIONS (CONT'D)

<u>Figure</u>		<u>Page</u>
33	Superimposed Impulse, $(p\tau_o)$, versus Critical Duration Time, τ_{ocr} , Preloaded Model B, $\bar{\epsilon} = 0.02$	80
34	Constant Load, p , versus Critical Duration Time, τ_{ocr} , Preloaded Model C, $\Lambda = 5.0$	86
35	Constant Load, p , versus Critical Duration Time, τ_{ocr} , Preloaded Model C, $\Lambda = 6.0$	87
36	Constant Load, p , versus Critical Duration Time, τ_{ocr} , Preloaded Model C, $\Lambda = 8.0$	88
37	Impulse, $(p\tau_o)$, versus Critical Duration Time, τ_{ocr} , Preloaded Model C, $\Lambda = 5.0$	89
38	Impulse, $(p\tau_o)$, versus Critical Duration Time, τ_{ocr} , Preloaded Model C, $\Lambda = 6.0$	90
39	Impulse, $(p\tau_o)$, versus Critical Duration Time, τ_{ocr} , Preloaded Model C, $\Lambda = 8.0$	91
40	Geometry of Model A with Damping	95
41	Geometry of Model B with Damping	100
42	Geometry of Model C with Damping	106

LIST OF TABLES

<u>Table</u>		<u>Page</u>
1	Critical Ideal Impulse, $(p\tau_o)_{cr}$, Model A	59
2	Critical Dynamic Load, P_{cr_∞} , Constant Load of Infinite Duration, Model A	60
3	Critical Ideal Impulse, $(p\tau_o)_{cr}$, Model B	70
4	Critical Dynamic Load, P_{cr_∞} , Constant Load of Infinite Duration, Model B	72
5	Critical Ideal Impulse, $(p\tau_o)_{cr}$, Model C	82
6	Critical Loads, Constant Magnitude, Infinite Duration, Model C	
7	Critical Conditions for Constant Load of Finite Duration in the Presence of Damping, Model A	99
8	Critical Conditions for Constant Load of Finite Duration in the Presence of Damping, Model B	105
9	Critical Conditions for Constant Load of Finite Duration in the Presence of Damping, Model C	111

SECTION I

INTRODUCTION

Dynamic stability or instability of elastic structures has drawn considerable attention in the past thirty years. The importance of the subject lies primarily in the constant demand for lightweight efficient structures, which requires a good understanding of how structures respond to loads that induce dynamic effects.

The term "Dynamic Stability" encompasses many classes of problems and it has been used, by the various investigators, in connection with a particular study. Therefore it is not surprising that there are various interpretations of the meaning of the term.

The class of problems falling in the category of parametric excitation are the best defined, conceived and understood problems of dynamic stability. An excellent treatment and bibliography can be found in the book by V. V. Bolotin [1]. As a matter of fact, Bolotin applies the term "Dynamic Stability" only to problems of parametric excitation.

In general, problems which deal with stability of motion have concerned for many years researchers in many fields of engineering. Definitions for stability and related criteria, as developed through the years, are given by I. J. Stoker [2]. Additional references [3-6] provide the necessary details as applied to a variety of problems. Some of these criteria find wide uses in problems of stability and control of aircraft [7], control theory [8], and many problems in fluid mechanics, combustion and, to a certain extent, elastic structures under dynamic conditions.

Moreover, many authors refer to problems of the "follower force" type

as problems of dynamic stability [9-10]. The primary reason for this is that critical conditions can be obtained (in many cases) only through the use of the "kinetic" or "dynamic" approach to static stability problems (flutter instead of divergence type of instability).

In addition, problems of aeroelastic instability and flow-induced instability (fluid flowing through pipes) also fall under the general heading of dynamic stability.

A large class of structural problems that has received attention recently and does qualify as a category of dynamic stability is that of impulsively loaded configurations and configurations which are suddenly loaded with loads of constant magnitude and infinite duration. These two types of loads may be thought of as mathematical idealizations of blast loads of (a) large decay rates and small decay times and (b) small decay rates and large decay times respectively. In addition, these types of loads may be considered as representative of impact loads. Of course, there are other physical explanations for such loads. For both types of loads mentioned above the concept of dynamic stability is related with the observation that for sufficiently small values of the loading the system simply oscillates (linearly or non-linearly) about the near static equilibrium point and the corresponding amplitudes of oscillation are sufficiently small. If the loading is increased, some systems will experience large amplitude oscillations or in general divergent type of motion. For this phenomenon to happen the configuration (turns out) must possess two or more static equilibrium positions and "tunneling-through" [11] occurs by having trajectories that can pass through an unstable static equilibrium point. Consequently, the methodologies developed by the various

investigators (including criteria and estimates) are for structural configurations that exhibit snap-through buckling, when loaded quasi-statically.

Solutions to such problems started appearing in the open literature in the early 1950's. Hoff and Bruce [12] considered the dynamic stability of a pinned half-sine arch under a half-sine distributed load. The ideal impulse problem as well as the case of a suddenly applied load with constant magnitude and infinite duration were considered in this report. Budiansky and Roth [13] in studying the axisymmetric behavior of a shallow spherical cap under suddenly applied loads defined the load to be critical, when the transient response increases suddenly with very little increase in the magnitude of the load. This concept was adopted by numerous investigators (see [14]) in the subsequent years because it is tractable to computer solutions. This concept was used by Budiansky and Hutchinson [15] in estimating the critical load (suddenly applied) for imperfection sensitive systems. Through this criterion, they related the dynamic critical load to the static one. Finally, the concept was generalized in a subsequent paper by Budiansky [16] in attempting to predict critical conditions for imperfection sensitive structures under time dependent loads. Conceptually, one of the best efforts in the area of dynamic buckling, under impulsive and suddenly applied loads, is the work of Hsu and his collaborators [17-20]. In his studies, he defined sufficiency conditions for stability and sufficiency conditions for instability, thus finding upper and lower bounds for the critical impulse or critical sudden load. Independently, Simitses [21] in dealing with the dynamic buckling of shallow arches and spherical caps termed the lower bound as a minimum possible critical load (MPCL) and the upper bound as a minimum guaranteed critical load (MGCL).

The purpose of the present work is to investigate the concept of dynamic stability of structural elements subjected to step-loads and develop the related criteria and estimates for finding critical conditions. The step load consists of a suddenly applied load of constant magnitude and finite duration t_0 , and the investigation will include the two extreme cases of $t_0 \rightarrow \infty$ and $t_0 \rightarrow 0$ (ideal impulse). Moreover, the effect of various parameters (small damping and preloading) on the critical conditions is studied. The developed solution methodology is demonstrated through simple mechanical models of one-and two-degrees of freedom. Section I deals with the introduction to the subject of dynamic stability of structural elements. Section II presents a detailed static buckling analysis of the models. Section III presents the concept of dynamic stability for impulsively loaded systems, which is demonstrated through the same models. Section IV gives a detailed treatment of systems loaded suddenly with constant load of infinite duration. Section V extends these concepts for the case of suddenly applied loads of constant magnitude and finite duration. Sections VI and VII deal with the study of the effects of preloading and small damping on the dynamic critical conditions.

SECTION II

GEOMETRY AND STATIC ANALYSIS OF THREE MECHANICAL MODELS

Model A. Geometrically Imperfect Model

Geometry of the Model

Consider the model shown on Fig. 2-1. This model consists of two rigid bars of equal length, L , pinned together. The left bar is pinned on an immovable support, A , while the right end of the second bar is pinned on a movable support, C , and loaded by a horizontal constant-directional force P . A linear spring of stiffness k connects the bar common pin, B , to an immovable support, D , which is L units directly below support A . The initial geometric imperfection, θ_0 is an angle between the horizontal line, joining supports A and C , and bar AB (or BC). The deformed position is characterized by angle θ , as shown (in its positive direction).

Static Stability Analysis of the Model

The stability analysis of this model under quasi-static application of the load P is performed by employing the energy approach. Through this approach, equilibrium is characterized by

$$\frac{dU_T}{d\theta} = 0 \quad (2.1)$$

where U_T is the total potential, and the character of equilibrium (stable or unstable) by the sign of the second derivative.

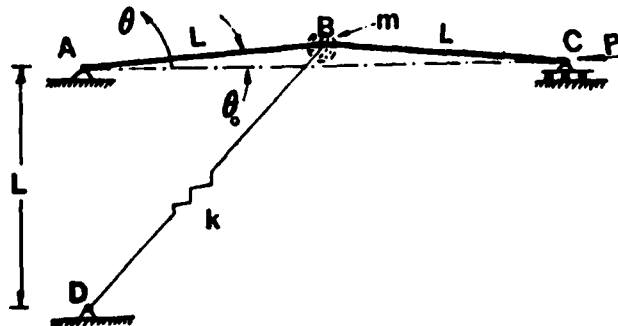


Fig. 2-1 Geometry and Sign Convention for Model A.

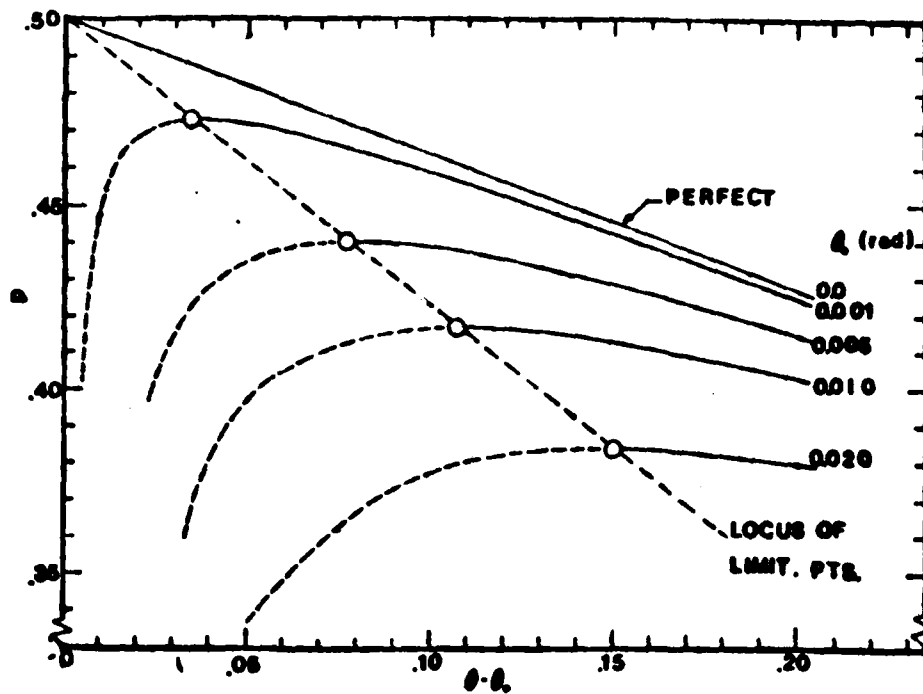


Fig. 2-2 Load-Displacement Curves (Model A).

The total potential is:

$$\bar{U}_T^P = \frac{U_T}{kL^2} = \left[\sqrt{1 + \sin \theta} - \sqrt{1 + \sin \theta_0} \right]^2 - p (\cos \theta_0 - \cos \theta) \quad (2.2)$$

where $p = 2P/kL$, and \bar{U}_T^P denotes the nondimensionalized total potential. The superscript p implies "under load p ".

The static equilibrium points are characterized by

$$p = [\sqrt{1+\sin\theta} - \sqrt{1+\sin\theta_0}] \frac{\cot\theta}{\sqrt{1+\sin\theta}} \text{ for } \theta_0 \neq 0 \quad (2.3)$$

Note that, for $\theta_0 = 0$ equilibrium is characterized by

$$\begin{aligned} &\text{either} && \theta = 0 \\ &\text{or} && p = \cot\theta (\sqrt{1+\sin\theta} - 1)/\sqrt{1+\sin\theta} \end{aligned} \quad (2.4)$$

Equilibrium positions are plotted on Fig. 2 as p versus $\theta - \theta_0$ for various values of the geometric imperfection θ_0 . The stability test reveals that the dashed line positions are stable, while the solid line positions are unstable and snapping (violent buckling) takes place through the existence of a limit point. Also note that positions characterized by negative values for $\theta - \theta_0$ (not shown herein) are stable and there is no possibility of buckling. Therefore, our interest lies in the area of $\theta_0 > 0$ and $\theta - \theta_0 > 0$. It is assumed, for simplicity, that the bars are weightless and the mass m of the system is concentrated on the joint B.

Model B. Load Eccentricity Model

Model B, shown on Fig. 3, is representative of eccentrically loaded structural systems, exhibiting limit point instability. The bar is rigid and of length L ; the spring is linear of stiffness k and the load eccentricity is denoted by e . The static stability analysis for this model is presented in Ref [23]. The bar is assumed to be weightless and the mass, m , of the system is concentrated on the top of the rod, point B.

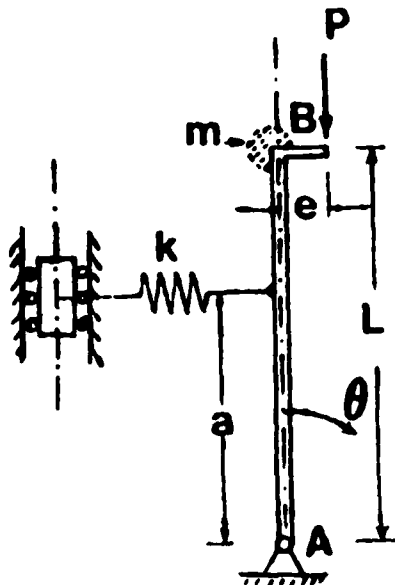


Fig. (2.3) Geometry and Sign Convention for Model B

The expression for the total potential is given by

$$U_T^P = \frac{1}{2}ka^2 \sin^2 \theta - PL \left(1 - \cos \theta + \frac{e}{L} \sin \theta \right)$$

In nondimensionalized form this expression becomes

$$\bar{U}_T^P = \frac{U_T^P}{\frac{1}{2}ka^2} = \sin^2 \theta - 2p \left(1 - \cos \theta + \bar{e} \sin \theta \right) \quad (2.5)$$

where $p = \frac{PL}{ka^2}$ is the nondimensionalized load and $\bar{e} = \frac{e}{L}$ is the nondimensionalized eccentricity.

Furthermore, equilibrium is characterized by

$$p = \frac{\sin \theta}{\tan \theta + \bar{e}} \quad (2.6)$$

and critical load (see Ref. [23]) is given by

$$p_{cr} = [1 + \bar{e}^{2/3}]^{-3/2} \quad (2.7)$$

2.4 Model C. A Snap-Through Model

Consider the model shown on Fig. (2-4), which consists of three equal length rigid bars. The three bars are pinned to each other, and they are connected with rotational springs of stiffness β (linear). The left bar is pinned onto an immovable support, while the right bar is pinned onto a movable support, which in turn is connected to a wall through a linear extensional spring (horizontal) of stiffness k (linear). The middle bar is originally horizontal and the loading consists of two equal concentrated forces, P , applied at the ends of the middle bar and remaining vertical. The original angle between the horizontal line, joining the supports and the end bars is α . The angle between the horizontal and the left bar in a deformed state is θ , while the angle between the horizontal and the right bar is φ .

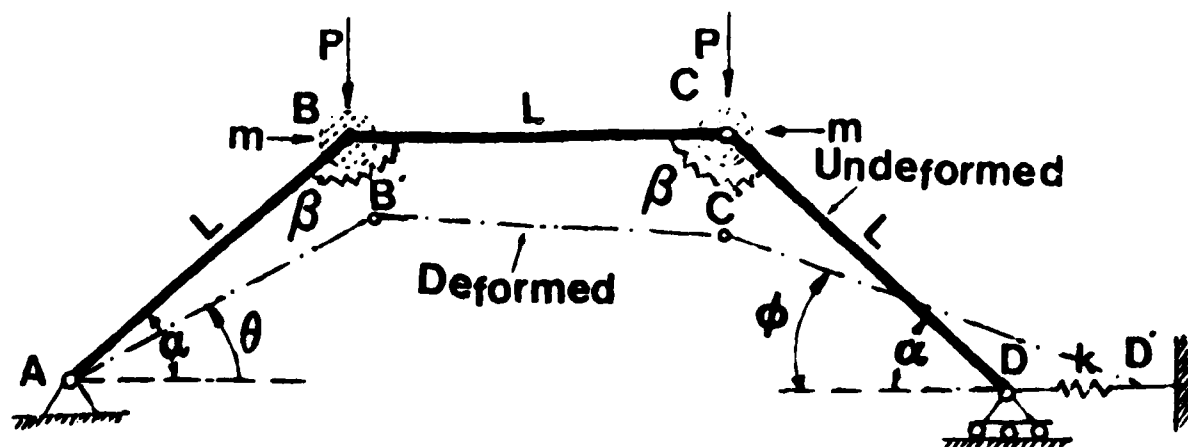


Fig. (2.4) Geometry and Sign Convention for Model C

This is a two-degree-of-freedom model, and as it will be seen, from the ensuing discussion, certain new features enter into the solution.

Assuming that α , θ , and φ are small angles such that their sine can be well approximated by the angle itself and the cosine by one minus half of the angle squared, then the expression for the total potential is approximated by

$$U_T^P = \frac{1}{2} \beta [5\theta^2 + 5\varphi^2 - 2\alpha^2 - 8\varphi\theta - 20\alpha - 2p\alpha] + \frac{kL^2}{2} (\alpha^2 - \theta^2 - \varphi^2 + \varphi\theta)^2 - PL(2\alpha - \theta - \varphi) \quad (2.8)$$

Note that for the above equation to be dimensionally correct the following order of magnitude must apply to the various terms. If α , θ and φ are taken to be small numbers (of order δ), then β must be of order $\delta^2 \times (kL^2)$, PL of order $\delta^3 \times (kL^2)$ and U_T^P of order $\delta^4 \times (kL^2)$.

The independent variables are φ and θ and the symmetric response mode is characterized by $\theta = \varphi$.

New variables r and s , are introduced such that the symmetric response is characterized by $s = 0$.

These are

$$\begin{aligned} \theta &= \sqrt{\tilde{\beta}} (r-s) \\ \varphi &= \sqrt{\tilde{\beta}} (r+s) \end{aligned} \quad (2.9)$$

or

$$\begin{aligned} r &= (\theta + \varphi)/2\sqrt{\tilde{\beta}} \\ s &= (\varphi - \theta)/2\sqrt{\tilde{\beta}} \end{aligned} \quad (2.10)$$

where $\tilde{\beta} = \beta/kL^2$ is a nondimensionalized rotational spring stiffness parameter. Through introduction of additional nondimensionalized parameters

$$\hat{U}_T = \frac{U_T}{\tilde{\beta}^2 kL^2} ; \quad p = \frac{P}{kL\tilde{\beta}^{3/2}} \quad (2.11)$$

and by letting

$$\alpha^2 = \bar{\beta}\Lambda, \quad (2.12)$$

the following expression for the total potential is obtained.

$$\bar{U}_T^P = (r^2 + 9s^2 - 2\sqrt{\Lambda} r + \Lambda) + \frac{1}{2} (\Lambda - r^2 - 3s^2)^2 - 2p (\sqrt{\Lambda} - r) \quad (2.13)$$

Note that, on the basis of the nondimensionalization, the order of magnitude of the new parameters is as follows: (a) $\bar{\beta}$ is of order δ^2 ; (b) U_T is of order one; (c) r and s are of order one; (d) Λ is of order one; and (e) p is of order one.

It can easily be shown that, if $\bar{\beta} = 0$ (no rotational springs), the system is unstable for zero load, $P = 0$, and thus the $\bar{\beta} = 0$ case is excluded from the present discussion, which also allows the nondimensionalization given by Eqs. (2-12) and (2-13) (division by a nonzero number). In the case $\bar{\beta} = 0$, upon the application of a very small load P , the system snaps through an asymmetric mode ($s \neq 0$).

Static Analysis of the Model

The static analysis is performed by employing the energy approach.

For equilibrium

$$\frac{\partial \bar{U}_T^P}{\partial r} = 0 = 2(r - \sqrt{\Lambda}) - (\Lambda - r^2 - 3s^2) 2r + 2p \quad (2.14)$$

$$\frac{\partial \bar{U}_T^P}{\partial s} = 0 = 18s - (\Lambda - r^2 - 3s^2) 6s \quad (2.15)$$

By introducing a new load parameter

$$Q = P - \sqrt{\Lambda} \quad (2.16)$$

the equilibrium equations, Eqs. (2-14) and (2-15) become

$$\begin{aligned}(\Lambda - 1 - r^2 - 3s^2) r &= Q \\ s(\Lambda - 3 - r^2 - 3s^2) &= 0\end{aligned}\tag{2.17}$$

There are two possible solutions to Eqs. (2.14)

(i) Symmetric response $s \equiv 0$, and

$$(\Lambda - 1 - r^2) r = Q\tag{2.18}$$

(ii) Existence of asymmetric response, $s \neq 0$

$$\begin{aligned}\Lambda - 3 &= r^2 + 3s^2 \\ 2r &= Q\end{aligned}\tag{2.19}$$

The equilibrium positions, Eqs. (2-17) are plotted on Fig. 2-5 for all Q , and on Fig. 2.6 as a load-deflection, Q - r curve.

On the basis of the results and by performing the stability test (second derivatives), the following conclusions are drawn.

(a) For $\Lambda < 1$ there is no possibility of buckling and asymmetric response ($s \neq 0$).

(b) For $1 \leq \Lambda \leq 3$ the response is symmetric ($s \equiv 0$) and buckling occurs through the limit point (pt. C on Fig. 2-6), positions between A and C are stable, and the critical load is given by

$$\begin{aligned}Q_{cr} &= 2\sqrt{\frac{\Lambda - 1}{3}} \\ p_{cr} &= \sqrt{\Lambda} + 2\sqrt{\frac{\Lambda - 1}{3}}\end{aligned}\tag{2.20}$$

(c) For $3 < \Lambda < 4$ there is a possibility of asymmetric modes, but for this range of Λ -values, point B is to the left of point C (Fig. 2-6), i.e.

$$\sqrt{\frac{\Lambda-1}{3}} > \sqrt{\Lambda-3} \quad (2.21)$$

and buckling still occurs through the limit point. Therefore, P_{cr} is given by Eq. (2.20).

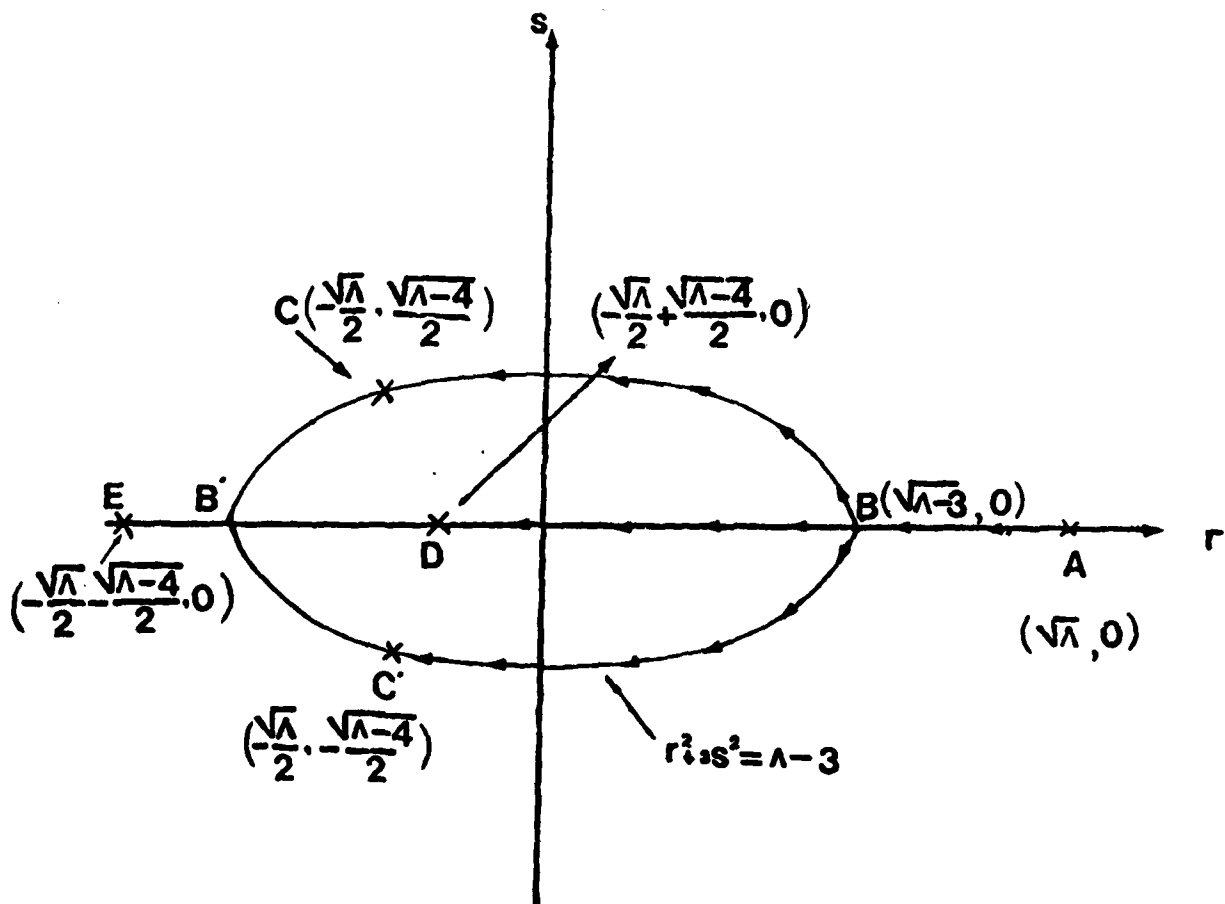


Fig. 2-5 Locus of Static Equilibrium Positions (model C).

(d) For $\Lambda > 4$ buckling occurs through the existence of unstable bifurcation (Pt. B), positions A to B are stable, positions BCO and BO are unstable, and the critical load is given by

$$Q_{cr} = 2\sqrt{\Lambda - 3} \quad , \quad \text{or} \quad (2-22)$$

$$P_{cr} = \sqrt{\Lambda} + 2\sqrt{\Lambda - 3}$$

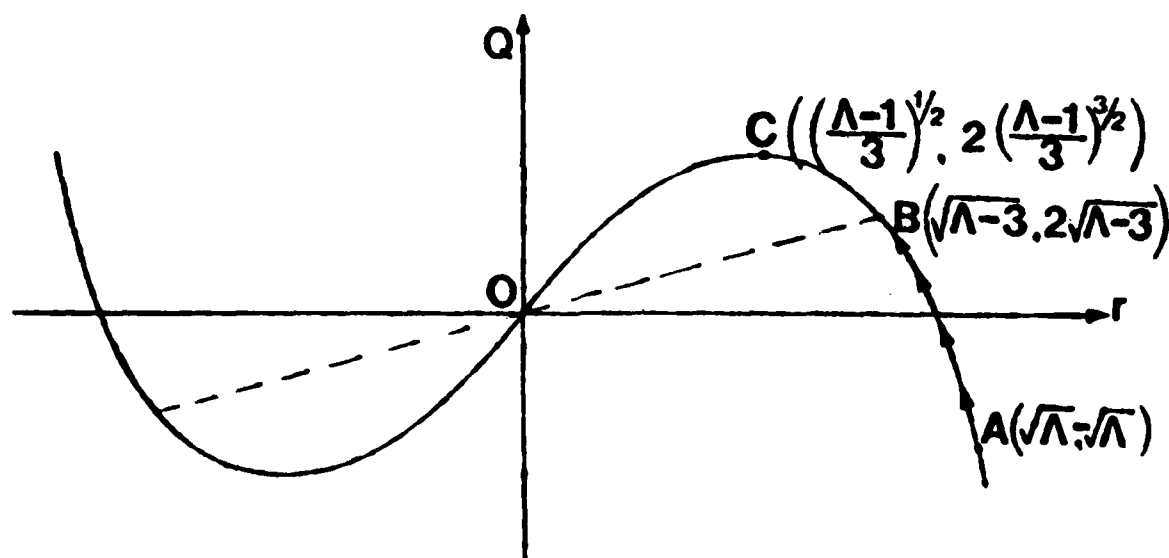


Fig. 2.6 Load-Displacement Curve for Model C.

SECTION III

IDEAL IMPULSE

Statement of the Problem:

Given a structural configuration subjected to loads that fall under the category of an ideal impulse, is there a possibility of dynamic instability, and if yes, what is the level of the impulse for this occurrence? Clearly, before one can estimate the critical condition, one must define what is meant by dynamic instability. Some systems, regardless of the magnitude of the impulse, will simply oscillate, linearly or nonlinearly, about the null positions. Others, if the impulse is small will oscillate, but as the impulse increases they have a tendency to move away from the null position. Finally, there is a group of systems, which behave a little differently from the second group. For small impulses they simply oscillate, but as the impulse increases a certain value is reached at which and beyond which the system will oscillate but with a higher amplitude than that for impulses smaller than this certain value. Regardless, though, of the particular case one can always associate the magnitude of oscillation amplitude to the value of the impulse. In such cases a critical impulse can be related to a maximum amplitude (this is the case in deflection limited designs).

There is always a relation between the system behavior under impulsive loads and the static equilibrium characteristics of the system. In the groups discussed above, the first corresponds to systems which have unique and stable load-deflection equilibrium states, or a stable post-buckling bifurcational branch. The other two correspond to systems that exhibit either limit point instability or an unstable bifurcational branch in the post-buckling region. The emphasis, therefore, is placed on the last two groups

and criteria for stability and estimates of critical conditions are presented through the models discussed in Section II.

Model A

Consider Model A shown on Fig. 2-1, assume that the bars are weightless and that the mass of the system is concentrated at point B. Furthermore, assume that the load, P , is suddenly applied with very short duration time, T_0 , and that the impulse (PT_0) , is imparted instantaneously into the system as initial kinetic energy.

Through impulse-momentum one obtains the following relation

$$(PT_0) = \frac{1}{2} \left(\frac{mL \dot{\theta}_0}{\sin \theta_0} \right) \quad (3.1)$$

where $\dot{\theta}_0 = d\theta/dt$ at $\theta = \theta_0$.

Since the system is conservative, then

$$\bar{U}_T^0 + T^0 = \text{const.} = T_1^0 \quad (3.2)$$

where \bar{U}_T^0 denotes the total potential "under zero load", T^0 is the kinetic energy, given by

$$T^0 = \frac{1}{2} mL^2 \dot{\theta}^2 \quad (3.3)$$

Note that T_1^0 is the initial kinetic energy imparted instantaneously by the impulsive load.

Finally the expression for \bar{U}_T^0 is given by

$$\bar{U}_T^0 = [\sqrt{1 + \sin \theta} - \sqrt{1 + \sin \theta_0}]^2 \quad (3.4)$$

In order to understand the "concept" of stability or instability under an impulsive load for this one degree of freedom model, let us consider Fig. 3.1, which is a plot of \bar{U}_T^0 versus $\theta - \theta_0$.

According to Eq. (3.2), and since T^0 is positive definite, motion is possible if and only if

$$T_i^0 - U_T^0 \geq 0 \quad (3.5)$$

This implies that, for a given initial kinetic energy, Eq. (3.3), and consequently a given impulse, say $\bar{T}_i^0 = D$ (see Fig. 3.1 - total potential presented in nondimensionalized form), motion is confined in the region $\theta_I < \theta - \theta_0 < \theta_{II}$. It is clearly seen then that, as long as $\bar{T}_i^0 = D < (\sqrt{2} - \sqrt{1 + \sin \theta_0})^2$, the motion of the system is bounded and it contains only the stable "zero load" static equilibrium point, B. Such a motion is termed "unbuckled". For the motion to cease to be "unbuckled", i.e. to become unbounded and cease to include only the initial stable static equilibrium point, B, D must be, at least, equal to the value of \bar{U}_T^0 at the unstable point C. Then that point (C) can be reached with zero velocity and the motion can become unbounded. Clearly if D is even slightly higher than the \bar{U}_T^0 - value at point C, the motion does become unbounded and it can contain other static equilibrium points, such as point C. Such a motion is called "buckled" and a critical condition exists when the impulse is large enough to satisfy the relation

$$\bar{T}_i^0 = \bar{U}_T^0(C) \quad (3.6)$$

Introducing nondimensionalized time and load parameters

$$\tau = \tau (2k/m)^{1/2} \quad \tau_o = \tau_o \left(\frac{2k}{m} \right)^{1/2} \quad (3.7)$$

$$p = 2P/kL$$

then

$$\bar{T}_i^o = \frac{T_o}{kL} = \frac{1}{2} \left(\frac{m}{k} \right) \dot{\theta}^2 = \left(\frac{d\theta}{d\tau} \right)_{\theta_o}^2 \quad (3.8)$$

From Eq. (3.1) one obtains

$$(p\tau_o) = \frac{2}{\sin \theta_o} \left(\frac{d\theta}{d\tau} \right) \quad (3.9)$$

Use of Eqs. (3.6), (3.4) (3.8) and (3.9) yields the expression for the critical impulse or

$$(p\tau_o)_{cr} = 2[\sqrt{2} - \sqrt{1 + \sin \theta_o}] / \sin \theta_o \quad (3.10)$$

Two observations are worth mentioning at this point: (a) Because this is a one degree of freedom model, the critical impulse $(p\tau_o)_{cr}$ given by Eq. 3.1 represents both the minimum possible (MPCL) and minimum guaranteed (MGCL) values as defined in Ref. 21. In other words Hsu's (17-18) "sufficient condition for stability and instability" boundaries are coincident; (b) Although the concept presented so far is clear and it leads to a criterion and estimate of the critical condition, it might be impractical when applied to real structures. In the particular example shown so far, it is clear that, according to the presented concept of dynamic instability, "buckled" motion is possible if the system is allowed to reach the position $\theta = \pi/2$. In many cases such positions may be considered excessive, especially in deflection-

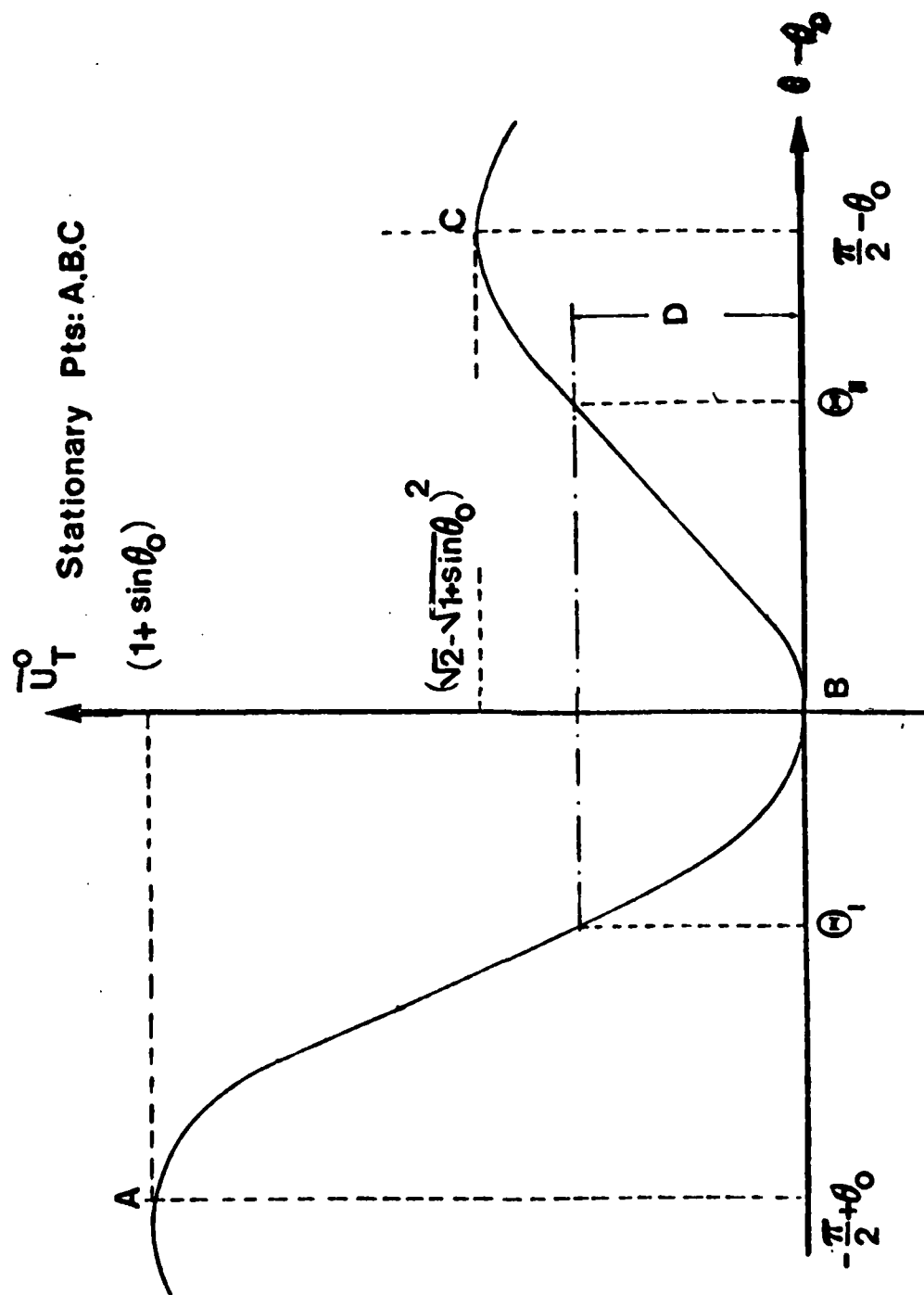


Fig. 3.1 "Zero-Load" Total Potential versus $\theta - \theta_0$ (Model A).

limited designs. In such cases, if θ cannot be larger than a specified value, then the allowable impulse is smaller and its value can be found from Eq. (3.6), if C is replaced by the maximum allowable value of θ , say θ_L . In this case

$$(p\tau_o)_{cr} = 2[\sqrt{1 + \sin\theta_L} - \sqrt{1 + \sin\theta_o}]/\sin\theta_o \quad (3.11)$$

Related with this discussion is the broad definition of stability proposed by Hoff (22): "A structure is in stable state, if admissible finite disturbances of its initial state of static or dynamic equilibrium, are followed by displacements whose magnitudes remain within allowable bounds during the required lifetime of the structure."

Model B

Following the same notion as for Model A, the expression for the critical impulse, $(p\tau_o)_{cr}$ is given by

$$(p\tau_o)_{cr} = \frac{I}{e} \quad (3.12)$$

where

$$\tau = \left(\frac{ka^2}{I}\right)^{1/2} t, \quad p = \frac{PL}{ka^2} \quad (3.13)$$

and I is the bar moment of inertia about the hinge.

The expression for the total potential, the kinetic energy, and impulse-momentum are given by (respectively)

$$U_T = \frac{1}{2} ka^2 \sin^2\theta - PL(1 - \cos\theta + \frac{e}{L} \sin\theta) \quad (3.14)$$

$$T = \frac{1}{2} I \left(\frac{d\theta}{dt}\right)^2 \quad (3.15)$$

$$(p\tau_o) = \left(\frac{I}{e}\right) \frac{d\theta}{dt} \quad (3.16)$$

where I is the moment of inertia of the mass m about the hinge.

In this case also, if the design is deflection limited, Θ_L , then $U_T^0\left(\frac{\pi}{2}\right) = \frac{1}{2} ka^2$ must be replaced by $U_T^0(\Theta) = \frac{1}{2} ka^2 \sin^2 \Theta_L$ and the allowable impulse in this case is given by

$$(p\tau_o)_{\text{allowable}} = \frac{L}{e} \sin \Theta_L \quad (3.17)$$

Another similar approach that may be used for finding critical impulses is presented herein through Model B. It makes use of Eq. (3.2), but instead of associating critical conditions with characteristics on the "zero load" total potential, the critical condition is associated with characteristics of the phase plane.

Eq. (3.2) for this model, in nondimensionalized form becomes

$$\dot{\theta}^2 + \sin^2 \theta = \left[(p\tau_o) \frac{e}{L} \right]^2 \quad (3.18)$$

where $\dot{\theta} = d\theta/d\tau$.

Clearly, if $\left[(p\tau_o) \frac{e}{L} \right]^2 < 1$, Eq. (3.18) denotes a closed curve about the null position $\dot{\theta} = \theta = 0$ in the phase plane. In this case the motion is called "unbuckled". (See Fig. 3.2). When $\left[p\tau_o \left(\frac{e}{L} \right) \right] = 1$, Eq. (3.18) denotes a curve which can escape the closed loop and thus the motion becomes "buckled". Therefore,

$$(p\tau_o)_{\text{cr}} = \frac{L}{e} \quad (3.19)$$

Model C

In order to simplify matters, it is assumed that the three bars are weightless and that the impulse is imparted into the system through two

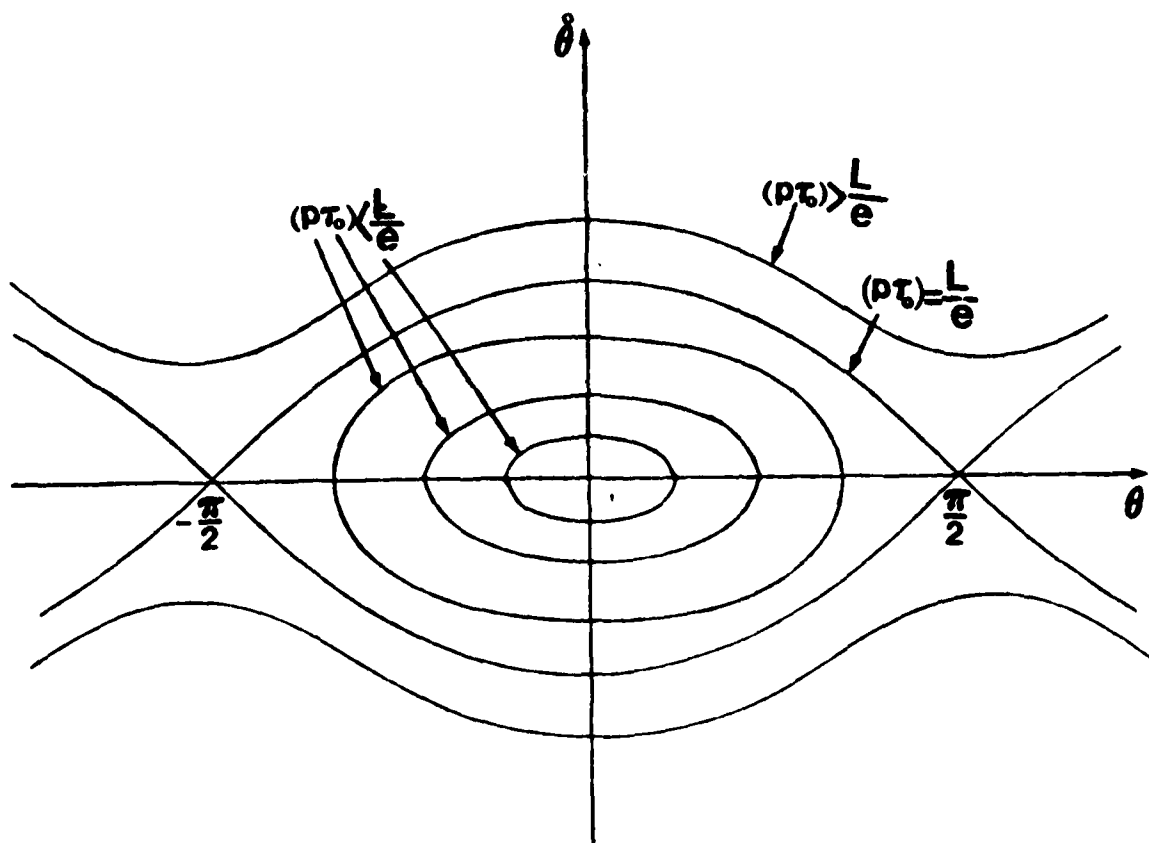


Fig. 3. 2. Phase Plane Curves for Model B

masses, m , at points B and C. This is also used in determining the initial, kinetic energy of the system. Thus

$$(p\tau_0) = 2mL \sqrt{\beta} \left(\frac{dr}{dt} \right) \Big|_{r = \sqrt{\Lambda}} \quad (3.20)$$

and

$$T_1^0 = mL^2 \beta \left(\frac{dr}{dt} \right) \Big|_{r = \sqrt{\Lambda}}^2$$

where T_0 is the small duration time.

Introduction of the new nondimensionalized parameters

$$\tau = \left(\frac{\bar{B}k}{2m} \right)^{1/2} \quad \text{and} \quad \bar{T}_1 = T_1 / \bar{B}^2 k l^2, \quad (3.21)$$

yields

$$(p\tau_0) = \left(\frac{dr}{d\tau} \right) \Big|_{r = \sqrt{\Lambda}} \quad (3.22)$$

The concept of dynamic stability is similar to the one used for Models A and B.

$$\bar{U}_T^0 + \bar{T}^0 = \bar{T}_1^0 \quad (3.23)$$

A critical condition exists, if the impulse, $(p\tau_0)$, imparts sufficient kinetic energy into the system so it can reach, with zero velocity, an unstable static equilibrium point on the "zero-load" total potential, \bar{U}_T^0 , and thus the motion can become unbounded.

Clearly, then from Eqs. (3.22) and (3.23)

$$(p\tau_0)_{cr} = \sqrt{2} (\bar{T}_1^0)^{1/2} = \sqrt{2} \bar{U}_T^0 \text{ (unst. st. pt.)} \quad (3.24)$$

Thus, before $(p\tau_0)_{cr}$ can be found, one must have knowledge of all stationary points and of their character (stable, unstable, etc.). Starting with the expression for \bar{U}_T^0 [Eq. (2.11) with $p = 0$], requiring equilibrium, and performing a stability analysis the following results are obtained.

Stationary points and their character

Pt. 1 at $(\sqrt{\Lambda}, 0)$	Stable (Relative Minimum)
Pt. 2 at $[(-\sqrt{\Lambda} + \sqrt{\Lambda-4})/2, 0]$	Unstable (Relative Maximum)
Pt. 3 at $[(-\sqrt{\Lambda} - \sqrt{\Lambda-4})/2, 0]$	Stable (Relative Minimum)
Pt. 4 at $[-\sqrt{\Lambda}/2, \sqrt{\Lambda-4}/2]$	Unstable (Saddle Point)
Pt. 5 at $[-\sqrt{\Lambda}/2, -\sqrt{\Lambda-4}/2]$	Unstable (Saddle Point)

We observe that there are two possibilities of the motion becoming unbounded; (a) by reaching Pt. 2 with zero velocity, in which case the system will definitely move toward Pt. 3 (far stable point); in this case the corresponding critical impulse is termed (MGCL) because \bar{U}_T^0 (Pt. 2) is the largest of all \bar{U}_T^0 (Stationary pts). Thus, regardless of the path of motion in the r, s space, starting from $(\sqrt{\Lambda}, 0)$, the motion will enclose at least one unstable point and will become unbounded; (b) by reaching either Pt. 4 or Pt. 5, in which case there is a single possibility of the motion becoming unbounded and enclosing one unstable point; note that, in this case, there is a possibility of unbounded motion, but this is not guaranteed, because the system can simply oscillate in the r, s space bounded by lines of equal potential, to \bar{U}_T^0 (Pt. 4) enclosing only the near static stable point, Pt. 1, and either of the "saddle" points, Pt. 4 or Pt. 5; thus, the corresponding critical impulse is called (MPCL).

(MPCL) and (MGCL) denote upper and lower bounds of $(p\tau_o)_{cr}$.

By Eq. (3.24),

$$(MPCL) \quad (p\tau_o)_{cr} = 3\sqrt{\Lambda - 1} \quad (3.25)$$

$$(MGCL) \quad (p\tau_o)_{cr} = \left[5\Lambda - 2 - 3\sqrt{\Lambda^2 - 4\Lambda} + \frac{1}{4} (\Lambda + 2 + \sqrt{\Lambda^2 - 4\Lambda})^2 \right]^{1/2}$$

Note that critical conditions can exist only for $\Lambda \geq 4$. If $\Lambda \geq 4$, there is no far stable static equil. pt. on the "zero-load" total potential.

The results are plotted on Fig. 3.3.

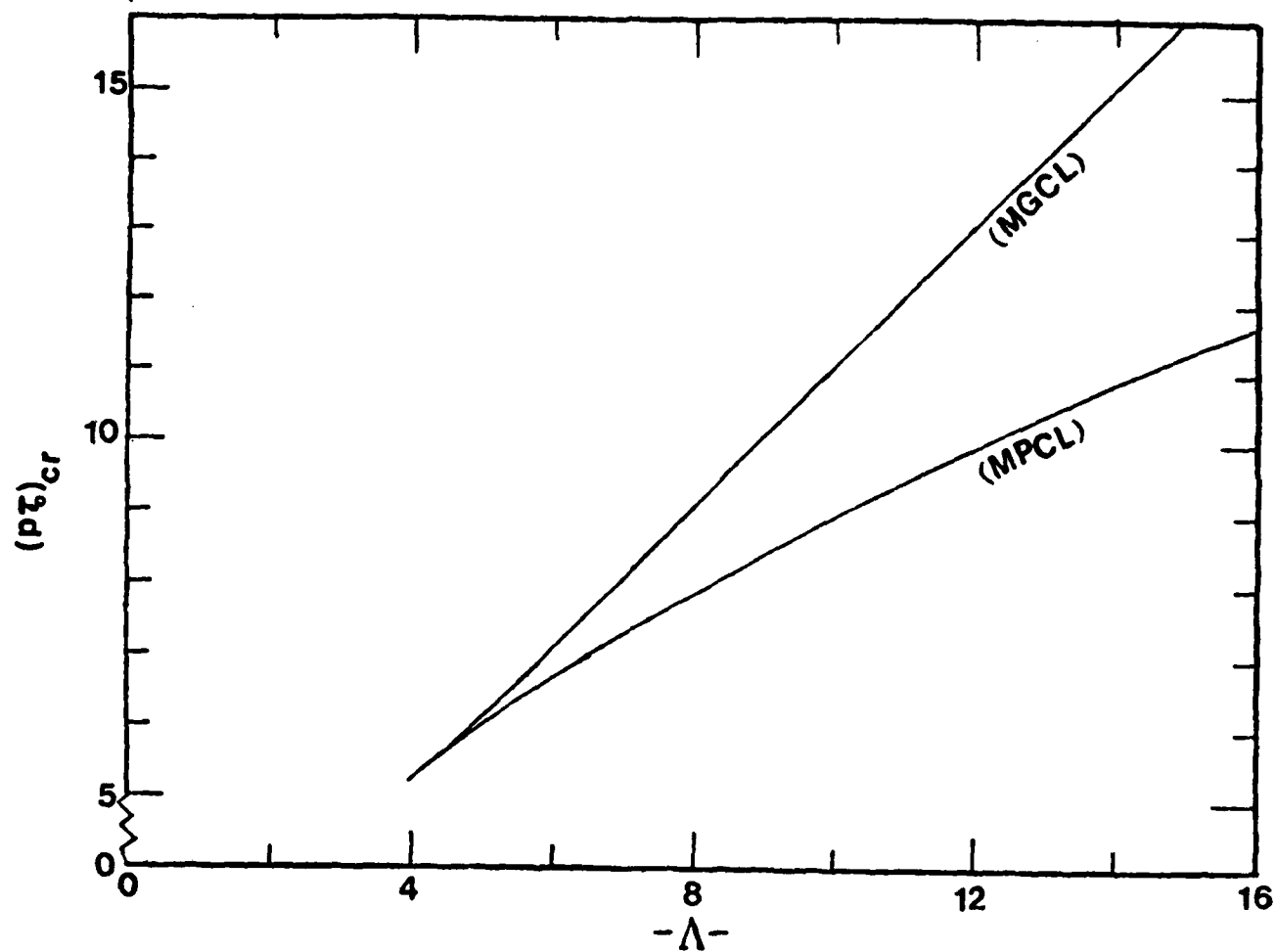


Fig. 3. 3 Upper and Lower Bounds for the Critical Ideal Impulse (Model C).

SECTION IV

CONSTANT LOAD OF INFINITE DURATION

The concept of stability, for this type of loads is also based on the definition of "buckled" and "unbuckled" motion as for the ideal impulse. Moreover, the criterion for stability and the related procedure for estimating critical conditions will be presented through the same three models.

Model A

For this case, the sum of the total potential and kinetic energy is zero

$$\bar{U}_T^P + \bar{T}^P = 0 \quad (4.1)$$

Fig. 4. 1 shows plots of \bar{U}_T^P versus $\theta - \theta_0$ for various values of the applied load, p . It is seen from this figure that for $p < 0.432$ motion is confined between the origin and $\theta - \theta_0 = A$, or the motion is "unbuckled". A critical condition exists when the motion can become unbounded by including position A'' (buckled motion). Thus, the critical load is found by solving the following equations

$$\bar{U}_T^P = 0 \text{ and } p = [\sqrt{1 + \sin \theta} - \sqrt{1 + \sin \theta_0}] \frac{\cot \theta}{\sqrt{1 + \sin \theta}} \quad (4.2)$$

with

$$\frac{d^2 \bar{U}_T^P}{d\theta^2} < 0$$

The inequality condition ensures that $\bar{U}_T^P = 0$ at an unstable equilibrium point. The simultaneous solution of Eqs. (4.2) yields the dynamic critical load and the corresponding position of the unstable static point, A'' on Fig. 4.1.

The results, for this model, are presented graphically on Fig. 4.2.

For this load case, also (MPCL) and (MGCL) are one and the same level.

Model B

For this model, the critical condition is estimated through the simultaneous solution of the following equations

$$\begin{aligned}
 U_T^P &= \frac{1}{2}ka^2 \sin^2 \theta - PL(1 - \cos \theta + \frac{e}{L} \sin \theta) = 0 \\
 ka^2 \sin \theta \cos \theta - PL(\sin \theta + \frac{e}{L} \cos \theta) &= 0 \\
 \text{and } \frac{d^2 U_T^P}{d\theta^2} &< 0 \text{ (at the solution)}
 \end{aligned} \tag{4.3}$$

The results are presented graphically on Fig. 4.3 as p_{cr} versus e/L . For this model, critical conditions are also related to characteristics of the phase plane curves. Fig. 4.4 shows plots of \bar{U}_T versus θ for various values of p , as well as $\dot{\theta}$ versus θ (phase plane).

The energy balance equation, in nondimensionalized form is

$$\dot{\theta}^2 + \sin^2 \theta - p(1 - \cos \theta + \frac{e}{L} \sin \theta) = 0 \tag{4.4}$$

Clearly from Fig. 4.4. if $p < p_{cr\infty}$ the motion is "unbuckled", which implies that for these loads the system simply oscillates about the static stable equilibrium position (A_1 or A_2). The load p is critical, ($p_{cr\infty}$) if the motion can escape through point B_3 ("buckled motion").

Note that for single degree of freedom models $p_{cr\infty}$ corresponds to both the lower and upper bounds (MPCL & MGCL).

Model C

The concept of dynamic stability is similar to the one used for one-

degree-of-freedom models. The only difference is that, in this case, there is a lower bound (MPCL) and an upper bound (MGCL). The lower bound corresponds to loads for which there is a possibility of "buckled" motion, while the upper bound corresponds to loads for which the motion will definitely be "buckled". Because the existence of bounds is dependent upon the value of Λ , the discussion will be based on the range of Λ values.

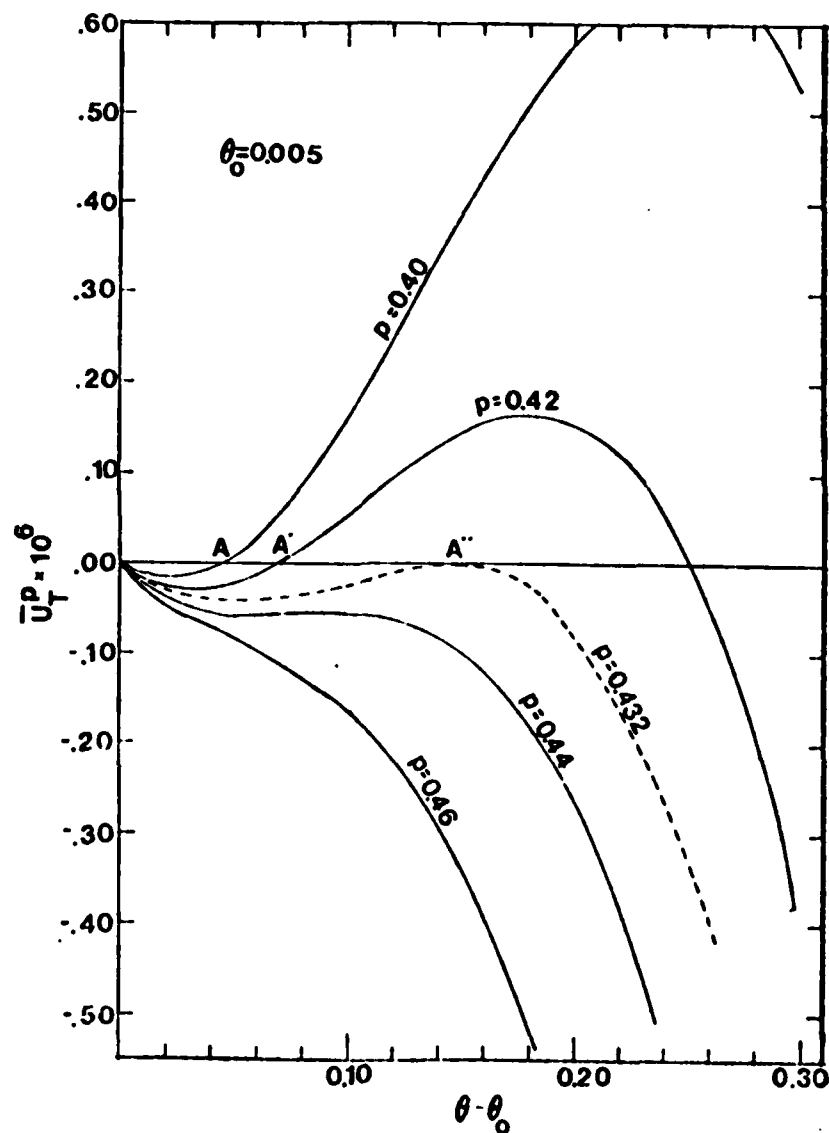


Fig. 4.1. Total Potential versus Displacement for Various Loads (Model A).

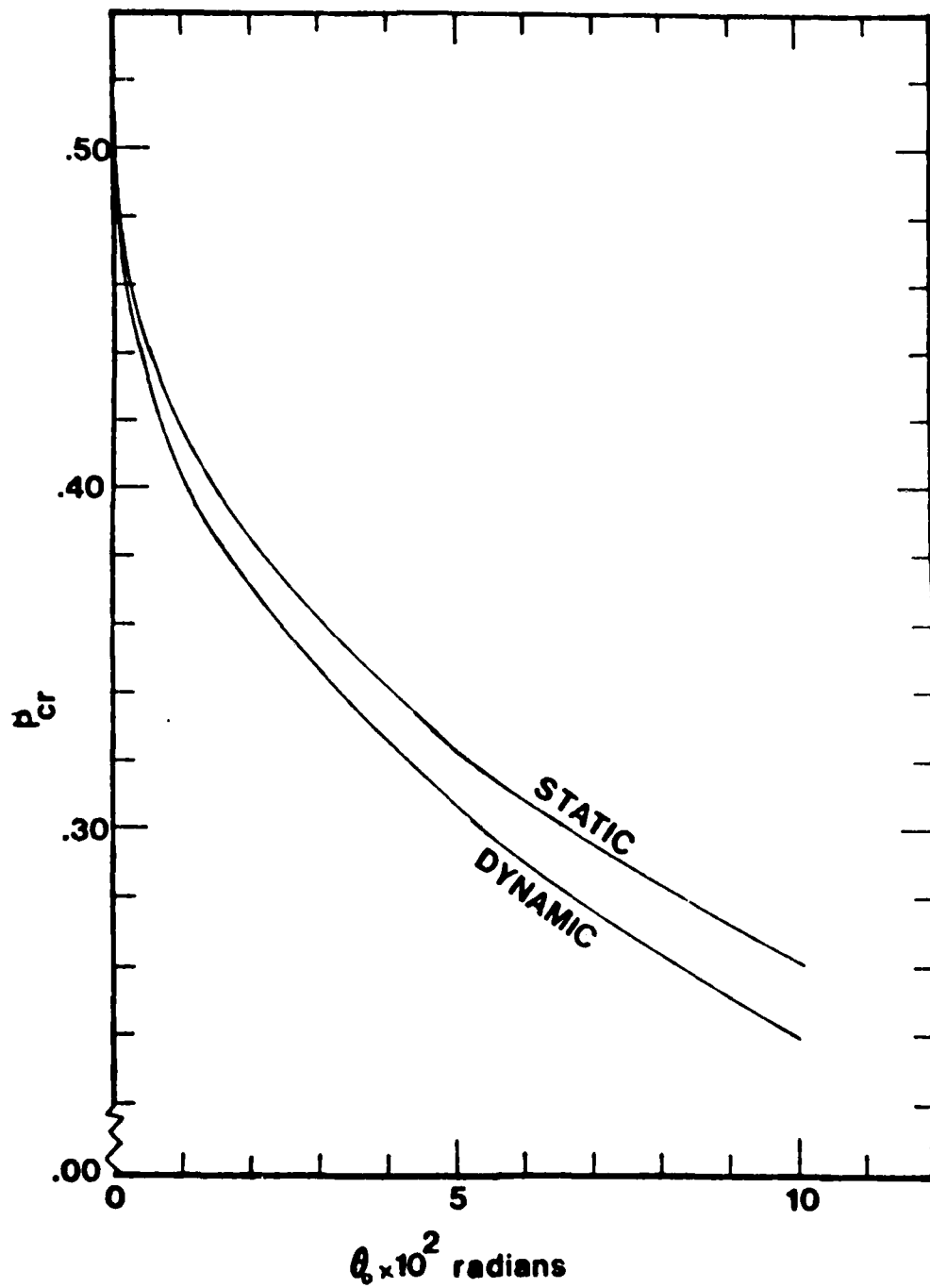


Fig. 4.2. Static and Dynamic Critical Loads (Model A).

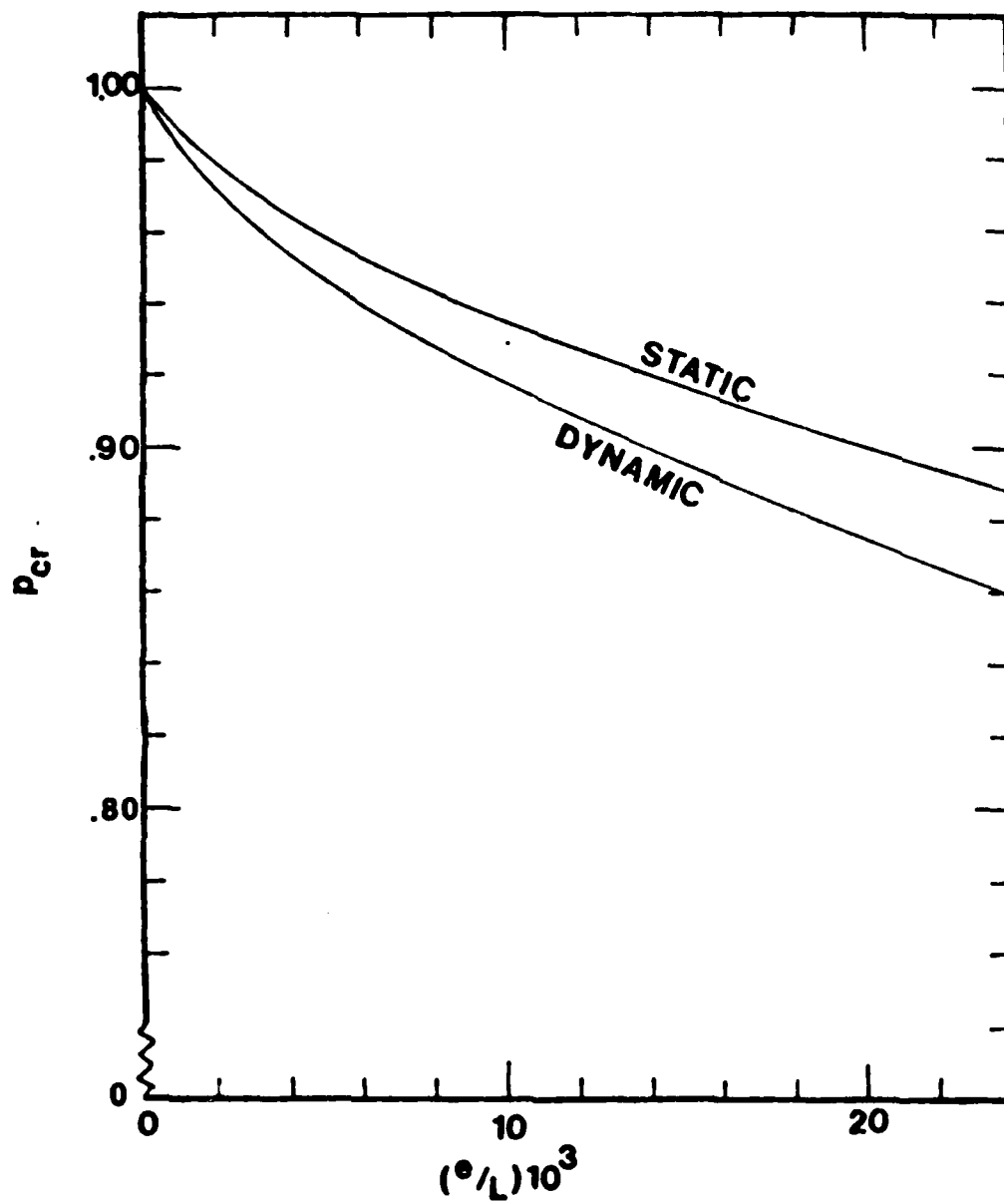


Fig. 4.3. Static and Dynamic Critical Loads (Model B).

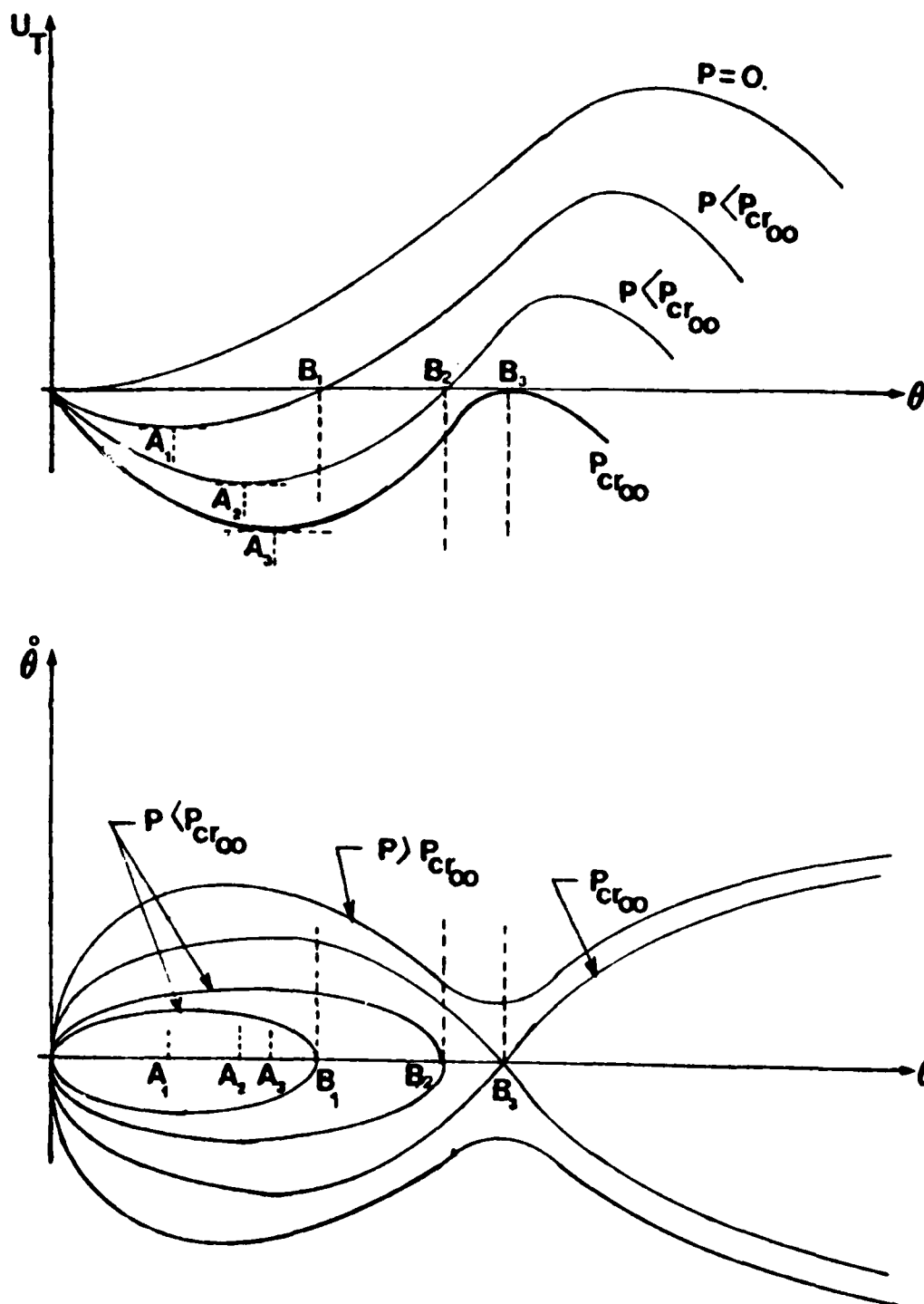


Fig. 4.4. Critical Conditions for Model B Constant Load of Infinite Duration

(a) For $\Lambda < 3$ there are no saddle points and the system behaves as a one-degree-of-freedom system. Therefore, for this case the governing equations are

$$\bar{U}_T^P = 0 \quad ; \quad (\Lambda - 1 - r^2) r = Q;$$

and

$$\frac{d^2 \bar{U}_T^P}{dr^2} < 0 \text{ at the solution} \quad (4.5)$$

Note that, for this case, "buckled" motion is both possible and guaranteed. Thus the upper and lower bounds are coincident.

(b) For $\Lambda > 3$, there exist "saddle" points on the total potential, in addition to the relative maximum point. All three are unstable static equilibrium points (stationary points). Therefore, the motion can become "buckled" either through a saddle point or through the relative maximum point. It will next be shown that, in certain instances, "buckled" motion is possible and in others guaranteed. Before proceeding with the analysis the following observations are made:

Parenthesis 1: For a specified load the total potential has a lower value at a "saddle" point than at a relative maximum point. This can be proven through computation of \bar{U}_T^P at the corresponding points.

Parenthesis 2: Regardless of the value of p and Λ (for $\Lambda > 3$), the total potential at any s position, but a fixed r -position ($r = \bar{r} < \sqrt{\Lambda - 3}$) has a higher potential than that of a position characterized by $r = \bar{r}$ and an s -position on the ellipse

$$r^2 + 3s^2 = \Lambda - 3 \quad (4.6)$$

Note that the ellipse, Eq. 4.6, defines the locus of static equilibrium points ("saddle" points).

Proof: Let $\Delta \bar{U}_T^P$ denote the difference in total potential, between the any s-position and that of an s-position on the ellipse ($r = \bar{r}$). Then, from Eqs. (2.11 and 4.6)

$$\begin{aligned}\Delta \bar{U}_T^P &= [\bar{r}^2 + 9s^2 - 2\sqrt{\Lambda} \bar{r} + \Lambda + \frac{1}{2} (\Lambda - \bar{r}^2 - 3s^2)^2 - 2p(\sqrt{\Lambda} - \bar{r})] \\ &\quad - [4\Lambda - \frac{9}{2} - 2\bar{r}^2 - 2\sqrt{\Lambda} \bar{r} - 2p(\sqrt{\Lambda} - \bar{r})] \\ &= 3(\bar{r}^2 + 3s^2 - \Lambda) + \frac{9}{2} + \frac{1}{2} (\Lambda - \bar{r}^2 - 3s^2)^2 \\ &= \frac{1}{2} (\Lambda - 3 - \bar{r}^2 - 3s^2)^2 \geq 0 \quad \text{Q. E. D.} \quad (4.7)\end{aligned}$$

Clearly, the difference is zero when s is on the ellipse and positive for all other s.

Parenthesis 3: For $p \geq \sqrt{\Lambda} + 2\sqrt{\Lambda - 3}$ [loads higher than the static critical load - see Eq. (2.20)], if $r_1 < r_2 \leq \sqrt{\Lambda - 3}$, then the total potential on the ellipse, Eq. (4.6), is higher at r_2 than at r_1 .

Proof:

$$\text{Let} \quad \Delta \bar{U}_T^P = \bar{U}_T^P(r_2) - \bar{U}_T^P(r_1) \quad (4.8)$$

Then, by Eqs. (2.11) and (4.8)

$$\Delta \bar{U}_T^P = 2(r_2 - r_1) [p - \sqrt{\Lambda} - (\bar{r}_2 + \bar{r}_1)] \quad (4.9)$$

Since $r_2 - r_1$ is positive $\Delta \bar{U}_T^P$ is positive if $p > \sqrt{\Lambda} + (\bar{r}_2 + \bar{r}_1)$.

But $p \geq \sqrt{\Lambda} + 2\sqrt{\Lambda - 3}$, thus

if $\sqrt{\Lambda} + 2\sqrt{\Lambda - 3} > \sqrt{\Lambda} + (r_2 + r_1)$ then

definitely $p > \sqrt{\Lambda} + (r_2 + r_1)$.

Clearly, from the statement of the parenthesis $2\sqrt{\Lambda - 3} > r_2 + r_1$, which

concludes the proof.

As the load is increased from zero, at low values of p , the zero potential lines in the rs -space enclose only the near static equilibrium point and the motion is "unbuckled". At some value of the load the first unstable point(s), at which the total potential can become zero, is (are) the "saddle" point(s) according to Parenthesis 1. At this load there is a possibility of "buckled" motion through the saddle point. This load, then, is called MPCL. The governing equations for finding this critical load, as well as the corresponding position (sr coordinates) of the saddle point are:

$$\bar{U}_T^P = (r^2 + 9s^2 - 2\sqrt{\Lambda}r + \Lambda) + \frac{1}{2} (\Lambda - r^2 - 3s^2)^2 - 2p(\sqrt{\Lambda} - r) = 0$$

$$(\Lambda - 1 - r^2 - 3s^2)r = p - \sqrt{\Lambda}$$

$$\Lambda - 3 - r^2 - 3s^2 = 0 \quad (4.10)$$

Note that "saddle" points are unstable, thus, there is no need for applying the stability requirements.

The solution to Eqs. (4.6) yields

$$(\text{MPCL}): P_{\text{cr}\infty} = 3(\sqrt{\Lambda} - 1)$$

$$\text{and "saddle" point at } r = \sqrt{\Lambda} - \frac{3}{2}; s = \pm (\sqrt{\Lambda} - \frac{7}{4})^{\frac{1}{2}}. \quad (4.11)$$

The solutions to Eqs. (4.5) and (4.10) are plotted on Fig. (4.5).

As far as the case of the upper bound is concerned (MGCL), there are two ways through which a guaranteed "buckled" motion can be achieved. One way is to require \bar{U}_T^P at the relative maximum unstable static point to be zero.

In this case the motion is definitely buckled and the critical load can be obtained from the solution of Eqs. (4.5). The second way is for loads which are equal to static critical load for asymmetric buckling ($\sqrt{\Lambda} + \sqrt{\Lambda - 3}$). In this case, although the total potential at the relative maximum point is higher than zero, guaranteed "buckled" motion can be achieved because of Parentheses 2 and 3. In this latter case, P_{cr} (MGCL) is given by the expression for the static load. Both results are shown graphically on Fig. 4.5.

Note, that the upper bound is the smallest load computed, either by the solutions of Eqs. (4.5) (for $\sqrt{\frac{7}{4}} \leq \Lambda \leq 7.3$), or by the static critical load (for $\Lambda \geq 7.3$). Moreover, for very large Λ -values the upper and lower bounds approach each other ($3\sqrt{\Lambda}$).

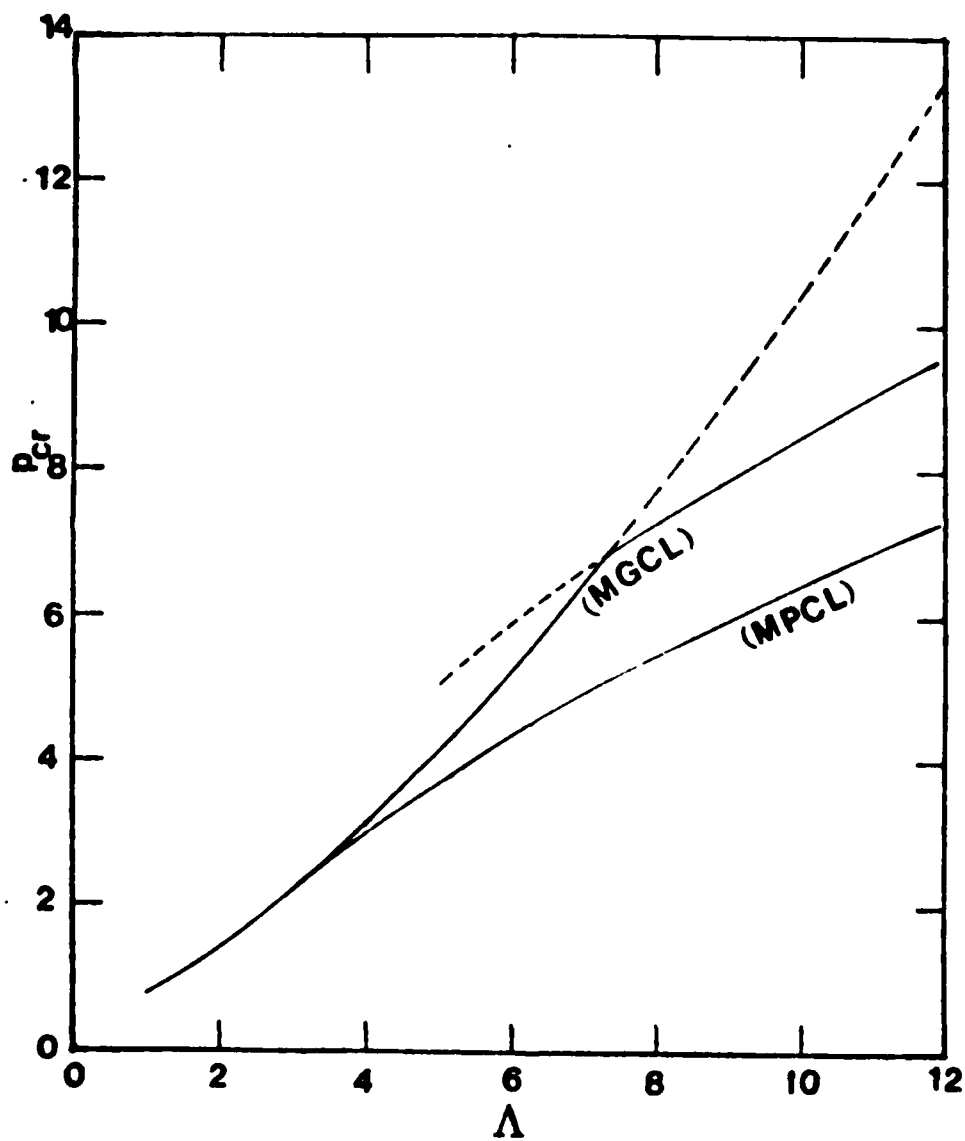


Fig. 4.5. Upper and Lower Bounds for the Critical Load (Infinite Duration).
(Model C).

SECTION V

CONSTANT LOAD OF FINITE DURATION

Statement of the Problem

Consider a model at its natural (unloaded) position. At time $t = 0$ a constant load P is applied suddenly on the system and it acts only for a finite duration time $t = T_0$. After the release of the force P , the system moves because of the imparted energy during the action of the load P_0 . The concept of dynamic stability for this particular load case is similar to the concept used in the cases of "ideal impulse" (Section III) and of "constant load of infinite duration" (Section IV). Thus, for all three cases the concept of dynamic stability is based on the definition of "buckled" and "unbuckled" motion.

If the energy imparted into the system, through the load P , is insufficient for the system to reach the unstable static equilibrium point on the "zero load" total potential, with zero velocity (zero kinetic energy) the motion is called "unbuckled". In this case, the system is dynamically stable. Consequently, the criterion for dynamic stability requires that the dynamically stable system possess total energy (at the release time, T_0) at a level below the level of the potential at its unstable static equilibrium point for the "zero-load" system. This is fully substantiated by mathematical arguments in the next section. On each individual model, the criterion is invoked and estimates for critical conditions are found. The extreme cases of $T_0 \rightarrow \infty$ (constant load of infinite duration) and $T_0 \rightarrow 0$ (ideal impulse) are special cases of the present one.

General Procedure

Since the system is conservative during the action of the load, then

$$U_T^P + T^P = 0 \quad \text{for } 0 \leq t \leq T_0 \quad (5.1)$$

where T_0 is the time of release of the load P . Similarly,

$$U_T^O + T^O = U_T^O(T_0) + T^O(T_0) \quad \text{for } t > T_0 \quad (5.2)$$

The continuity of the kinetic energy at the time of release, T_0 , is expressed by

$$T^O(T_0) = T^P(T_0) \quad (5.3)$$

Use of Eqs. (5.1) and (5.3) into Eq. (5.2) yields

$$U_T^O + T^O = U_T^O(T_0) - U_T^P(T_0) \quad \text{for } t \geq T_0 \quad (5.4)$$

If L_u^O indicates the position of the unstable static equilibrium point for $P = 0$, the critical condition is met (buckled motion is possible), if the load P , acting for time T_0 , imparts sufficient energy into the system to equal the potential $U_T^O(L_u^O)$ of the "zero-load" system at the unstable position L_u^O . Thus, the stability criterion is expressed by

$$U_T^O(T_0) - U_T^P(T_0) \leq U_T^O(L_u^O) \quad (5.5)$$

The equality sign implies a critical condition, while the inequality refers to a dynamically stable situation.

Note that Eq. (5.5) relates the applied load P and the release position, L_p (one equation in two unknown quantities, if one views the release position L_p at time T_0 , as one quantity). In addition, through equation (5.1), one may relate the applied load, P , the release position, L_p , and the release time, T_0 , for a specified path of motion. For one-degree-of-freedom systems there is only one path, but for two-degree-of-freedom systems there are several paths;

for such cases, the path is determined through the brachistochrone problem of the system. This is so, because one may view the problem as follows: Find the smallest time T_0 for a given load P such that the motion can become "buckled".

A critical condition is obtained by specifying the load and finding, through the simultaneous solution of the above two mentioned equations, the corresponding release time, T_{0cr} .

These steps are next clearly demonstrated for each one of the three models.

Model A

For this particular model, the unstable stationary points on the "zero-load" total potential are located at $\theta = \pm \pi/2$ [see Eq. (2.2)]. Then, Eq. (5.5), with the equality sign), becomes

$$p (\cos \theta_0 - \cos \theta_{cr}) = [\sqrt{2} - \sqrt{1 + \sin \theta_0}]^2 \quad (5.6)$$

where θ_{cr} is the release position, L_p , of the system. Note that $\theta_{cr} = 0(T_{0cr})$.

This equation, Eq. (5.6), is one of the two needed equations for finding a critical condition. Before finding the second equation, from Eq. (5.1), the following simplifications are introduced.

First, it is assumed that the bars of the system are weightless and the mass, m , of the system is concentrated at joint B (see Fig. 2.1). With this, the kinetic energy of the system is given by

$$T = \frac{1}{2} mL^2 \left(\frac{d\theta}{dt} \right)^2 \quad (5.7)$$

Next, the following nondimensionalized time parameter, τ , is introduced.

$$\tau = t \left(\frac{2k}{m} \right)^{\frac{1}{2}} \quad (5.8)$$

Finally, the kinetic energy, T , is nondimensionalized in a manner similar

to the total potential

$$\bar{T} = T/kL^2 \quad (5.9)$$

Then Eq. (5.1) becomes

$$\bar{U}_T^P + \bar{T}^P = \bar{U}_T^P + \left(\frac{d\theta}{d\tau}\right)^2 = 0 \quad (5.10)$$

The critical condition is obtained from Eqs. (5.6) and (5.10). The approach one may use is as follows: first specify the value of p (these values must be larger than the critical load corresponding to the infinite duration case) and through Eq. (5.6) solve for θ_{cr} ; then use Eq. (5.10) to find the corresponding duration time τ_o , or

$$\tau_{o_{cr}} = \int_{\theta_o}^{\theta_{cr}} \frac{d\theta}{\sqrt{-\bar{U}_T^P}} \quad (5.11)$$

where \bar{U}_T^P is given by Eq. (2.2).

Note that computationally it is much simpler to assign values of θ_{cr} (starting with $\theta_o + \theta_1$, where θ_1 is a small increment and increase it to values approaching the angle corresponding to the infinite duration case) and solve for p and $\tau_{o_{cr}}$ from Eqs. (5.6) and (5.11) respectively.

A computer program is written and data are obtained through the Georgia Tech high speed digital computer CYBER 70, Model 74-28. These data are presented graphically on Figs. 5.1 and 5.2. Fig. 5.1 shows critical condition, for various imperfection angles, θ_o , in terms of p and $\tau_{o_{cr}}$. Note that as the critical release time, $\tau_{o_{cr}}$, is increased, the corresponding load approaches the value of p_{cr} for the infinite duration case. The same data are presented on Fig. 5.2 as plots of $(p\tau_o)_{cr}$ versus $\tau_{o_{cr}}$. Through this figure, it is shown that as $\tau_{o_{cr}} \rightarrow 0$ the values of $(p\tau_o)_{cr}$ approach the critical impulse values,

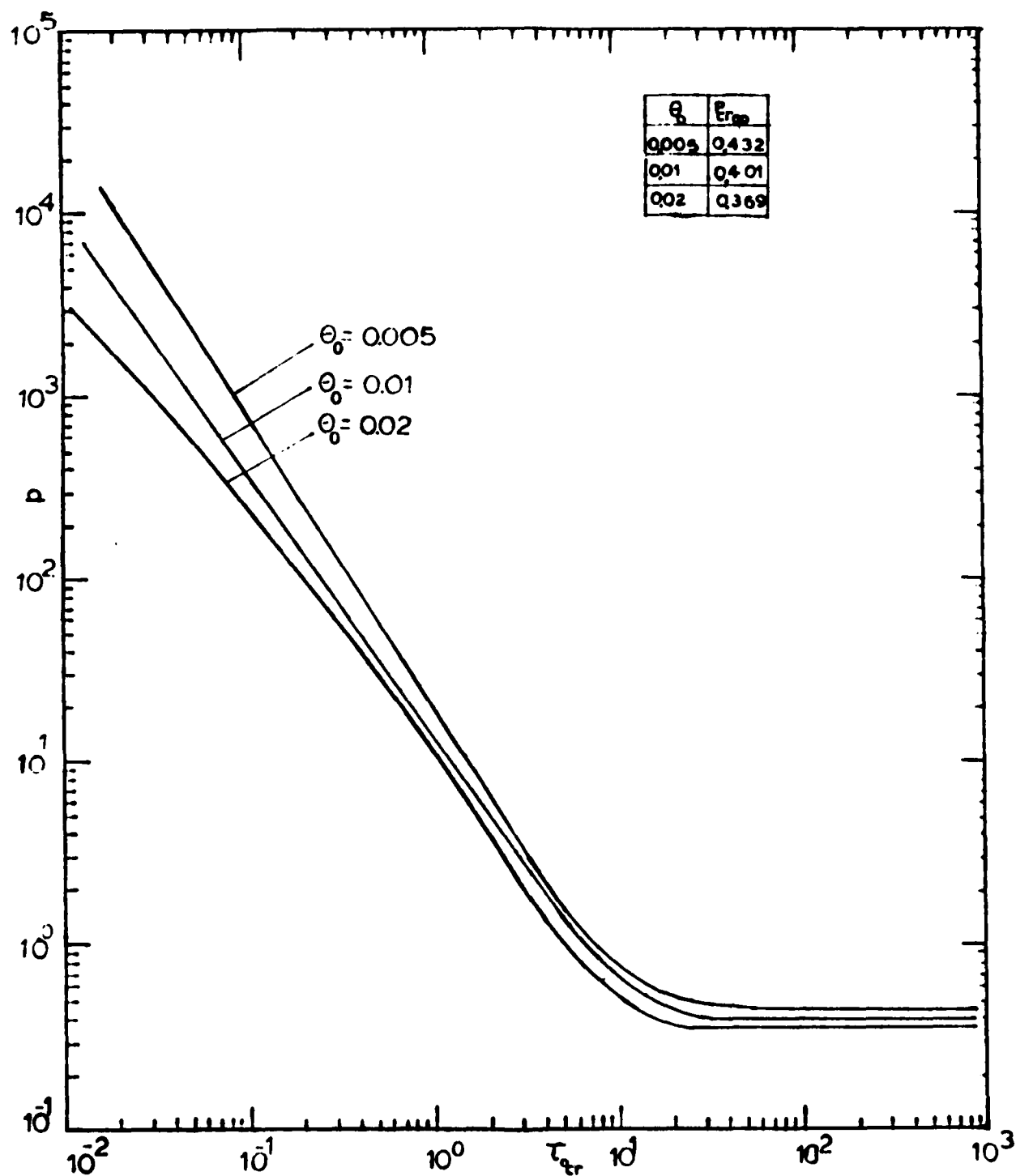


Fig. 5.1. Constant load, p , versus critical duration time, τ_{cr} , (Model A).

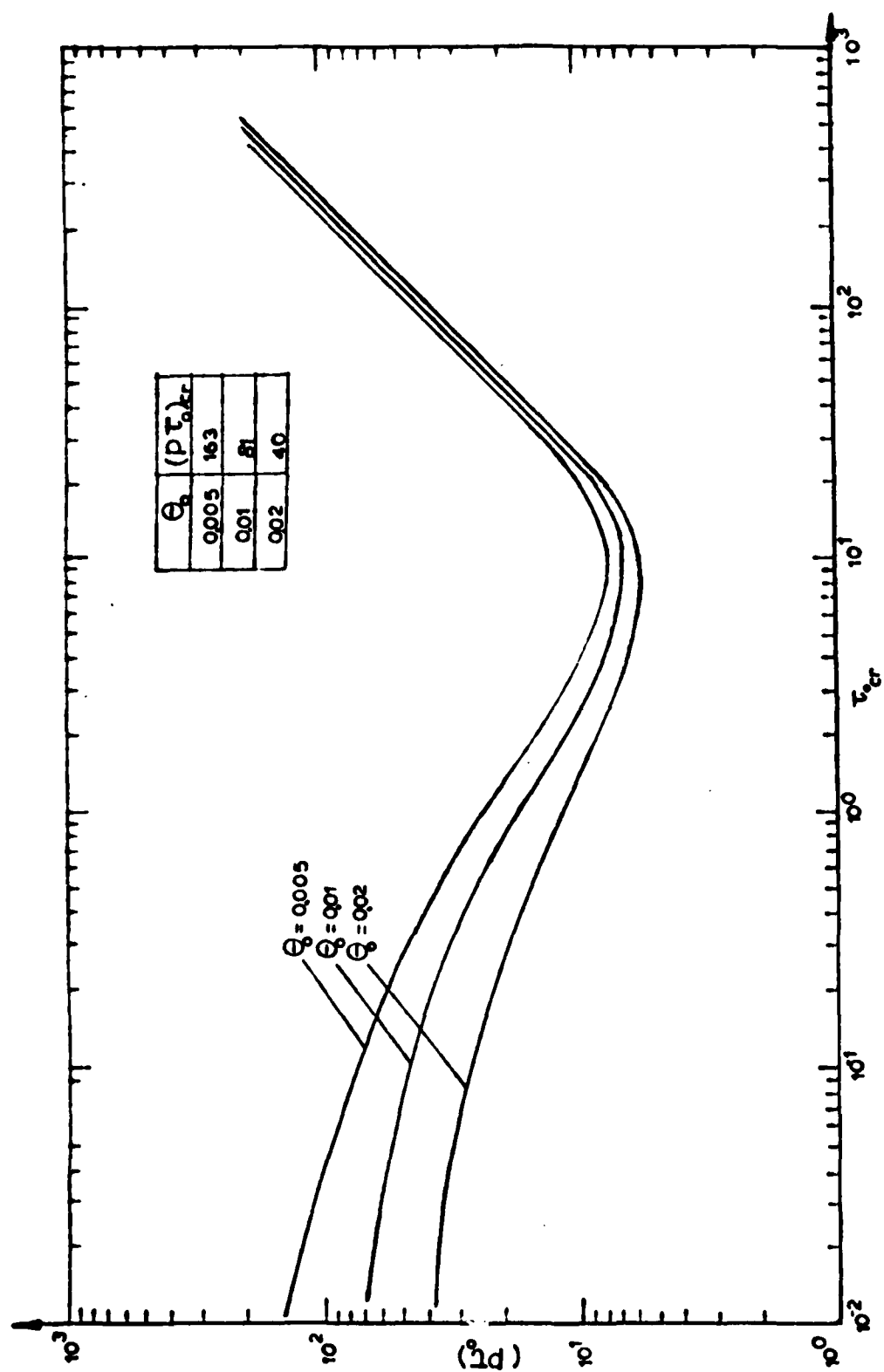


Fig. 5.2. Impulse, $(p\tau_o)$, versus critical Duration Time, τ_{ocr} , (Model A).

as obtained in Section III.

Model B

For this particular model the unstable stationary points on the "zero-load" total potential are also located at $\theta = \pm \pi/2$ [see Eq. (2.5)]. Then, Eq. (5.5) becomes

$$2p(1 - \cos \theta_{cr} + \bar{e} \sin \theta_{cr}) = 1 \quad (5.12)$$

where $\bar{e} = e/L$, $p = PL/ka^2$ and θ_{cr} is the position of the system at the critical time of release, τ_{ocr} .

According to the nondimensionalization employed for this model in Section III, the kinetic energy and time parameters are

$$\bar{T} = \dot{\theta}^2, \quad \tau = (ka^2/I)^{1/2} t \quad (5.13)$$

where

$$\dot{\theta} = d\theta/d\tau.$$

For this model then, Eq. (5.1) becomes

$$\bar{U}_T^p + \dot{\theta}^2 = 0 \quad (5.14)$$

From Eq. (5.14) one may solve for the critical duration time, τ_{ocr} , or

$$\tau_{ocr} = \int_0^{\theta_{cr}} \frac{d\theta}{\sqrt{-\bar{U}_T^p}} \quad (5.15)$$

where the expression for \bar{U}_T^p is given by Eq. (2.5). For this model as well as for model A, a computer program is written and data are generated for finding critical conditions (p and corresponding τ_{ocr}). Computationally, values of θ_{cr} are assigned and the value of p is found from Eq. (5.12). Then, the critical release time τ_{ocr} is evaluated from Eq. (5.15). The generated data are presented graphically on Figs. 5.3 and 5.4. Note that, as the duration

time becomes large, the corresponding load approaches the critical value for the case of constant load of infinite duration, $P_{cr\infty}$ (see Fig. 5.3). Similarly, as the duration time approaches zero the corresponding $(p\tau_o)_{cr}$ approaches the value of the critical impulse (see Fig. 5.4). This value is equal to $1/\bar{e}$ and it can also be derived analytically from Eqs. (5.12) and (5.15). If the expression for \bar{U}_T^p is used in Eq. (5.15), one obtains

$$\tau_{o_{cr}} = \int_0^{\theta_{cr}} \frac{d\theta}{\sqrt{\frac{1 - \cos\theta + \bar{e} \sin\theta}{1 - \cos\theta_{cr} + \bar{e} \sin\theta_{cr}} - \sin^2\theta}} \quad (5.16)$$

Next it is observed that as the critical duration (release) time becomes very small the corresponding release position, θ_{cr} , also becomes very small, for every fixed value of \bar{e} . Then, for very small θ_{cr} values; and consequently θ -values, Eq. (5.16) can be written as

$$\begin{aligned} \tau_{o_{cr}} &= \int_0^{\theta_{cr}} \left(\frac{\theta}{\theta_{cr}}\right)^{-\frac{1}{2}} d\theta = \theta_{cr} \int_0^{\theta_{cr}} \left(\frac{\theta}{\theta_{cr}}\right)^{-\frac{1}{2}} \frac{d\theta}{\theta_{cr}} \\ &= 2\theta_{cr} \left(\frac{\theta}{\theta_{cr}}\right)^{\frac{1}{2}} \Big|_0^{\theta_{cr}} = 2\theta_{cr} \end{aligned} \quad (5.17)$$

Similarly, from Eq. (5.12)

$$p = \frac{1}{2\bar{e}\theta_{cr}} \quad (5.18)$$

Thus,

$$(p\tau_o)_{cr} = 1/\bar{e}.$$

Model C

The expression for the "zero load" total potential is given by

$$\bar{U}_T^0 = \left(\frac{2}{r} + 9s^2 - 2\sqrt{\Lambda} r + \Lambda\right) + \frac{1}{2} (\Lambda - r^2 - 3s^2)^2 \quad (5.19)$$

Starting with \bar{U}_T^0 , requiring equilibrium and performing a static stability

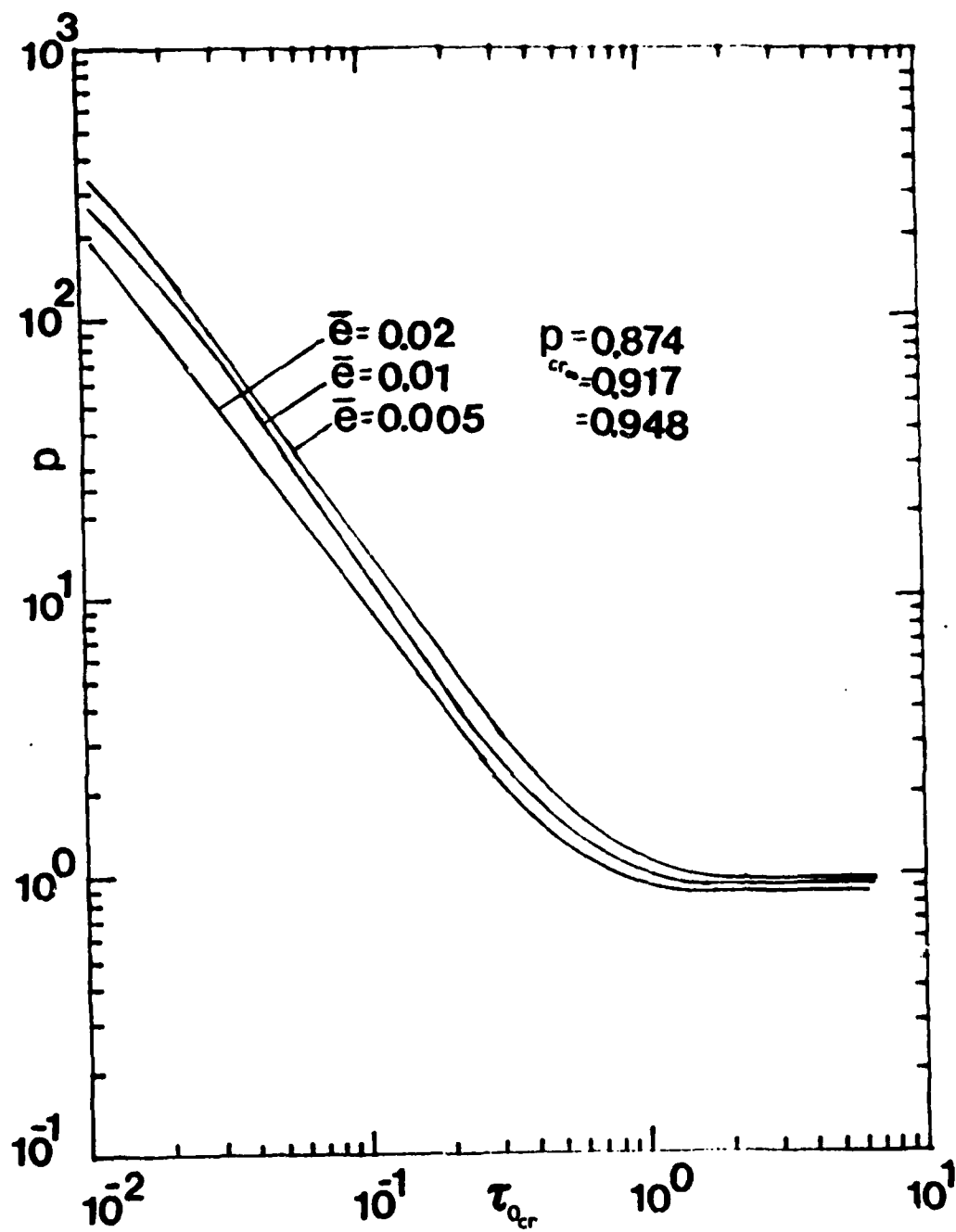


Fig. 5.3. Constant load, p_{cr} , versus Critical Duration Time, $\tau_{0_{cr}}$, (Model P).

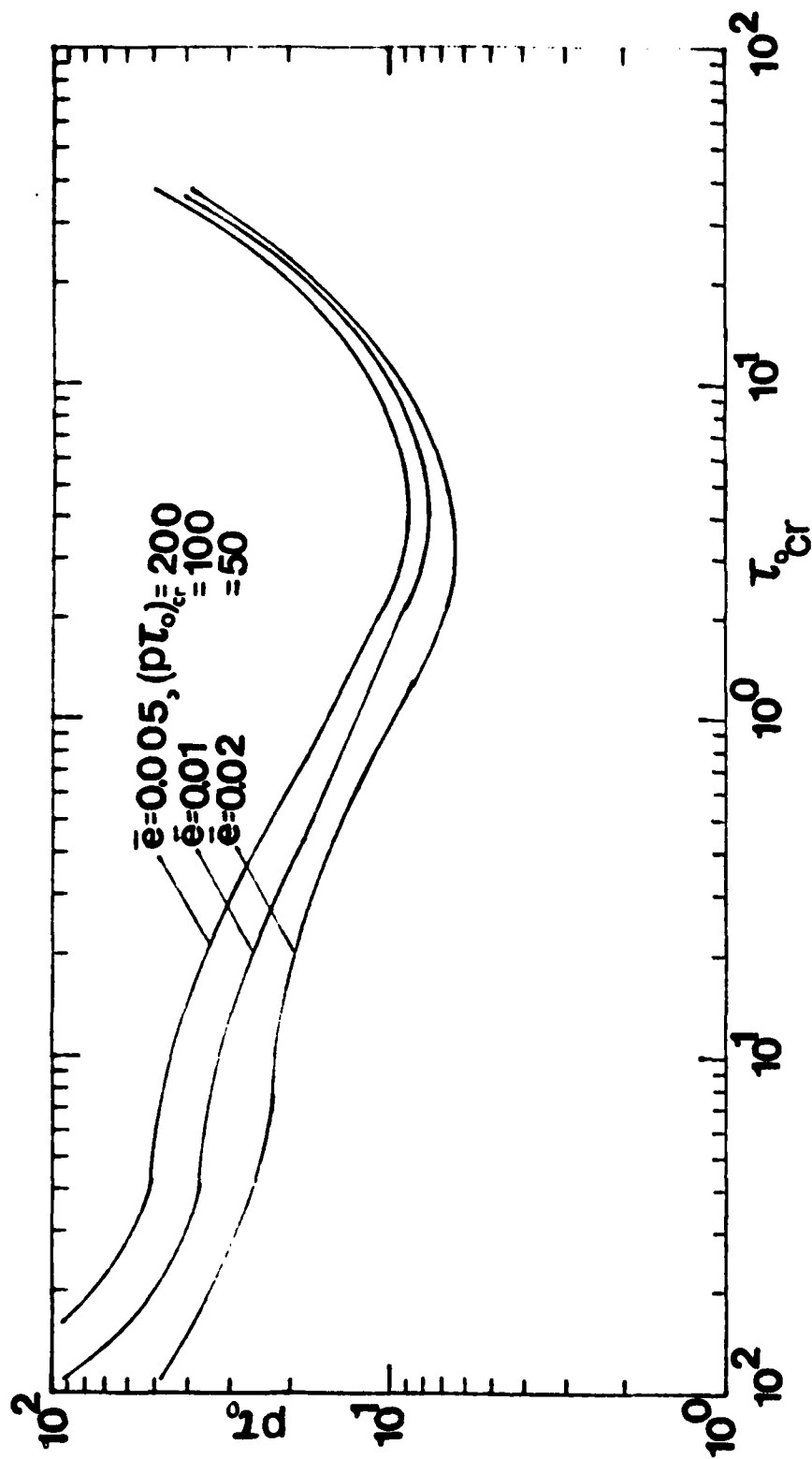


Fig. 5.4. Impulse, (pr_0) , versus critical Duration Time, τ_{0cr} , (Model B).

analysis the following stationary points are obtained (see Section III).

Pt. 1 at $(\sqrt{\Lambda}, 0)$	Stable (Relative min)
Pt. 2 at $\left[(\sqrt{\Lambda} - \sqrt{\Lambda-4})/2, 0 \right]$	Unstable (Relative max)
Pt. 3 at $\left[(\sqrt{\Lambda} + \sqrt{\Lambda-4})/2, 0 \right]$	Stable (Relative min)
Pt. 4 at $\left[-\sqrt{\Lambda}/2, \sqrt{\Lambda-4}/2 \right]$	Unstable (Saddle point)
Pt. 5 at $\left[-\sqrt{\Lambda}/2, -\sqrt{\Lambda-4}/2 \right]$	Unstable (Saddle point)

For simplicity, it is assumed that the three bars are weightless and the only massive parts of the system are two masses, m , concentrated at the joints B and C. Moreover, the nondimensionalized kinetic energy is expressed by $\bar{T} = \frac{T}{\bar{\theta}^2 k L^2}$, where T characterizes the kinetic energy and

$$\bar{T} = \frac{1}{2} \left[\left(\frac{dr}{d\tau} \right)^2 + \left(\frac{ds}{d\tau} \right)^2 \right] = \frac{1}{2} [1 + s'^2] \left(\frac{dr}{d\tau} \right)^2 \quad (5.20)$$

where

$$(\cdot) = \frac{\partial}{\partial \tau} \text{ and } \tau = t \left(\frac{\bar{\theta} k}{2m} \right)^{1/2}$$

Clearly, saddle points exist for $\Lambda > 4$. For this range of Λ -values, the "zero load" total potential value at the saddle points, pts. 4 & 5, is smaller than the corresponding value at the relative maximum, pt. 2. On the basis of this observation the motion can possibly become "buckled" through the "saddle" points, pts. 4 & 5. The corresponding condition for this case is a "possible critical condition". On the other hand if the imparted energy, by the applied force at the release time, is sufficient to reach the relative maximum (unstable) static equilibrium point, pt. 2, "buckled" motion is guaranteed and the corresponding critical condition is a guaranteed one. The former is termed sufficient condition for dynamic stability, while the latter sufficient condition for dynamic instability by Hsu [17].

Next, the computational procedure for finding the possible critical condition is outlined.

Through Eq.(5.5)(in a nondimensionalized form) one obtains

$$2\bar{p}(\sqrt{\Lambda}-r)|_{\tau=\tau_0} = \frac{9}{2}(\Lambda-1) \quad (5.21)$$

where τ_0 is the release time.

Moreover, Eq. (5.1) in nondimensionalized form holds for $(0 < \tau \leq \tau_0)$.

For a given path of motion, integration of Eq. (5.1), yields a relation between the time of release and the position at that instant. Note, that the problem has been cast in the following terms: for a given load, p , find the smallest release time, τ_{ocr} , such that the system may reach an unstable point (saddle point for the minimum possible critical condition) with zero velocity, Eq. (5.24). Since one is interested in obtaining the smallest release time, τ_{ocr} , and since the position at the time of release is path dependent, one can solve the problem by considering the associated brachistochrone problem. The brachistochrone problem makes use of Eq. (5.1) for this system, and through its solution one obtains the relation between the smallest release time, τ_{ocr} , the position at the instant of release, as well as the path that yields τ_{ocr} . The details of the solution to this brachistochrone problem are presented in Appendix A. The solution to the brachistochrone problem yields that the path is characterized by $s=0$ and the relation between τ_{ocr} and the position of the system, r_{cr} , at τ_{ocr} is

$$\tau_{ocr} = \int_{\sqrt{\Lambda}}^{r_{cr}} \frac{dr}{\sqrt{4\bar{p}(\sqrt{\Lambda}-r)-2(r-\sqrt{\Lambda})^2-(\Lambda-r^2)^2}} \quad (5.22)$$

Computationally, it is simpler for one to assign values of r_{cr} (starting with values close to the initial position, $r = \sqrt{\Lambda}$ and $s = 0$), solve for \bar{p} through Eq. (5.21) and then for τ_{ocr} through Eq. (5.22).

Note that for the case of the minimum guaranteed critical condition Eq. (5.21) is replaced by a comparable equation which employs the value of the "zero load" total potential at the relative maximum unstable static point.

Numerical results are presented graphically on Figs. 5.5 and 5.6, for the minimum possible critical condition only, and various values of Λ . The curves of Fig. 5.5 depict critical conditions in terms of applied load, \bar{p} , versus critical release time, τ_{ocr} . One may observe that as the τ_{ocr} increases, the corresponding load approaches, asymptotically, the value of \bar{p}_{cr} for the infinite duration time. Fig. 5.6 presents the same results as Fig. 5.5, but in terms of $(pr_o)_{cr}$ versus critical release time τ_{ocr} . Note that as τ_{ocr} approaches zero, the value of $(pr_o)_{cr}$ approaches that of the critical ideal impulse.

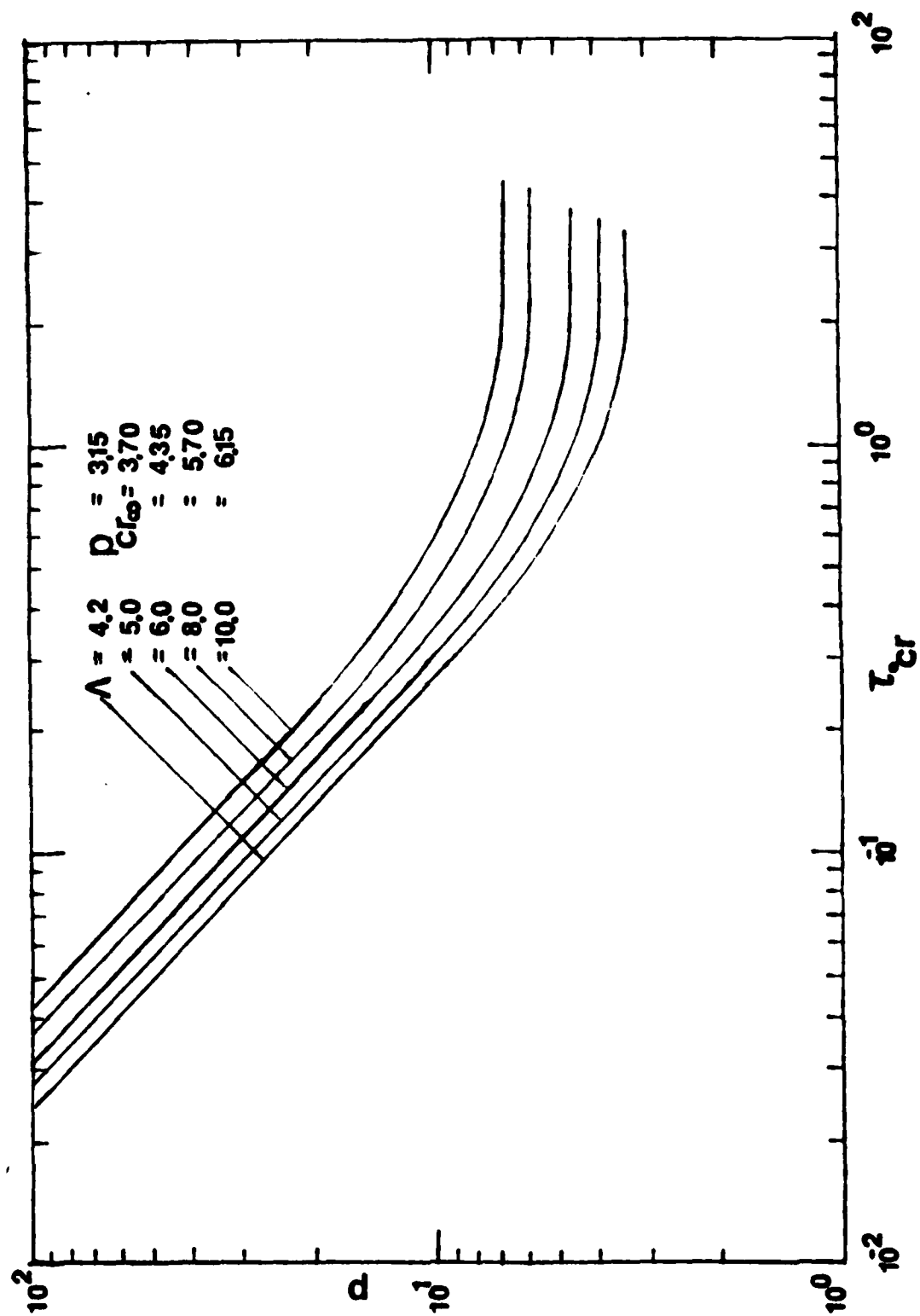


Fig. 5.5. Load, P , versus critical Duration Time, τ_{0cr} , Model C

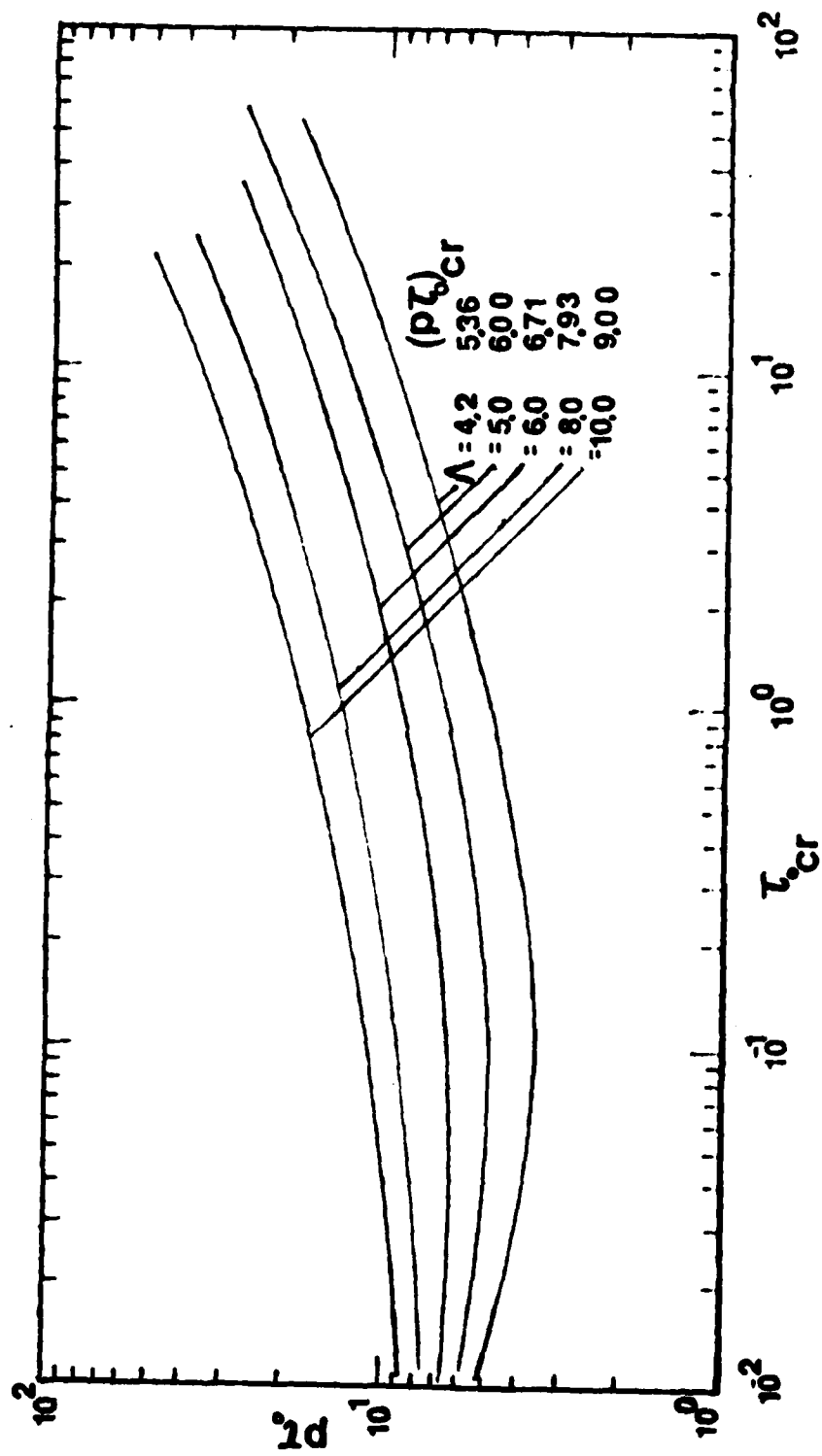


Fig. 5.6. Impulse, $(p\tau_0)$, versus critical Duration Time, τ_{0cr} , (Model C).

SECTION VI

THE INFLUENCE OF PRELOADING-CONSTANT LOAD OF FINITE DURATION

Statement of the Problem

Consider a model at its stable equilibrium position $L_S^{P_0}$, when subjected to an initial static load P_0 . At time $t = 0$ an additional constant load P is suddenly applied to the system and acts only for finite duration time $t = T_0$. After the release of the force P , the system moves because of the acquired total energy during the action of the load P . The system will be called dynamically stable if its motion is "unbuckled", in the sense described in previous sections. Since the systems under consideration exhibit either limit or unstable bifurcation point instability, the system is stable if the energy, imparted through the action of the load P , is insufficient for the system to reach the unstable static equilibrium point for " P_0 -load" total potential of the system with zero velocity (zero kinetic energy). For each individual model, the criterion is invoked and estimates for critical conditions are found. The extreme cases of $T_0 \rightarrow \infty$ (constant load of infinite duration) and $T_0 \rightarrow 0$ (Ideal Impulse) are treated as special cases.

General Procedure

The concept of Dynamic Stability and the general procedure as well are extensions of those used in the cases of the constant load of finite duration. The equilibrium positions of the preloaded system are given as solutions to

$$\frac{\partial U_T^{P_0}(L)}{\partial L} = 0 \quad (6.1)$$

where L is the position of the system. Thus, one may find all the " P_0 -load" static equilibrium positions including the near stable position $L_S^{P_0}$ as well as the unstable position $L_u^{P_0}$, through which "buckled" motion can be realized (see Fig. 6.1).

Keeping the same generalized coordinates for all models and the same expressions for the total potential and for the kinetic energy, one may apply the concepts already developed. These are next explained through the use of Fig. 6.1, which holds for one-degree-of-freedom systems, but the explanation is applicable to all finite-degree-of-freedom systems.

The system is initially loaded quasi-statically by load p_0 and it reaches point A ($L = L_S^{P_0}$; stable static equilibrium point). Then, a load p is applied suddenly for a time τ_0 (finite duration). At τ_0 the load p is removed.

A potential \bar{U}_T^P is defined, such that $\bar{U}_T^P = \bar{U}_T^{P_0}$ at $\tau = 0$ or $L = L_S^{P_0}$ (see Fig. 6.1).

$$\bar{U}_T^P = \bar{U}_T^{P_0+P} + \left[\bar{U}_T^{P_0} \left(L_S^{P_0} \right) - \bar{U}_T^{P_0+P} \left(L_S^{P_0} \right) \right] \quad (6.2)$$

Since the system is conservative, then during the action of p one may write

$$\bar{U}_T^P + \bar{T}^{P_0+P} = \bar{U}_T^{P_0} \left(L_S^{P_0} \right) ; 0 \leq \tau \leq \tau_0 \quad (6.3)$$

where \bar{T}^{P_0+P} is the kinetic energy of the system. This equation, Eq. (6.3), is equivalent to Eq. (5.1) of Section V. Making use of Eq. (6.2), Eq. (6.3) becomes

$$\bar{U}_T^{P_0+P} + \bar{T}^{P_0+P} = \bar{U}_T^{P_0+P} \left(L_S^{P_0} \right) ; 0 \leq \tau \leq \tau_0 \quad (6.4)$$

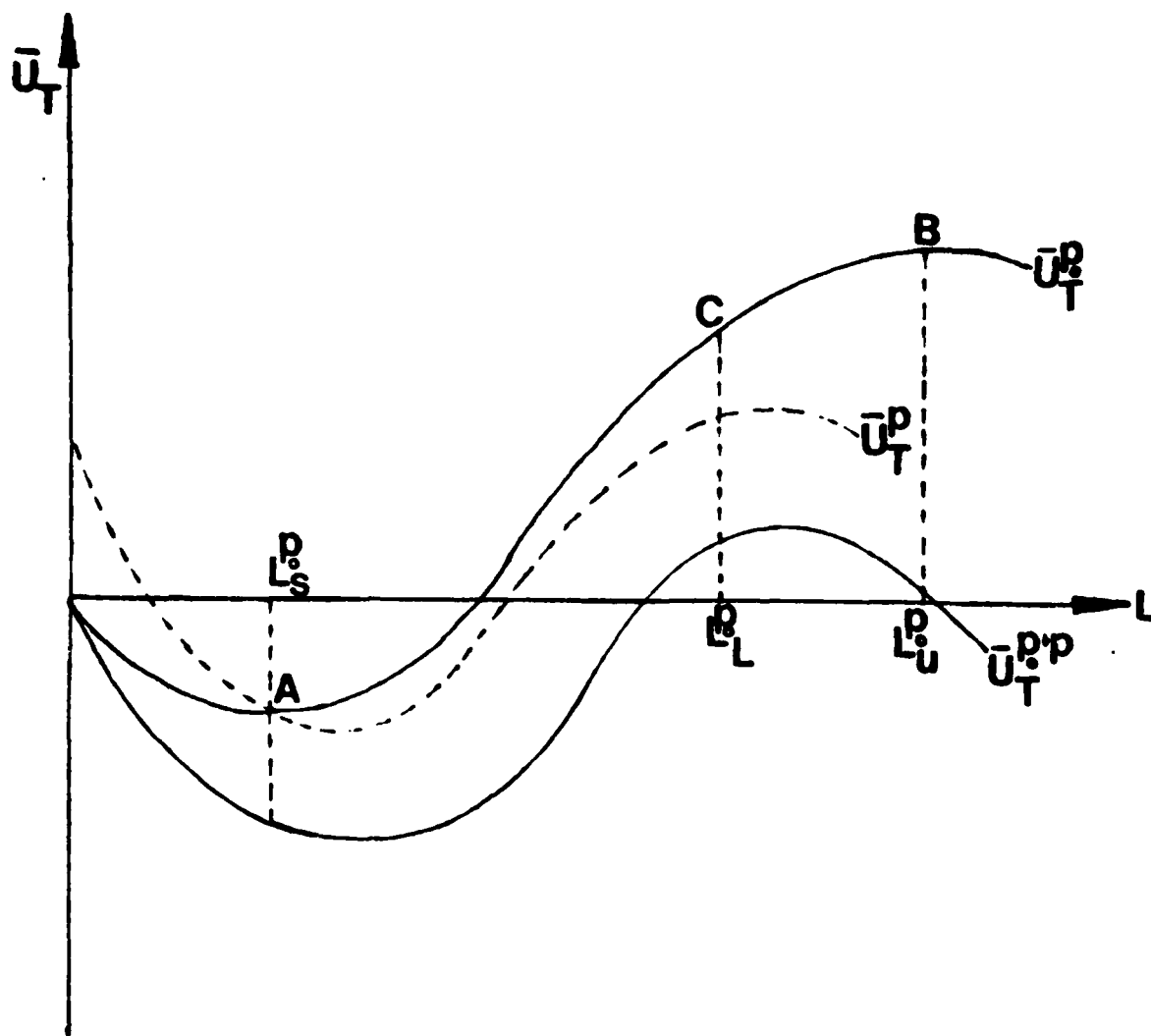


Fig. 6.1. Definitions of Total Potentials (One-degree-of-freedom system)

For times greater than τ_0 , the system is also conservative and conservation of energy yields

$$\bar{U}_T^P + \bar{T}^P = \bar{U}_T^{P_0}(\tau_0) + \bar{T}^{P_0}(\tau_0) ; \tau > \tau_0 \quad (6.5)$$

where the right-hand-side represents the level of the system energy at the release time τ_0 , and Eq. (6.5) is equivalent to Eq. (5.2) of Section V.

If the force p has imparted sufficient energy into the system, such that it can reach the unstable point B ($L = L_u^{P_0}$; see Fig. 6.1) on the " p_0 -load" potential with zero kinetic energy (velocity), then "buckled" motion is possible, and the system becomes dynamically unstable.

The governing equations for predicting critical conditions are obtained from Eqs. (6.4) and (6.5).

By requiring kinematic continuity at $\tau = \tau_0$ one may write

$$\bar{T}^{P_0+P}(\tau_0) = \bar{T}^{P_0}(\tau_0) \quad (6.6)$$

From Eq. (6.4) one may write

$$\bar{T}^{P_0+P} = \bar{U}_T^{P_0+P} \left(L_S^{P_0} \right) - \bar{U}_T^{P_0+P}(\tau_0) \quad (6.7)$$

Substitution of Eqs. (6.6) and (6.7) into Eq. (6.5) yields

$$\bar{U}_T^{P_0} + \bar{T}^{P_0} = \bar{U}_T^{P_0}(\tau_0) - \bar{U}_T^{P_0+P}(\tau_0) + \bar{U}_T^{P_0+P} \left(L_S^{P_0} \right) \quad (6.8)$$

for $\tau > \tau_0$

Next, a critical condition exists, if the system can reach point B (see Fig. 6.1) with zero kinetic energy $\left[\bar{T}^{P_0} \left(L_u^{P_0} \right) = 0 \right]$. Thus, denoting the critical condition by p, τ_{0cr} , one may write

$$\bar{U}_T^{P_0} \left(L_u^{P_0} \right) = \bar{U}_T^{P_0}(\tau_{0cr}) - \bar{U}_T^{P_0+P}(\tau_{0cr}) + \bar{U}_T^{P_0+P} \left(L_S^{P_0} \right) \quad (6.9)$$

Note that Eq. (6.9) relates p , $\tau_{o_{cr}}$ and the position of the system, L_{cr} , at the instant of the release of the force p . Please observe (as also explained in Section V) that the above described critical condition depends on the evaluation of two parameters, p and τ_o . One approach is to prescribe τ_o and find the corresponding p_{cr} and the other is to prescribe p and find the corresponding $\tau_{o_{cr}}$. The two are equivalent. Regardless of the approach, Eq. (6.9) relates three parameters p , $\tau_{o_{cr}}$ (or p_{cr} , τ_o) and L_{cr} (the position of the system taken as one parameter).

The second (needed) equation is obtained from Eq. (6.4). This equation (see Section V) is used to relate the load p , the time of release, τ_o , and the position of the system at the instant of release. In order to find, for a prescribed load, the position of the system at the instant of release, one must specify the path of motion. For one-degree-of-freedom systems there is only one path and this is easily accomplished [see Eqs. (5.13) and (5.17)]. On the other hand, for a multi-degree-of-freedom system there are numerous possible paths leading to a multitude of positions for a given release time. In such cases, if one is interested in finding a lower bound for the critical conditions, he may find the path that yields the smallest possible time. This may be accomplished by solving the corresponding "brachistochrone" problem (see Appendix A). The solution to the "brachistochrone" problem yields the path of motion which yields the smallest possible time. Thus, Eq. (6.4) along with the path of motion, relates the release time τ_o and system position at the instant of release [see Eq. (5.24)]. These steps are clearly demonstrated for each of the three models, in the subsequent articles.

Moreover, if one is dealing with a deflection limited design (the

position of the system cannot exceed $L_L^{P_0}$ - see Fig. 6.1), then $\bar{U}_T^{P_0}(L_u^{P_0})$ is replaced by $\bar{U}_T^{P_0}(L_L^{P_0})$, in the outlined computational procedure.

Parenthesis: The cases of ideal impulse and suddenly applied load of constant magnitude and infinite duration, may be obtained as special cases of the present procedure.

However, critical conditions for these two load cases may also be obtained independently.

For the ideal impulse case, one may relate the impulse to an initial kinetic energy, and from conservation of energy

$$\bar{U}_T^{P_0} + \bar{T}_i^{P_0} = \bar{U}_T^{P_0}(L_s^{P_0}) + \bar{T}_i^{P_0} \quad (6.10)$$

Then $\bar{T}_i^{P_0}$ is critical (related to the critical ideal impulse) if the system reaches position $L_u^{P_0}$ (pt B of Fig. 6.1) with zero kinetic energy.

Thus

$$\bar{T}_{i_{cr}}^{P_0} = \bar{U}_T^{P_0}(L_s^{P_0}) - \bar{U}_T^{P_0}(L_u^{P_0}) \quad (6.11)$$

For the second extreme case ($\tau \rightarrow \infty$), P_{cr} may be obtained from Eq. (6.3) or (6.4), which, for this case, holds true for all τ ($0 \leq \tau \leq \infty$). Thus, P_{cr} corresponds to the solution of

$$\bar{U}_T^{P_0 + P}(L_u^{P_0 + P}) = \bar{U}_T^{P_0 + P}(L_s^{P_0}) \quad (6.12)$$

where $L_u^{P_0 + P}$ denotes the unstable static equilibrium position of the system when the static load is equal to $p_0 + p$.

Model A

For this particular model, the static stability analysis is presented in Section V. The geometry of the model is given in Fig. 2.1 and the static response in Fig. 2.2.

In evaluating the effect of preloading three imperfection angles are chosen ($\theta_o = 0.005, 0.010, 0.020$), and for each θ_o - value the system is initially loaded quasistatically with a p_o -load smaller than the p_{cr} -static. Then, the system is loaded dynamically. The following values are used in the dynamic analysis:

$$\begin{array}{lll} \theta_o = 0.005 & ; & p_{cr} = 0.440 \quad ; \quad p_o = 0.340, 0.380, \text{ and } 0.420 \\ \theta_o = 0.010 & ; & p_{cr} = 0.415 \quad ; \quad p_o = 0.300, 0.360, \text{ and } 0.400 \\ \theta_o = 0.020 & ; & p_{cr} = 0.384 \quad ; \quad p_o = 0.300, 0.340, \text{ and } 0.370 \end{array}$$

First, the extreme cases ($\tau_o \rightarrow 0$ and $\tau_o \rightarrow \infty$) are analyzed, by employing Eqs (6.11) and (6.12) respectively.

The ideal impulse, $(p\tau_o)$ is related to the initial kinetic energy [in the nondimensionalized form; see Eqs. (3.8) and (3.9)] by the expression

$$(p\tau_o) = \frac{2}{\sin(\theta_s^{p_o})} \left[\tilde{T}_i^{p_o} \right]^{\frac{1}{2}} \quad (6.13)$$

where $\theta_s^{p_o}$ is the stable static position (angle θ) under p_o load.

The critical ideal impulse $(p\tau_o)_{cr}$, is obtained by substituting Eq. (6.11) into Eq. (6.13), or

$$(p\tau_o)_{cr} = \frac{2}{\sin(\theta_s^{p_o})} \left[\tilde{U}_T^{p_o}(\theta_u^{p_o}) - \tilde{U}_T^{p_o}(\theta_s^{p_o}) \right]^{\frac{1}{2}} \quad (6.14)$$

where $\theta_u^{p_o}$ is the unstable static position under p_o load, and the expression for the total potential is given by Eq. (2.2) by using p_o wherever p appears in the equation. The numerical results for all θ_o, p_o combinations are presented in tabular form on Table 6.1.

Table 6.1 Critical Ideal Impulse, $(p\tau_o)_{cr}$, Model A.

$\theta_o = 0.005$		$\theta_o = 0.010$		$\theta_o = 0.020$	
p_o	$(p\tau_o)_{cr}$	p_o	$(p\tau_o)_{cr}$	p_o	$(p\tau_o)_{cr}$
0	162.000	0	81.000	0	40.000
0.340	8.246	0.300	6.980	0.300	2.900
0.380	3.498	0.360	2.247	0.340	1.207
0.420	0.758	0.400	0.486	0.370	0.338
0.440	0	0.416	0	0.384	0

Note that the first row results are obtained from Eq. (3.10) of Section III. Note also that as the value of p_o approaches the value of the static critical load the additionally imposed (critical) impulse tends to zero. This is reflected by the results of the last row (Table 6.1).

The critical load for the case of $\tau_o \rightarrow \infty, p_{cr\infty}$, is obtained the following steps, for a given θ_o, p_o combination (a) solve Eq. (2.3) given below, for $\theta_s^{p_o}$ (stable position)

$$p_o = \left[\sqrt{1 + \sin \theta} - \sqrt{1 + \sin \theta_o} \right] \cot \theta / \sqrt{1 + \sin \theta} \quad (6.15)$$

(b) Static equilibrium positions are characterized by Eq. (2.3) for loading $p_o + p$, or

$$p + p_o = \left[\sqrt{1 + \sin \theta} - \sqrt{1 + \sin \theta_o} \right] \cot \theta / \sqrt{1 + \sin \theta} \quad (6.16)$$

(c) Eq. (6.12) for this model is given below.

$$\left[\sqrt{1 + \sin \theta} - \sqrt{1 + \sin \theta_o} \right]^2 - (p_o + p) (\cos \theta_o - \cos \theta) =$$

$$\left[\sqrt{1 + \sin \theta_s^{p_o}} - \sqrt{1 + \sin \theta_o} \right]^2 - p_o (\cos \theta_o - \cos \theta_s^{p_o}) \quad (6.17)$$

The simultaneous solution of Eqs. (6.16) and (6.17) yields $\theta_o^{p_o+p}$ and p_{cr_∞} . Note that since Eq. (6.17) must be satisfied at an unstable point $(\theta_u^{p_o+p})$ the stability test may be used to ensure this, or

$$\frac{d^2 U_T^{p_o+p}}{d\theta^2} \bigg|_{\theta_u^{p_o+p}} < 0$$

The numerical results for all θ_o , p_o combinations are presented in tabular form in Table 6.2.

Table 6.2 - Critical Dynamic Load, p_{cr_∞}
(Constant Load of Infinite Duration: Model A)

$\theta_o = 0.0005$			$\theta_o = 0.010$			$\theta_o = 0.020$		
p_o	p_{cr_∞}	$p_o + p_{cr_\infty}$	p_o	p_{cr_∞}	$p_o + p_{cr_\infty}$	p_o	p_{cr_∞}	$p_o + p_{cr_\infty}$
0	0.4320	0.4320	0	0.4010	0.4010	0	0.3690	0.3690
0.340	0.0940	0.4340	0.300	0.1090	0.4090	0.300	0.0751	0.3751
0.380	0.0560	0.4360	0.360	0.0517	0.4117	0.340	0.0396	0.3796
0.420	0.0165	0.4365	0.400	0.0136	0.4136	0.370	0.0116	0.3816
0.440	0	0.4400	0.4160	0	0.4160	0.384	0	0.3840

Note that the first row results of Table 6.2 are taken from Section IV.

The results of the last row reflect the fact that if the system is loaded quasistatically up to the limit point, then the additional suddenly applied

load that the system can withstand tends to zero.

Finally, for the case of constant load, p , applied suddenly for a finite duration, τ_o , critical conditions are obtained from the following steps:

- (a) From the static stability analysis obtain $\theta_s^{p_o}$ and $\theta_u^{p_o}$ for each p_o .
- (b) Use of Eq. (6.9) yields

$$p \left(\cos \theta_s^{p_o} - \cos \theta_{cr} \right) = \left[\sqrt{1 + \sin \theta_u^{p_o}} - \sqrt{1 + \sin \theta_o} \right]^2 - \left[\sqrt{1 + \sin \theta_s^{p_o}} - \sqrt{1 + \sin \theta_o} \right]^2 + p_o \left(\cos \theta_u^{p_o} - \cos \theta_s^{p_o} \right) \quad (6.18)$$

where θ_{cr} is the position θ at the instant of the release of the force p ($\tau = \tau_o$).

In Eq. (6.18) for a given, p_o , everything is known (p_o , θ_o , $\theta_s^{p_o}$, and $\theta_u^{p_o}$) except p and θ_{cr} . Therefore, Eq. (6.18) relates p and θ_{cr} for a critical condition to exist.

- (c) Since $\bar{T}^{p+p_o} = \left(\frac{d\theta}{d\tau} \right)^2$, then from Eq. (6.4) we may write

$$\frac{d\theta}{d\tau} = \bar{U}_T^{p_o+p} \left(\theta_s^{p_o} \right) - \bar{U}_T^{p_o+p} (\theta) \quad \text{or}$$

$$d\tau = \left[\bar{U}_T^{p_o+p} \left(\theta_s^{p_o} \right) - \bar{U}_T^{p_o+p} (\theta) \right]^{-\frac{1}{2}} d\theta \quad (6.19)$$

Integration from $\tau = 0$ to $\tau = \tau_o$ and use of the expression for the total potential [see Eq. (2.2)] yields

$$\tau_o = \int_{\theta_s}^{\theta_{cr}} \left\{ \left[\sqrt{1 + \sin \theta_s^{p_o}} - \sqrt{1 + \sin \theta_o} \right]^2 - \left[\sqrt{1 + \sin \theta} - \sqrt{1 + \sin \theta_o} \right]^2 \right. \\ \left. + (p_o + p) \left(\cos \theta_s^{p_o} - \cos \theta \right) \right\}^{-\frac{1}{2}} d\theta \quad (6.20)$$

Note that Eq. (6.20) also relates θ_{cr} to p .

A critical condition is characterized by (p, τ_o) that satisfies both equation, Eq. (6.18) and (6.20). This means that for a given release time, τ_o , find p_{cr} or for a given p find $\tau_{o_{cr}}$. Computationally, though it is easier to assign values of θ_{cr} , solve for p from Eq. (6.18) and then for the corresponding τ_o from Eq. (6.20).

A computer program has been written for these computations. Values of θ_{cr} are assigned, starting with $\theta_s^{p_o} + \delta\theta$, where $\delta\theta$ is very small, and computing the corresponding values of p and τ_o for each $\delta\theta$.

The results are presented graphically on Figs. 6.2 - 6.7 for the three values of θ_o . On the first three figures critical conditions appear as plots of p versus duration time, $\tau_{o_{cr}}$. Note that as $\tau_{o_{cr}}$ becomes larger and larger, the corresponding value of p approaches $p_{cr_{\infty}}$ (see Table 6.2). On the last three figures (6.5-6.7), critical conditions appear as plots of $(p\tau_o)_{cr}$ versus duration time, $\tau_{o_{cr}}$. On these figures, as $\tau_{o_{cr}} \rightarrow 0$, the corresponding value of $(p\tau_o)_{cr}$ approaches the critical ideal impulse (see Table 6.1).

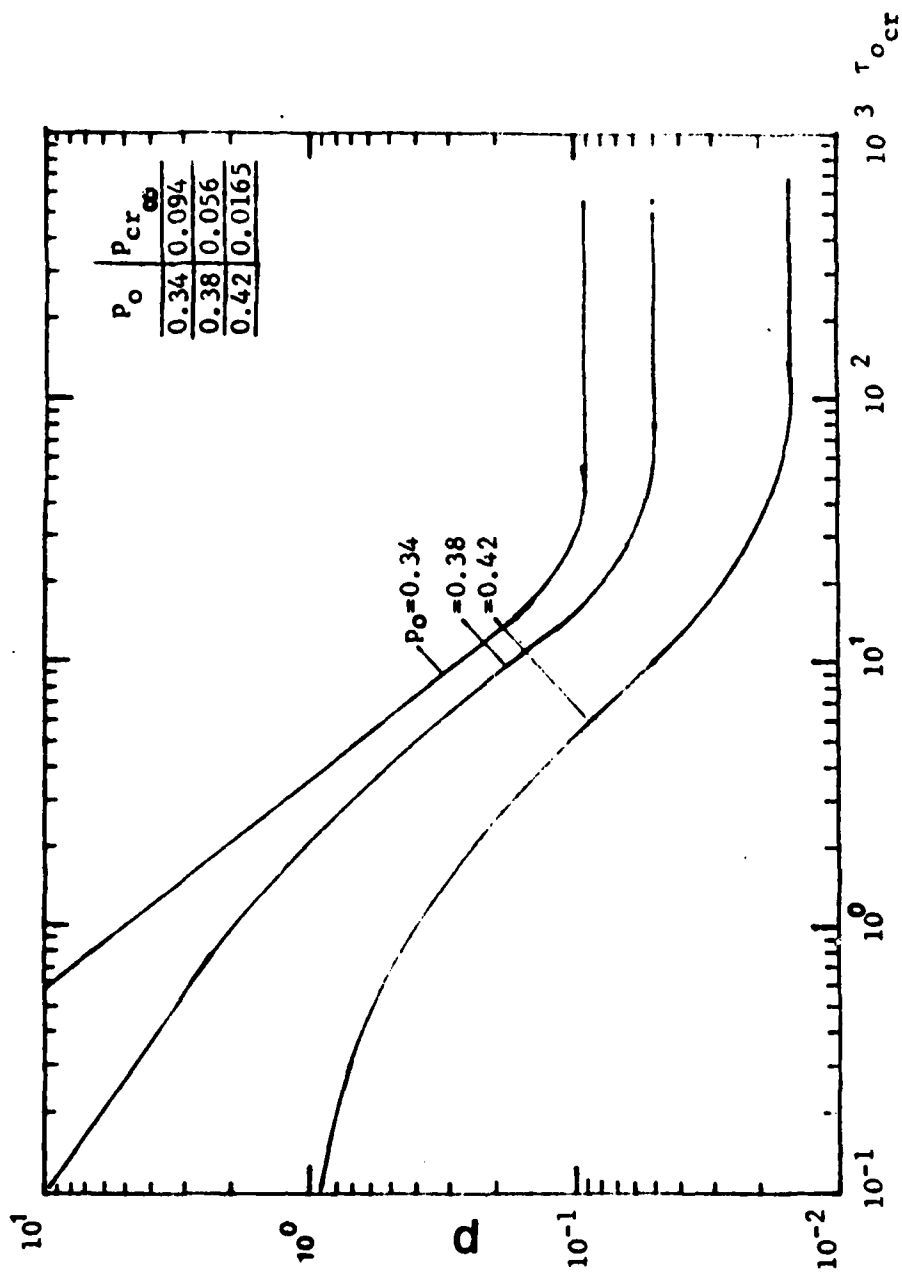


Fig. 6.2. Superimposed load, p , versus critical finite time duration, τ_{ocr} , preloaded Model A, $\theta_0 = 0.005$

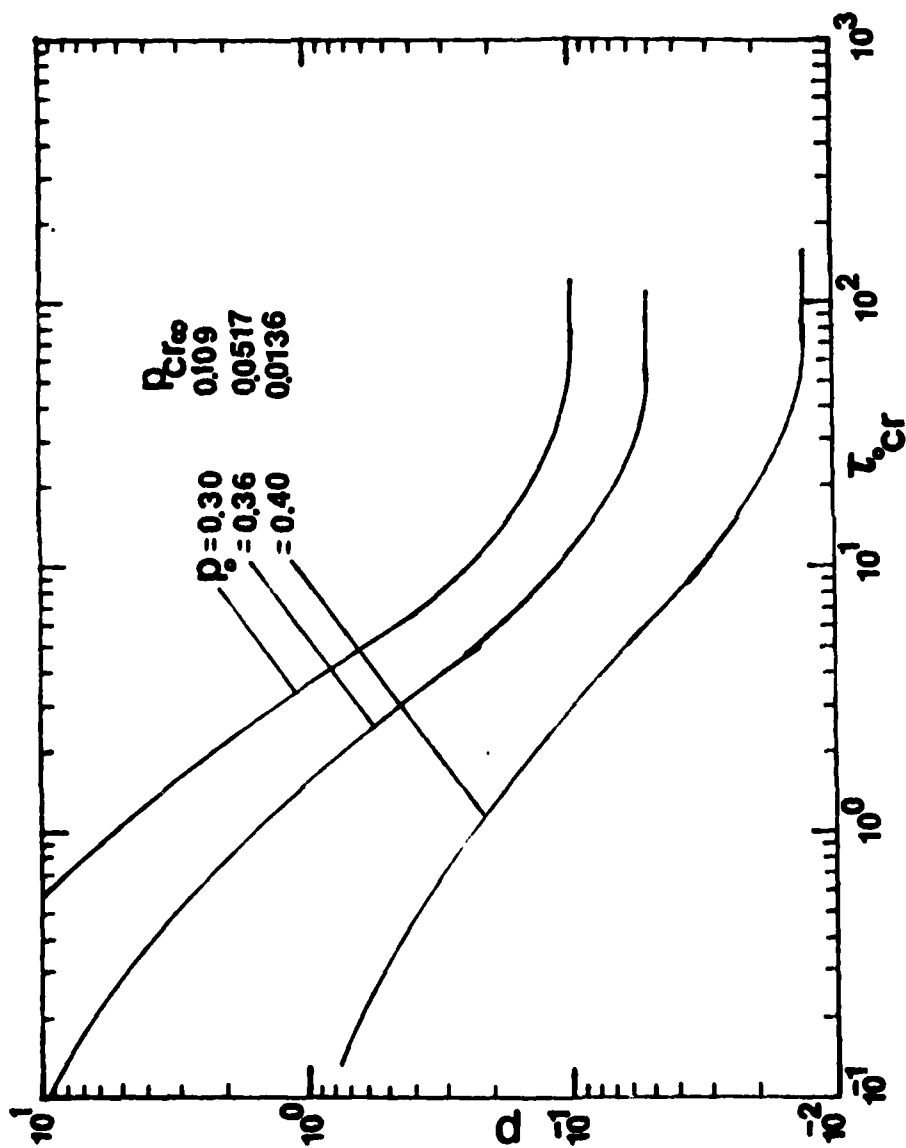


Fig. 6.3. Superimposed load, p , versus Critical Finite Time Duration, τ_{ocr} , Preloaded Model A, $\theta_o = 0.01$.

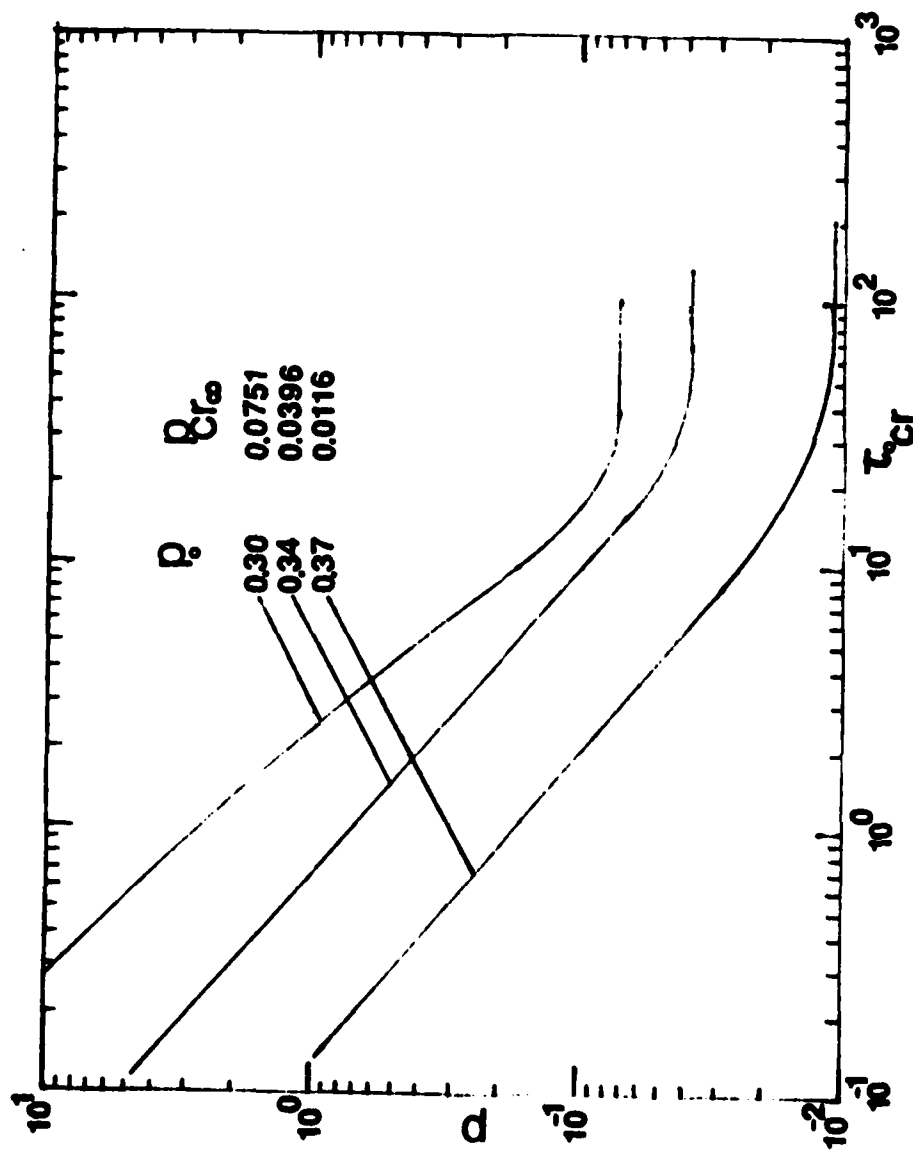


Fig. 6.4. Superimposed load, p , versus Critical Finite Time Duration, τ_{ocr} , Preloaded Model A, $\theta_o = 0.02$.

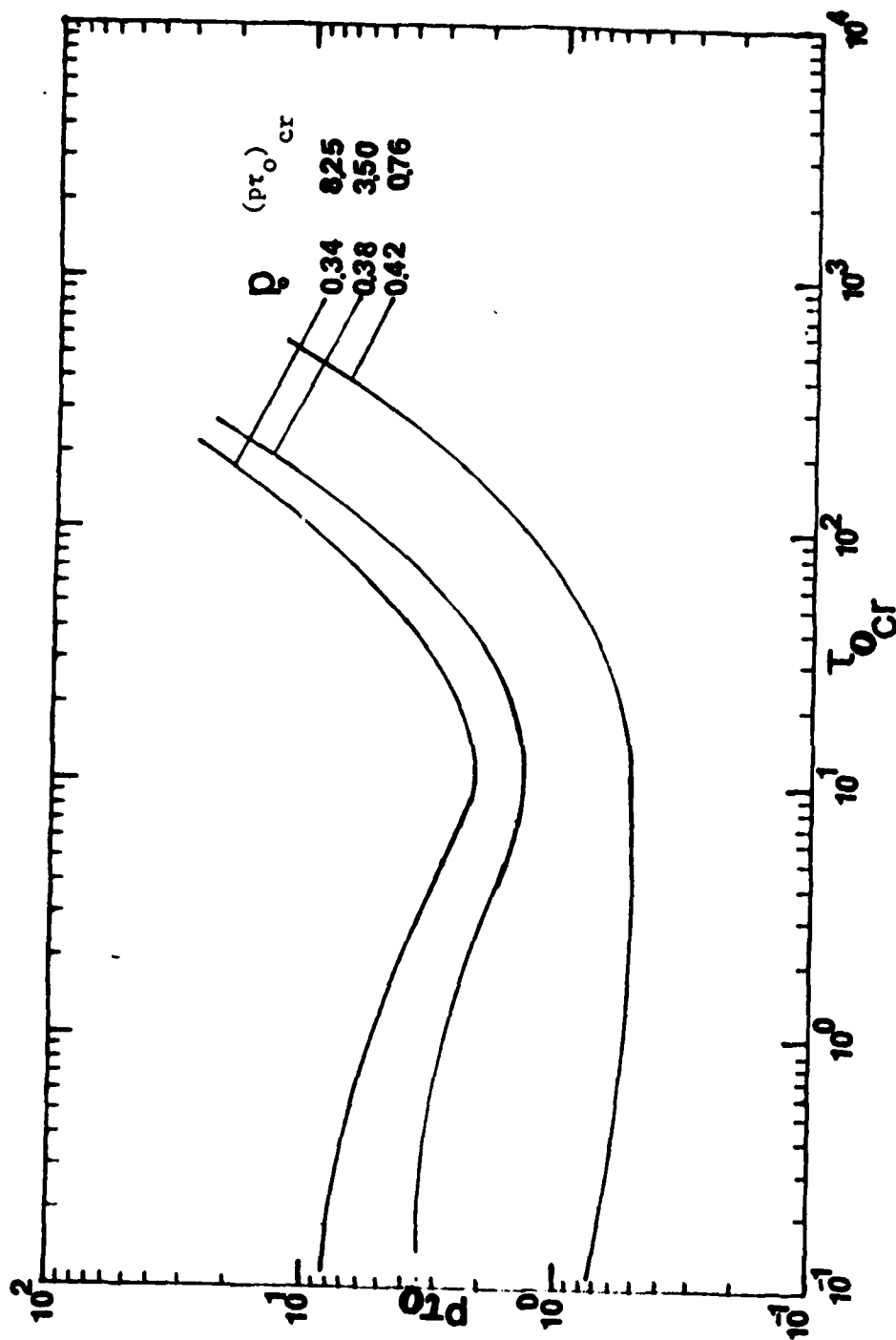


Fig. 6.5. Superimposed Impulse, (pr_0) , versus critical Duration Time, τ_{0cr} , Preloaded Model A, $\theta_0 = 0.005$

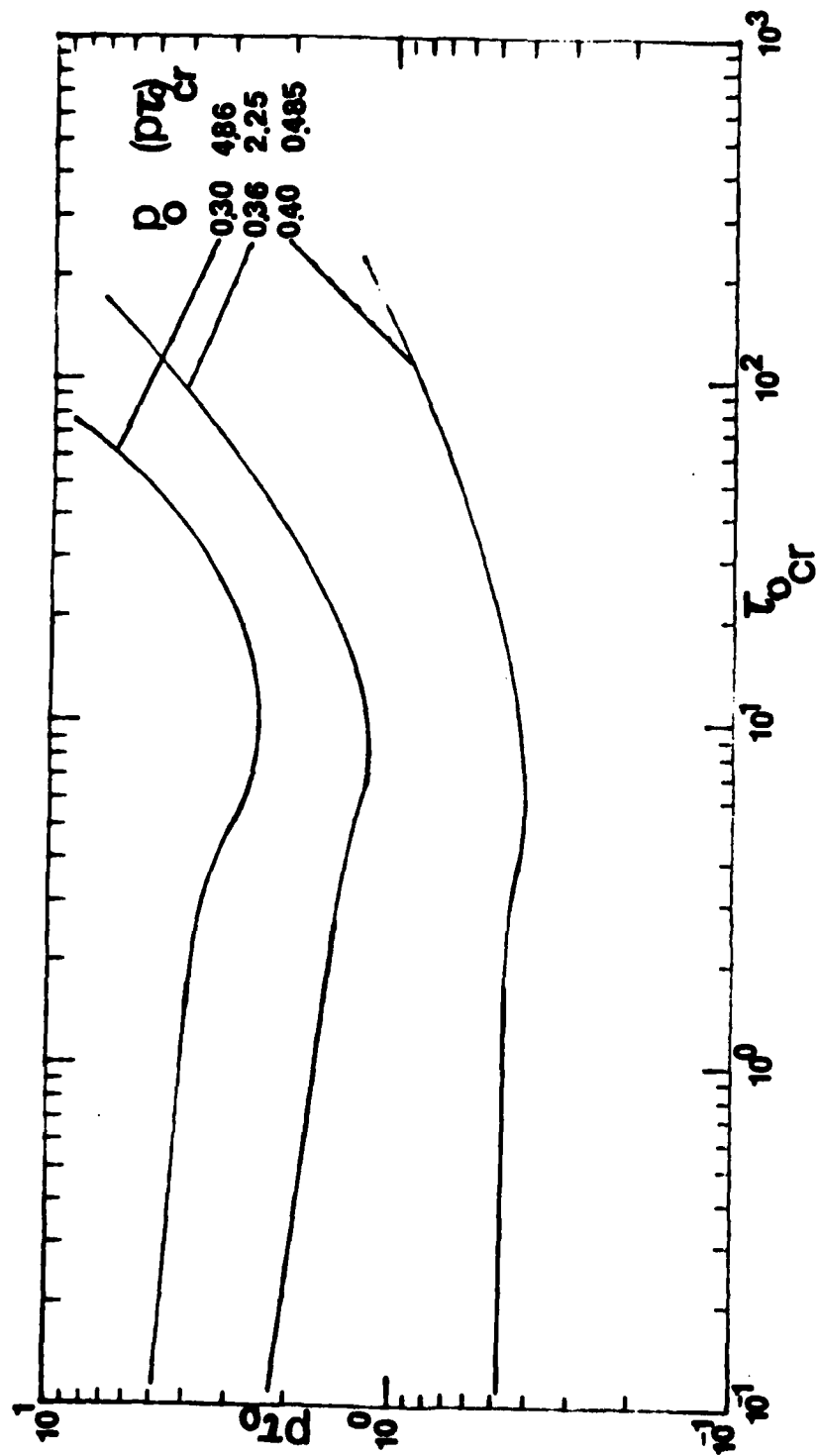


Fig. 6.6. Superimposed impulse, (pt_0) , versus critical time duration, τ_{0cr} , Preloaded Model A, $\theta_0 = 0.01$

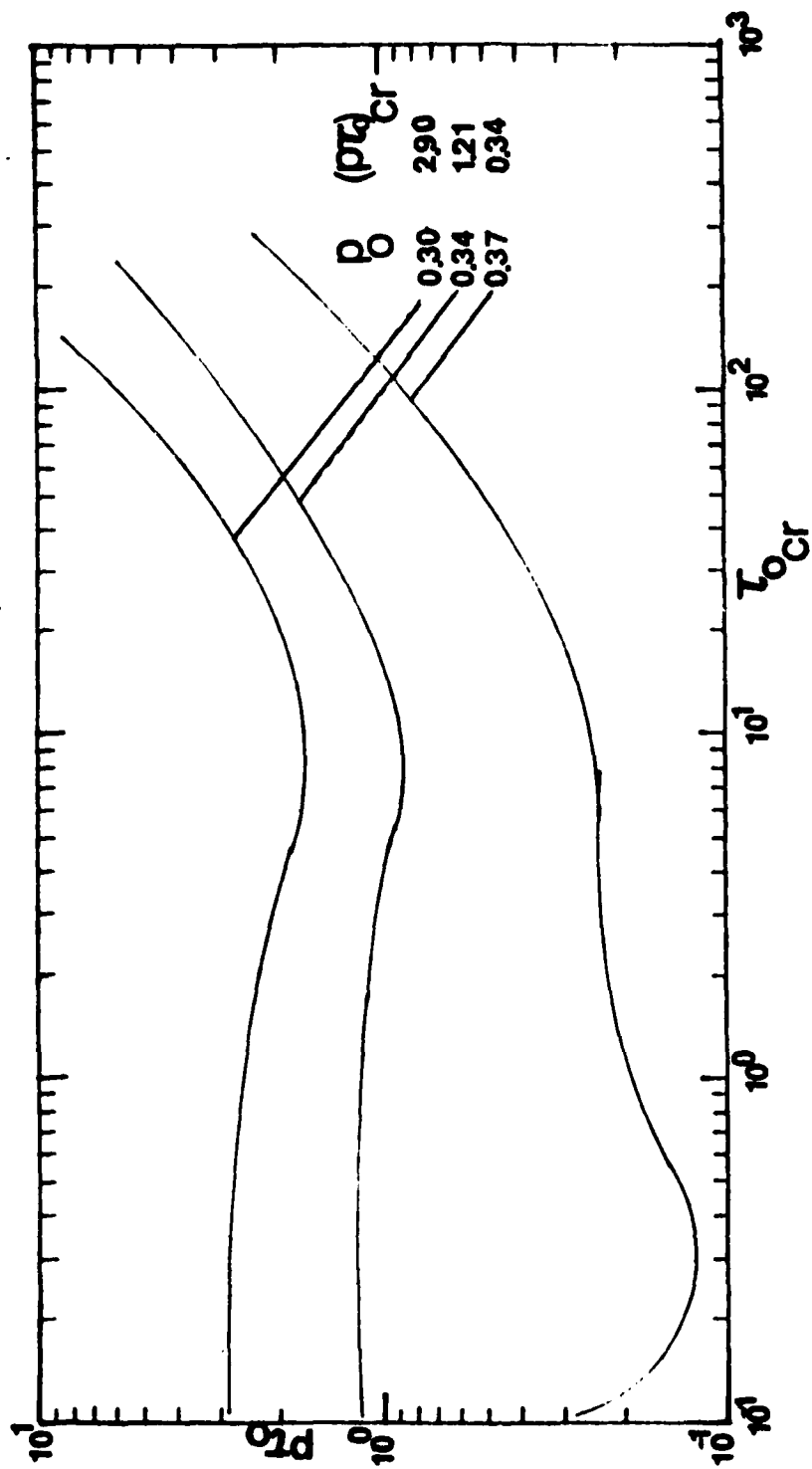


Fig. 6.7. Superimposed Impulse, (p^r) , versus Critical Duration Time, τ_{ocr} , Preloaded Model A, $\theta_o = 0.02$

Model B

For this particular model, the static stability analysis is presented in Section II. The geometry of the model is given in Fig. 2.3.

In evaluating the effect of preloading, three eccentricities are chosen ($\bar{e} = 0.005, 0.010, 0.020$), and for each \bar{e} -value the system is initially loaded quasi-statically with a p_o -load smaller than p_{cr} -static. Then, the system is loaded dynamically. The following values are used in the dynamic analysis:

$\bar{e} = 0.005$;	$p_{cr} = 0.955$;	$p_o = 0.35$,	0.40, and 0.50.
$\bar{e} = 0.010$;	$p_{cr} = 0.932$;	$p_o = 0.30$,	0.40 and 0.50.
$\bar{e} = 0.020$;	$p_{cr} = 0.898$;	$p_o = 0.30$,	0.40, and 0.50.

First, the extreme cases ($\tau_o \rightarrow 0$ and $\tau_o \rightarrow \infty$) are analyzed, by employing Eqs. (6.11) and (6.12) respectively.

The ideal impulse, $(p\tau_o)$ is related to the initial kinetic energy by the expression

$$(p\tau_o) = \frac{1}{\sin \theta_s^{p_o} + \bar{e} \cos \theta_s^{p_o}} \left[T_i^{p_o} \right]^{\frac{1}{2}} \quad (6.21)$$

where $\theta_s^{p_o}$ is the stable static position (angle θ) under p_o load.

The critical ideal impulse, $(p\tau_o)_{cr}$, is obtained by substituting Eq. (6.11) into Eq. (5.21), or

$$(p\tau_o)_{cr} = \frac{1}{\sin \theta_s + \bar{e} \cos \theta_s} \frac{p_o}{p_o} \left[\bar{U}_T^{p_o}(\theta_s) - \bar{U}_T^{p_o}(\theta_u) \right] \quad (6.22)$$

where $\theta_u^{p_o}$ is the unstable static position under p_o load, and the expression for the total potential is given by Eq. 2.5 by using p_o wherever p appears in the equation. The numerical results for all \bar{e} , p_o combinations are presented in tabular form on Table 6.3.

Table 6.3. Critical Ideal Impulse, $(p\tau_o)_{cr}$

(Model B)

$\bar{e} = 0.005$		$\bar{e} = 0.01$		$\bar{e} = 0.02$	
p_o	$(p\tau_o)_{cr}$	p_o	$(p\tau_o)_{cr}$	p_o	$(p\tau_o)_{cr}$
0	200	0	100	0	50
0.35	192	0.30	88	0.30	42
0.40	164	0.40	76	0.40	36
0.50	139	0.50	62	0.50	29
0.955	0	0.932	0	0.898	0

Note that the first row results are obtained from Eq. (3.24) of Section III. Note also that as the value of p_o approaches the value of

the static critical load the additionally imposed (critical) impulse tends to zero. This is reflected by the results of the last row (Table 6.3).

The critical load for the case of $\tau_o \rightarrow \infty$, $p_{cr} \rightarrow \infty$, is obtained by the following steps, for a given θ_o , p_o combination.

- a) Solve Eq. (2.6) given below, for $\theta_s^{p_o}$ (stable position)

$$p_o = \frac{\sin \theta_s^{p_o}}{\tan \theta_s^{p_o} + \bar{e}} \quad (6.23)$$

- (b) Static equilibrium positions are characterized by Eq. (2.6) for loading $p_o + p$, or

$$p + p_o = \frac{\sin \theta}{\tan \theta + \bar{e}} \quad (6.24)$$

- (c) Eq. (6.12) for this model is given below

$$\sin^2 \theta - 2(p_o + p)(1 - \cos \theta + \bar{e} \sin \theta) = \sin^2 \theta_s^{p_o} - 2 p_o (1 - \cos \theta_s^{p_o} + \bar{e} \sin \theta_s^{p_o}) \quad (6.25)$$

The simultaneous solution of Eqs. (6.24) and (6.25) yields $\theta_u^{p_o + p}$ and $p_{cr}^{p_o + p}$. Note that the same Eq. (6.25) must be satisfied at an unstable point $(\theta_u^{p_o + p})$. The stability test may be used to ensure this, or

$$\left. \frac{d^2 U_T}{d\theta^2} \right|_{\theta_u^{p_o + p}} < 0$$

The numerical results for all \bar{e} , p_o combinations are presented in tabular form on Table 6.4.

Table 6.4 - Critical Dynamic Load, $p_{cr\infty}$

(Constant Load of Infinite Duration: Model B)

$\bar{e} = 0.0005$			$\bar{e} = 0.010$			$\bar{e} = 0.020$		
p_o	$p_{cr\infty}$	$p_o + p_{cr\infty}$	p_o	$p_{cr\infty}$	$p_o + p_{cr\infty}$	p_o	$p_{cr\infty}$	$p_o + p_{cr\infty}$
0	0.948	0.948	0	0.912	0.912	0	0.85	0.85
0.35	0.60	0.95	0.30	0.62	0.92	0.30	0.59	0.89
0.40	0.54	0.94	0.40	0.52	0.92	0.40	0.48	0.88
0.50	0.45	0.95	0.50	0.42	0.92	0.50	0.38	0.88
0.955	0	0.955	0.932	0	0.932	0.898	0	0.898

Note that the first row results of Table 6.4 are taken from Section IV. The results of the last row reflect the fact that if the system is loaded quasi-statically up to the limit point, the additional suddenly applied load that the system can withstand tends to zero.

Finally, for the case of constant load, p , applied suddenly for a finite duration, τ_o , critical conditions are obtained from the following steps:

- From the static stability analysis obtain $\theta_s^{p_o}$ and $\theta_u^{p_o}$ for each p_o .
- Use of equation (6.9) yields

$$\begin{aligned}
 & 2p (\cos \theta_s^{p_o} - \bar{e} \sin \theta_s^{p_o} - \cos \theta_{cr} + \bar{e} \sin \theta_{cr}) = \\
 & = \sin^2 \theta_u^{p_o} - \sin^2 \theta_s^{p_o} - 2p_o (\cos \theta_s^{p_o} - \bar{e} \sin \theta_s^{p_o} - \\
 & - \cos \theta_u^{p_o} + \bar{e} \sin \theta_u^{p_o}) \quad (6.26)
 \end{aligned}$$

where θ_{cr} is the position θ at the instant of the release of the force p ($\tau = \tau_0$)

In Eq. 6.26, for a given geometry \bar{e} and static load p_0 , everything is known (p_0 , \bar{e} , $\theta_s^{p_0}$ and $\theta_u^{p_0}$) except p and θ_{cr} . Therefore, Eq. 6.26 relates p and θ_{cr} for a critical condition to exist.

c) Since $\bar{T}^{p+p_0} = \left(\frac{d\theta}{d\tau}\right)^2$, then from Eq. 6.4 one may write

$$\frac{d\theta}{d\tau} = \left[\bar{U}_T^{p_0+p}(\theta_s^{p_0}) - \bar{U}_T^{p_0+p}(\theta) \right]^{\frac{1}{2}}, \text{ or}$$

$$d\tau = \left[\bar{U}_T^{p_0+p}(\theta_s^{p_0}) - \bar{U}_T^{p_0+p}(\theta) \right]^{\frac{1}{2}} d\theta \quad (6.27)$$

Integration from $\tau = 0$ to $\tau = \tau_0$ and use of the expression for the total potential [see Eq. 2.5] yields

$$\tau_0 = \int_{\theta_s^{p_0}}^{\theta_{cr}} \left\{ \sin^2 \theta_s^{p_0} - \sin^2 \theta - \right.$$

$$\left. -2(p_0+p) \cdot (\bar{e} \sin \theta_s^{p_0} - \cos \theta_s^{p_0} - \bar{e} \sin \theta + \cos \theta) \right\}^{\frac{1}{2}} d\theta \quad (6.28)$$

Note that Eq. (6.28) also relates θ_{cr} to p .

A critical condition is characterized by (p, τ_0) that satisfies both equations, Eqs. (6.26) and (6.28). This means that for a given release time, τ_0 , find p_{cr} or for a given p find τ_{0cr} . Computationally, though, it is easier to assign values of θ_{cr} , solve for p from Eq. (6.26) and then for the corresponding τ_0 from Eq. (6.28).

A computer program has been written for these computations. Values

of θ_{cr} are assigned, starting with $\theta_s^{p_o} + \delta\theta$, where $\delta\theta$, is very small, and computing the corresponding values of p and τ_o for each $\delta\theta$.

The results are presented graphically on Figs. 6.8 - 6.13 for the three values of θ_o . On the first three figures critical conditions appear as plots of p versus duration time, $\tau_{o_{cr}}$. Note that as $\tau_{o_{cr}}$ becomes larger and larger, the corresponding value of p approaches p_{cr_∞} (see Table 6.4). On the last three figures (6.11 - 6.13) critical conditions appear as plots of $(p\tau_o)_{cr}$ versus duration time, $\tau_{o_{cr}}$. On these figures, as $\tau_{o_{cr}} \rightarrow 0$, the corresponding value of $(p\tau_o)_{cr}$ approaches the critical ideal impulse (see Table 6.3).

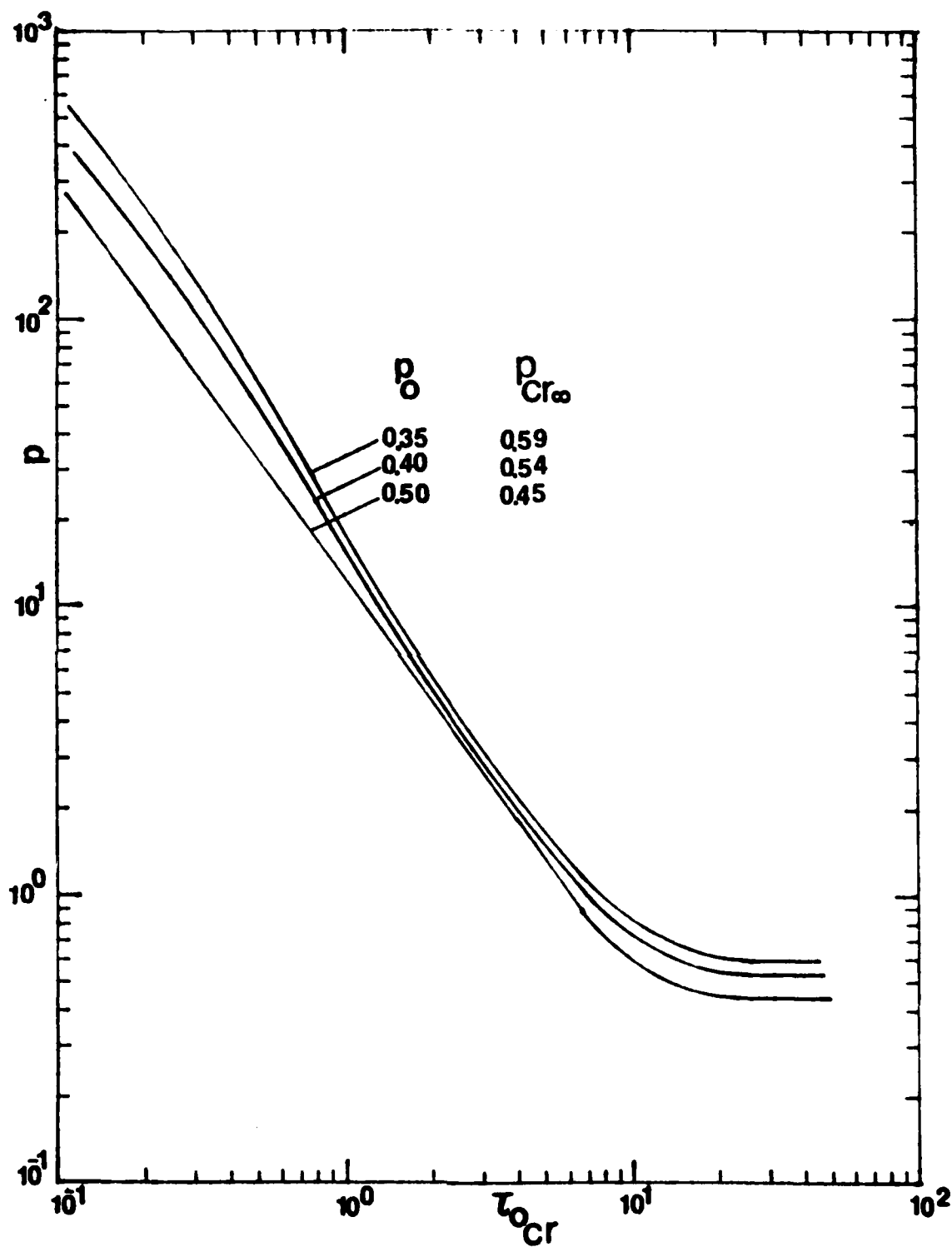


Fig. 6.8. Superimposed load, p , versus Critical Duration Time, τ_{ocr} ,
Preloaded Model B, $\bar{c} = 0.005$

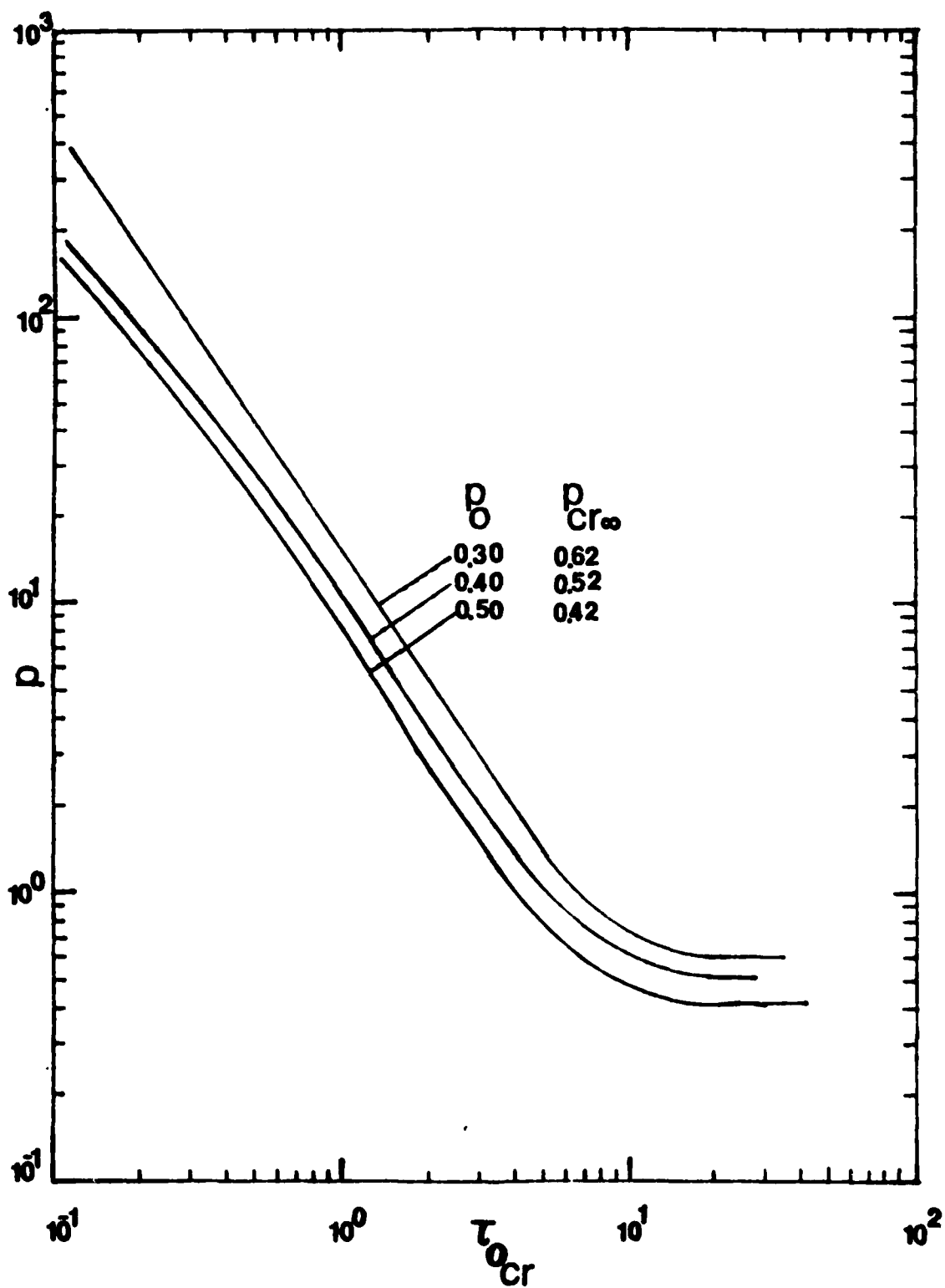


Fig. 6.9. Superimposed load, p , versus critical Duration Time, τ_{0cr} ,
Preloaded Model B, $e = 0.01$

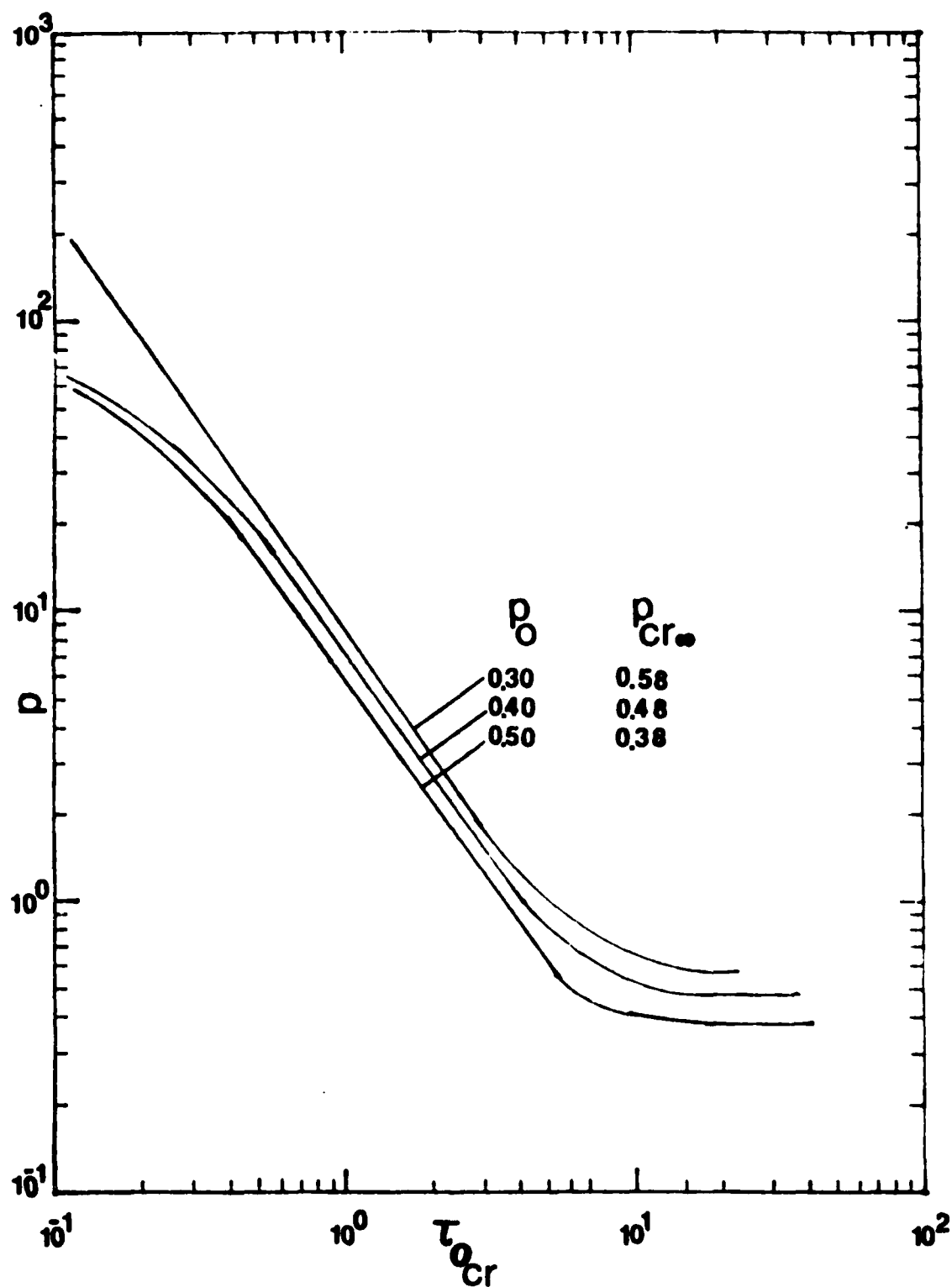


Fig. 6.10. Superimposed load, p , versus critical Duration Time, τ_{0cr} , Preloaded Model R, $c = 0.02$.

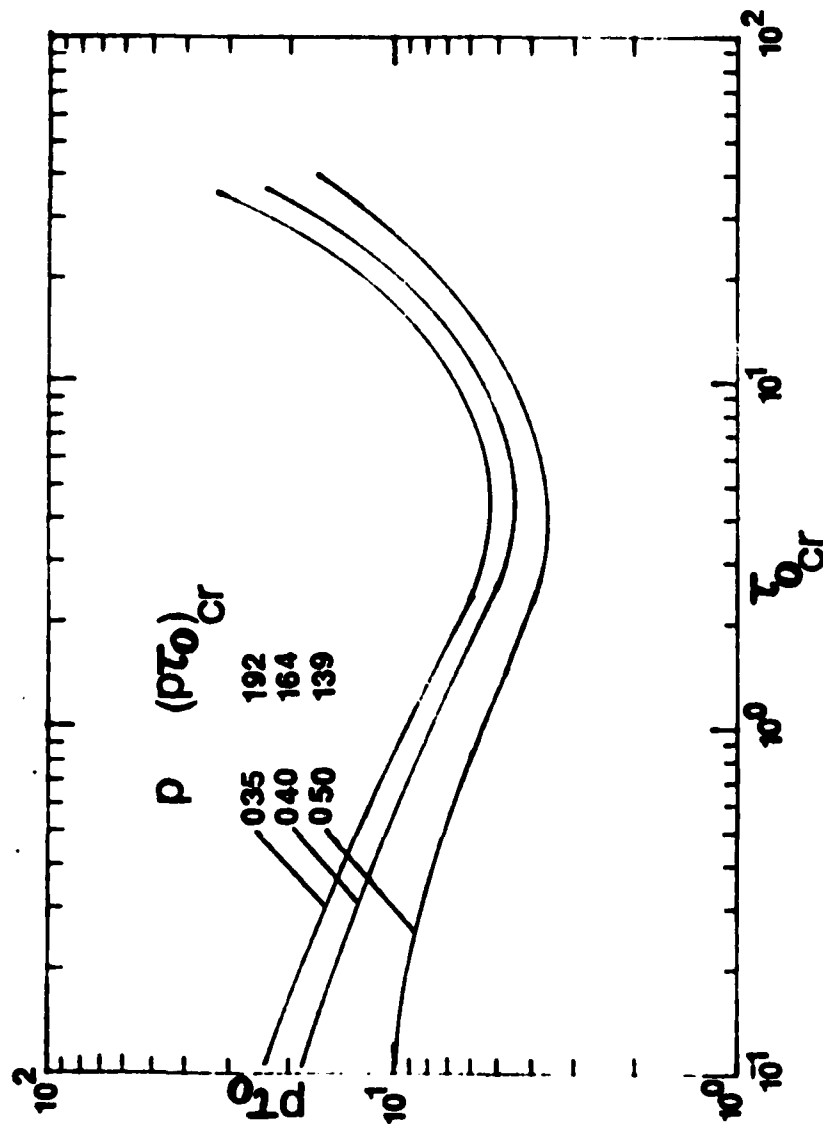


Fig. 6.11. Superimposed Impulse, $p\tau$, versus critical Duration Time, τ_{ocr} , Preloaded Model B, $\alpha = 0.005$

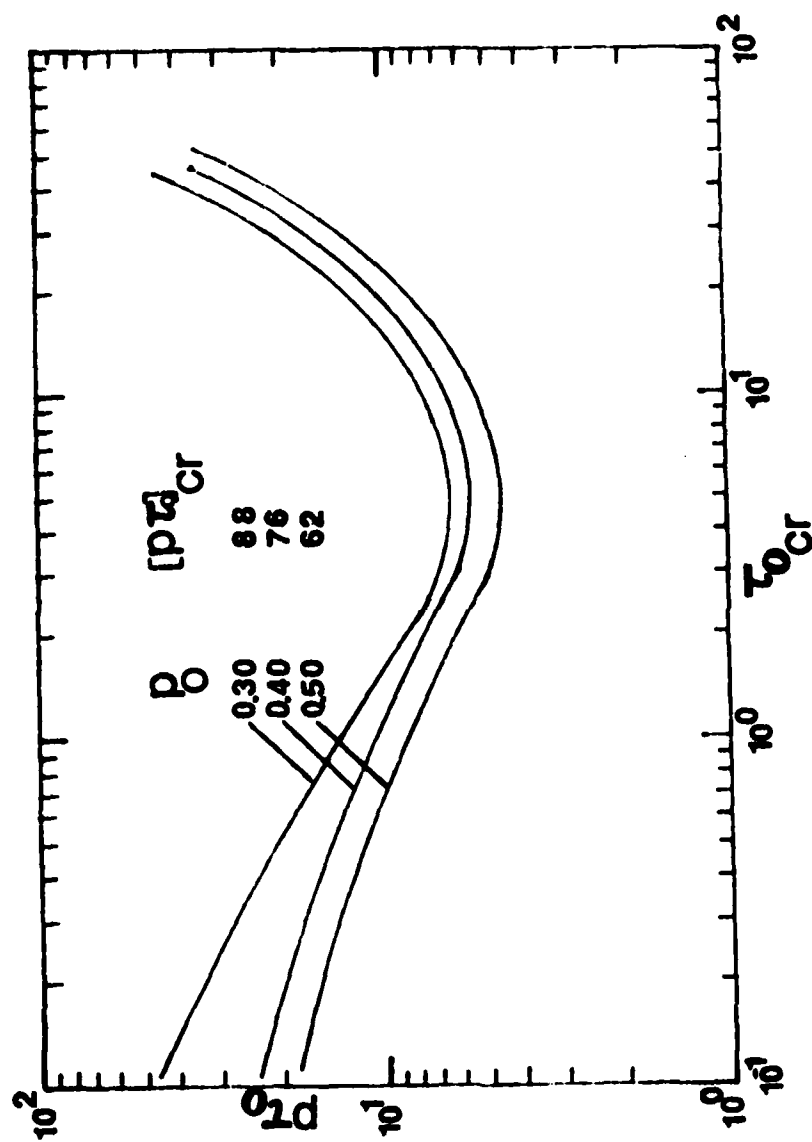


Fig. 6.12. Superimposed Impulse, p_0 , versus critical Duration Time, τ_{0cr} , Preloaded Model B, $\bar{e} = 0.01$

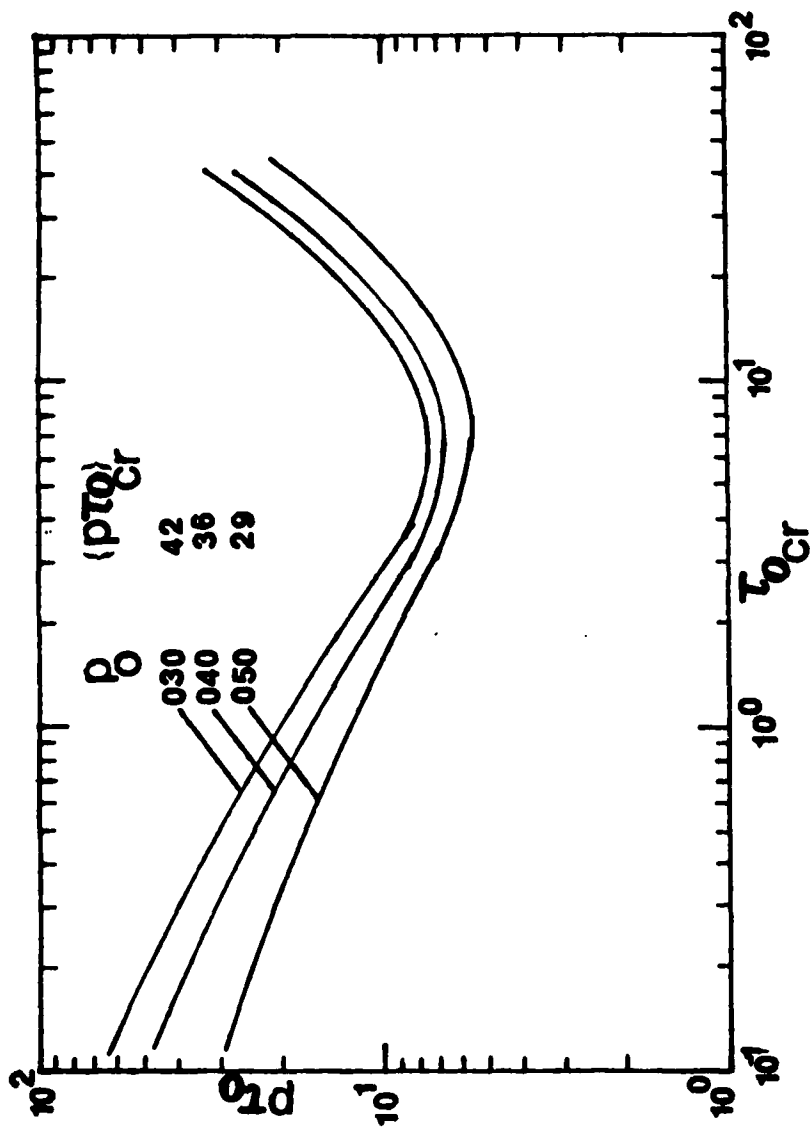


Fig. 6.13. Superimposed Impulse, p_0 , versus critical Duration Time, τ_{0cr} , Preloaded Model B, $\bar{\epsilon} = 0.02$

Model C.

For this particular model, the static stability analysis is presented in Section II. The geometry of the model is given on Fig. 2.4 and the static response on Fig. 2.6.

In evaluating the effect of prestress, three Λ -characteristic coefficients are chosen ($\Lambda = 5.0, 6.0, 8.0$), and for each Λ -value the system is initially loaded quasi-statically with a p_o -load smaller than the p_{cr} -static. Then, the system is loaded dynamically. The following values are used in the dynamic analysis.

$$\begin{aligned}\Lambda = 5.0 & \quad ; \quad p_{cr} = 5.154 \quad ; \quad p_o = 2.8, 3.4, 4.0 \\ \Lambda = 6.0 & \quad ; \quad p_{cr} = 6.000 \quad ; \quad p_o = 3.2, 3.8, 4.2 \\ \Lambda = 8.0 & \quad ; \quad p_{cr} = 7.310 \quad ; \quad p_o = 4.8, 5.4, 6.0\end{aligned}$$

First, the extreme cases ($\tau_o \rightarrow 0$ and $\tau_o \rightarrow \infty$) are analyzed, by employing Eqs. (6.11) and (6.12), respectively.

The ideal impulse, $(p\tau_o)$, is related to the initial kinetic energy in the nondimensionalized form [see Eqs. (3.22)] by the expression

$$(p\tau_o) = [2 \bar{T}_1^{p_o}]^{\frac{1}{2}} \quad (6.29)$$

where $\theta_s^{p_o}$ is the stable static position (angle θ) under p_o load. The critical ideal impulse, $(p\tau_o)_{cr}$, is obtained by substituting Eq. (6.11) into Eq. (6.13), or

$$(p\tau_o)_{cr} = \sqrt{2} \left[\bar{U}_T^{p_o}(\theta_s^{p_o}) - \bar{U}_T^{p_o}(\theta_u^{p_o}) \right]^{\frac{1}{2}} \quad (6.30)$$

where $\theta_u^{p_o}$ is the unstable static position under p_o load, and the expression for the total potential is given by Eq. (2.2) by using p_o wherever p appears in the equation. The numerical results for all p_o combinations are presented in tabular form on Table 6.5.

Table 6.5 - Critical Ideal Impulse, $(p\tau_o)_{cr}$, (Model C)

$\Lambda=5.0$		$\Lambda=6.0$		$\Lambda=8.0$	
p_o	$(p\tau_o)_{cr}$	p_o	$(p\tau_o)_{cr}$	p_o	$(p\tau_o)_{cr}$
0	6.00	0	6.71	0	7.93
2.8	3.06	3.2	3.39	4.8	3.04
3.4	2.32	3.8	2.67	5.4	2.31
4.0	1.32	4.2	1.67	6.0	1.44
5.154	0	6.0	0	7.31	0

Note that the first row results are obtained from Eq. (3.26) of Section III. Note also that as the value of p_o approaches the value of the static critical load the additionally imposed (critical) impulse tends to zero. This is reflected by the results of the last row (Table 6.5).

The critical load for the case of $\tau_0 \rightarrow \infty$, $p_{cr\infty}$, is obtained by the following steps, for a given Λ , p_0 combination

- a) Solve Eq. (2.17) given below for $r_s^{p_0}$ (stable position) and $s = 0$,

$$p_0 = (\Lambda - 1 - r_s^{p_0})^2 r_s^{p_0} + \sqrt{\Lambda} \quad (6.31)$$

- b) Static Saddle equilibrium positions are characterized by Eq. (2.19) for loading $p_0 + p$, or

$$r = \frac{p + p_0 - \sqrt{\Lambda}}{2} \quad (6.32)$$

$$r^2 + 3s^2 = \Lambda - 3$$

- c) Eq. (6.12) for this model is given below

$$\begin{aligned} (r^2 + 3s^2 - 2\sqrt{\Lambda}r + \Lambda) + \frac{1}{2}(\Lambda - r^2 - 3s^2)^2 - 2(p_0 + p)(\sqrt{\Lambda} - r) = \\ = r_s^{p_0} + \frac{1}{2}(\Lambda - r_s^{p_0})^2 - 2p_0(\sqrt{\Lambda} - r_s^{p_0}) \end{aligned} \quad (6.33)$$

The simultaneous solution of Eqs. (6.32) and (6.33) yields $r_u^{p_0+p}$ and $p_{cr\infty}$.

The numerical results for all Λ , p_0 combinations are presented in Tabular form on Table 6.6.

Table 6.6. Critical Loads (Constant Magnitude, Infinite Duration - Model C).

$\Lambda = 5.0$			$\Lambda = 6.0$			$\Lambda = 8.0$		
p_0	$p_{cr\infty}$	$p_0 + p_{cr\infty}$	p_0	$p_{cr\infty}$	$p_0 + p_{cr\infty}$	p_0	$p_{cr\infty}$	$p_0 + p_{cr\infty}$
0	3.70	3.70	0	4.35	4.35	0	5.70	5.70
2.8	1.48	4.28	3.2	1.68	4.88	4.8	1.59	6.39
3.4	1.17	4.57	3.8	1.22	5.02	5.4	1.21	6.61
4.0	.58	4.58	4.2	0.85	5.05	6.0	0.68	6.68
5.154	0	5.154	6.000	0.0	6.000	7.31	0.0	7.31

Note that the first row results of Table 6.6 are taken from Section IV.

The results of the last row reflect the fact that if the system is loaded quasi-statically up to the limit point, then the additional suddenly applied load that the system can withstand tends to zero.

Finally, for the case of constant load, p , applied suddenly for a finite duration, τ_0 , critical conditions are obtained from the following steps:

(a) From the static stability analysis obtain $r_s^{p_0}$ and $r_u^{p_0}$, $s_u^{p_0}$ for each p_0 .

(b) Use of Eq. (6.9) yields

$$2p (r_s^{p_0} - r_{cr}) = (r_u^{p_0})^2 + 9s_u^{p_0} - 2\sqrt{\Lambda} r_u^{p_0} + \Lambda + \frac{1}{2} (\Lambda - r_u^{p_0})^2 - (r_s^{p_0} - \sqrt{\Lambda})^2 - \frac{1}{2} (\Lambda - r_s^{p_0})^2 + 2p_0 (r_u^{p_0} - r_s^{p_0}) \quad (6.34)$$

where r_{cr} is the position r at the instant of the release of the force p ($\tau = \tau_0$).

In Eq. (6.34), for a given geometry, Λ , and Static load, p_0 , everything is known (p_0 , c , $r_s^{p_0}$, $r_u^{p_0}$ and $s_u^{p_0}$) except p and r_{cr} . Therefore, Eq. (6.34) relates p and r_{cr} for a critical condition to exist.

(c) Since $\bar{T}^{p+p_0} = \frac{1}{2}(1+s'^2) \left(\frac{dr}{d\tau}\right)^2$, then from Eq. 6.4 we may write

$$\frac{dr}{d\tau} = \left[\bar{U}_T^{p_0+p} (r_s^{p_0}) - \bar{U}_T^{p_0+p} (r, s) \right]^{1/2}, \text{ or}$$

$$d\tau = \left[\bar{U}_T^{p_0+p} (r_s^{p_0}) - \bar{U}_T^{p_0+p} (r, s) \right]^{-1/2} dr \quad (6.35)$$

Invoking the same techniques we used for the same problem but without prestress in Section V, the critical time τ_0 is computed on the symmetric path $s = 0$.

Integration from $\tau = 0$ to $\tau = \tau_0$ and use of the expression for the total potential [see Eq. 2.13] yields

$$\tau_0 = \int_{r_s^{p_0}}^{r_{cr}} \left[(r_s^{p_0} - \sqrt{\Lambda})^2 + \frac{1}{2} (\Lambda - r_s^{p_0})^2 - (r - \sqrt{\Lambda})^2 - \frac{1}{2} (\Lambda - r)^2 - \right]$$

$$- 2 (p + p_o)(r - r_s^{p_o}) \Big]^{-1} dr \quad (6.36)$$

Note that Eq. (6.34) also relates r_{cr} to p .

A critical condition is characterized by (p, τ_o) that satisfies both equation, Eqs. (6.34) and (6.36). This means that for a given release time, τ_o , find p_{cr} or for a given p find τ_{ocr} . Computationally, though it is easier to assign values of r_{cr} , solve for p from Eq. (6.34) and then for the corresponding τ_o from Eq. (6.36).

A computer program has been written for these computations. Values of r_{cr} are assigned, starting with $r_s^{p_o} + \delta r$, where δr is very small, and computing the corresponding values of p and τ_o for each δr .

The results are presented graphically on Figs. 6.14 - 6.17 for the three values of Λ . On the first three figures, critical conditions appear as plots of p versus duration time, τ_{ocr} . Note that as τ_{ocr} becomes larger and larger, the corresponding value of p approaches p_{cr_∞} (see Table 6.6). On the last three figures (6.17 - 6.79) critical conditions appear as plots of $(p\tau_o)_{cr}$ versus duration time, τ_{ocr} . On these figures, as $\tau_{ocr} \rightarrow 0$, the corresponding value of $(p\tau_o)_{cr}$ approaches the critical ideal impulse (see Table 6.5).

AD-A122 317

DYNAMIC STABILITY OF STRUCTURES: IMPERFECTION SENSITIVE
SYSTEMS ACTED UPON. (U) GEORGIA INST OF TECH ATLANTA
SCHOOL OF ENGINEERING SCIENCE AN. G J SIMITSES ET AL.

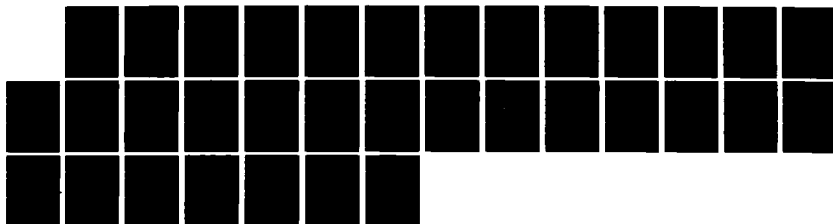
2/2

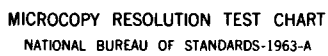
UNCLASSIFIED

MAY 81 AFMIL-TR-81-3040 F33615-79-C-3221

F/G 20/11

NL





MICROCOPY RESOLUTION TEST CHART
NATIONAL BUREAU OF STANDARDS-1963-A

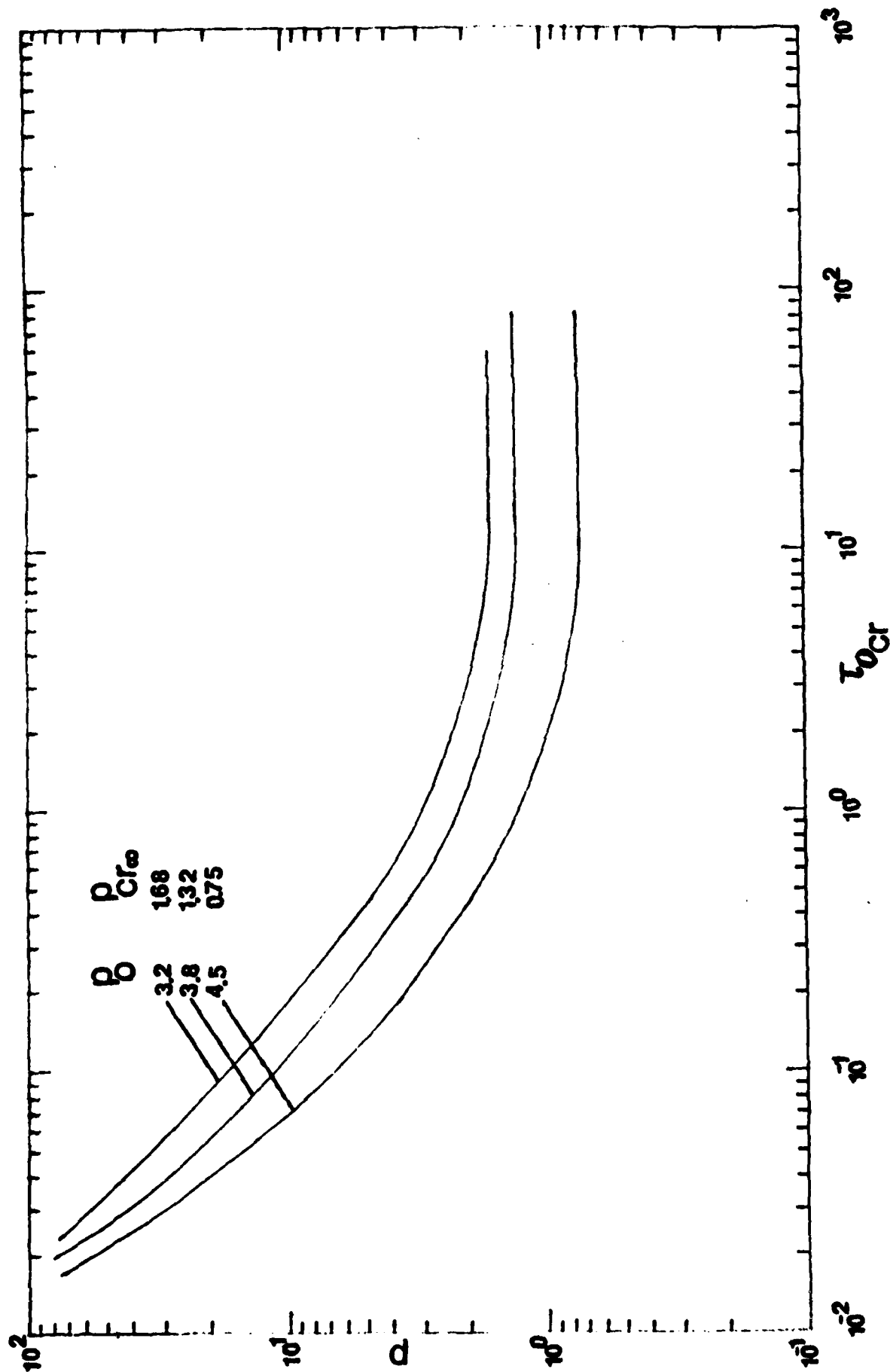


Fig. 6.14. Constant load, P , versus critical Duration Time, τ_{0cr} , Preloaded Model C, $\Lambda = 5.0$

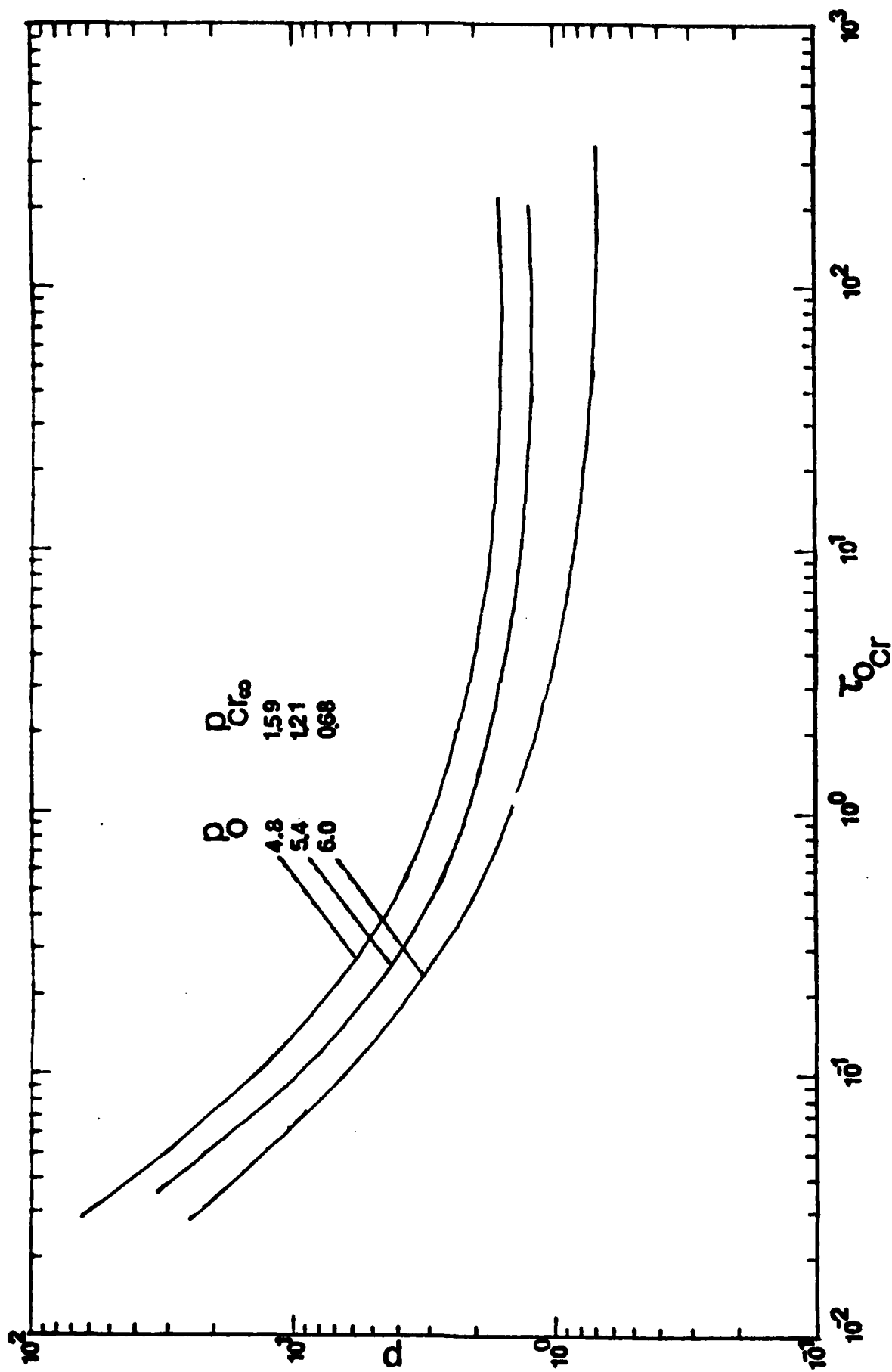


Fig. 6.15. Constant load, P , versus Critical Duration Time, τ_{cr} , preloaded Model C, $\Lambda = 6.0$

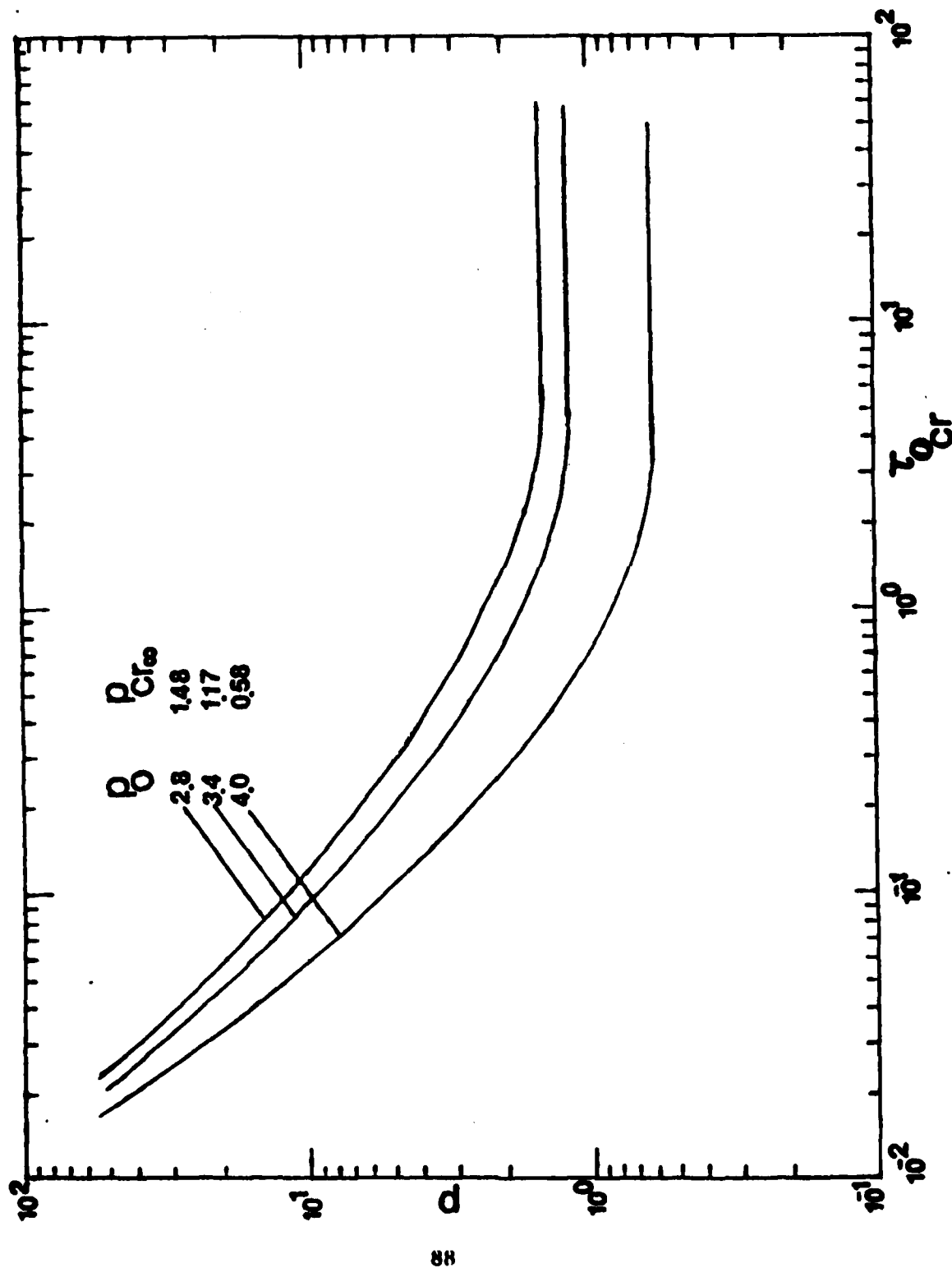


Fig. 6.16. Constant load, P , versus Critical Duration Time, τ_{ocr} , preloaded Model C, $\Lambda = 8.0$

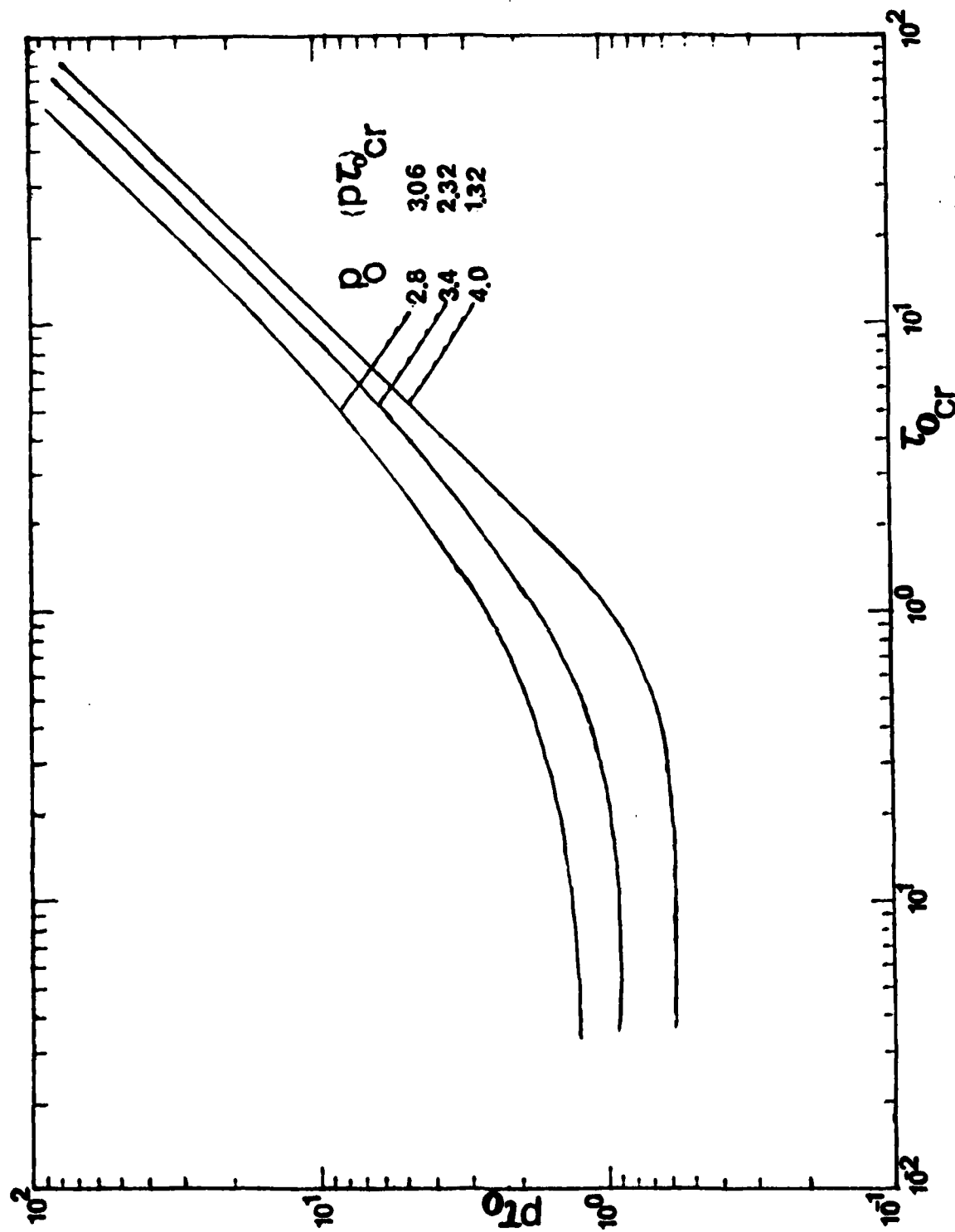


Fig. 6.17. Impulse, p_o , versus critical Time Duration, $\tau_{o_{cr}}$, preloaded Model C, $\lambda = 5.0$

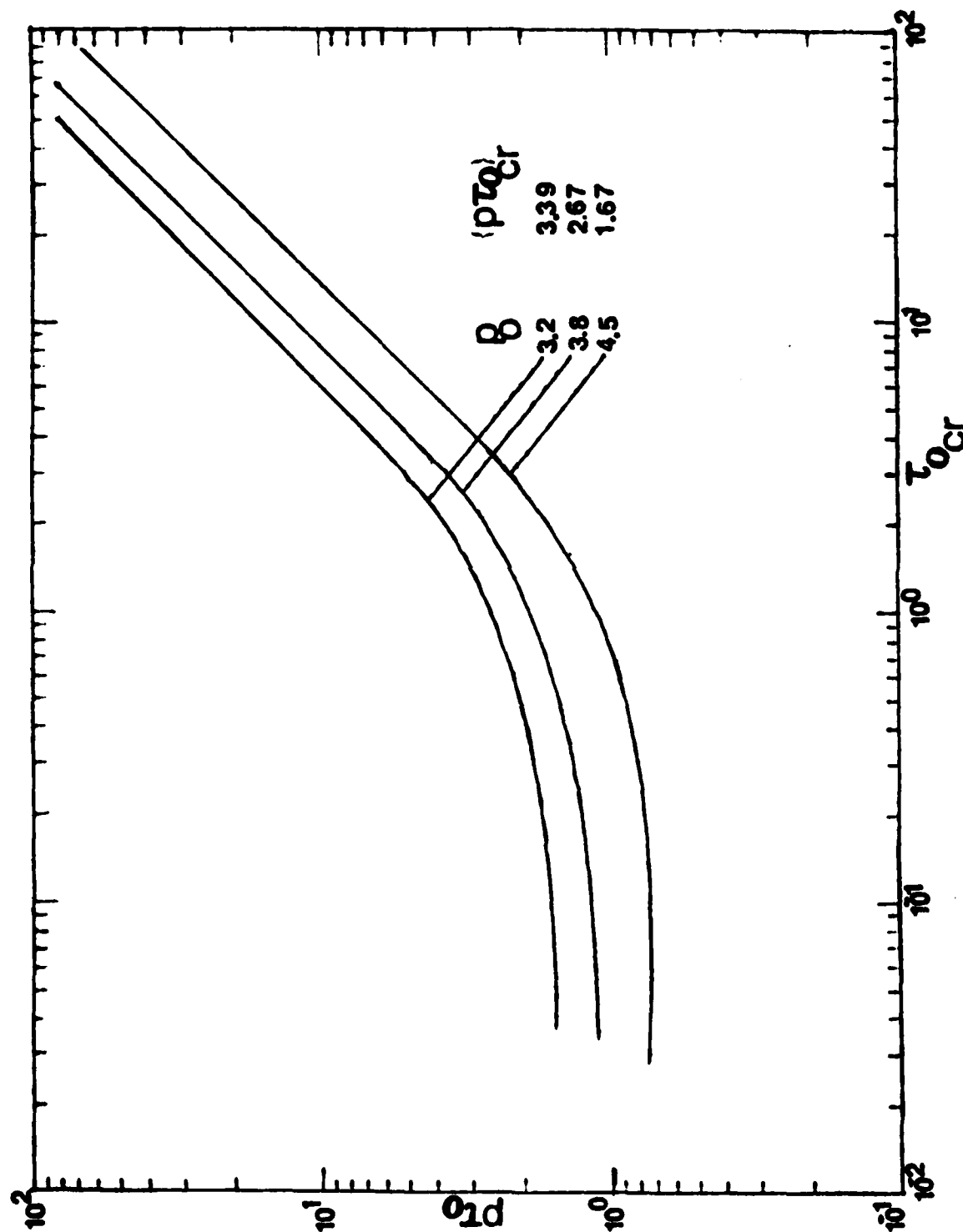


Fig. 5.15. Impulse, (p_0) , versus critical Duration Time, τ_{0cr} , preloaded Model C, $\lambda = 6.0$

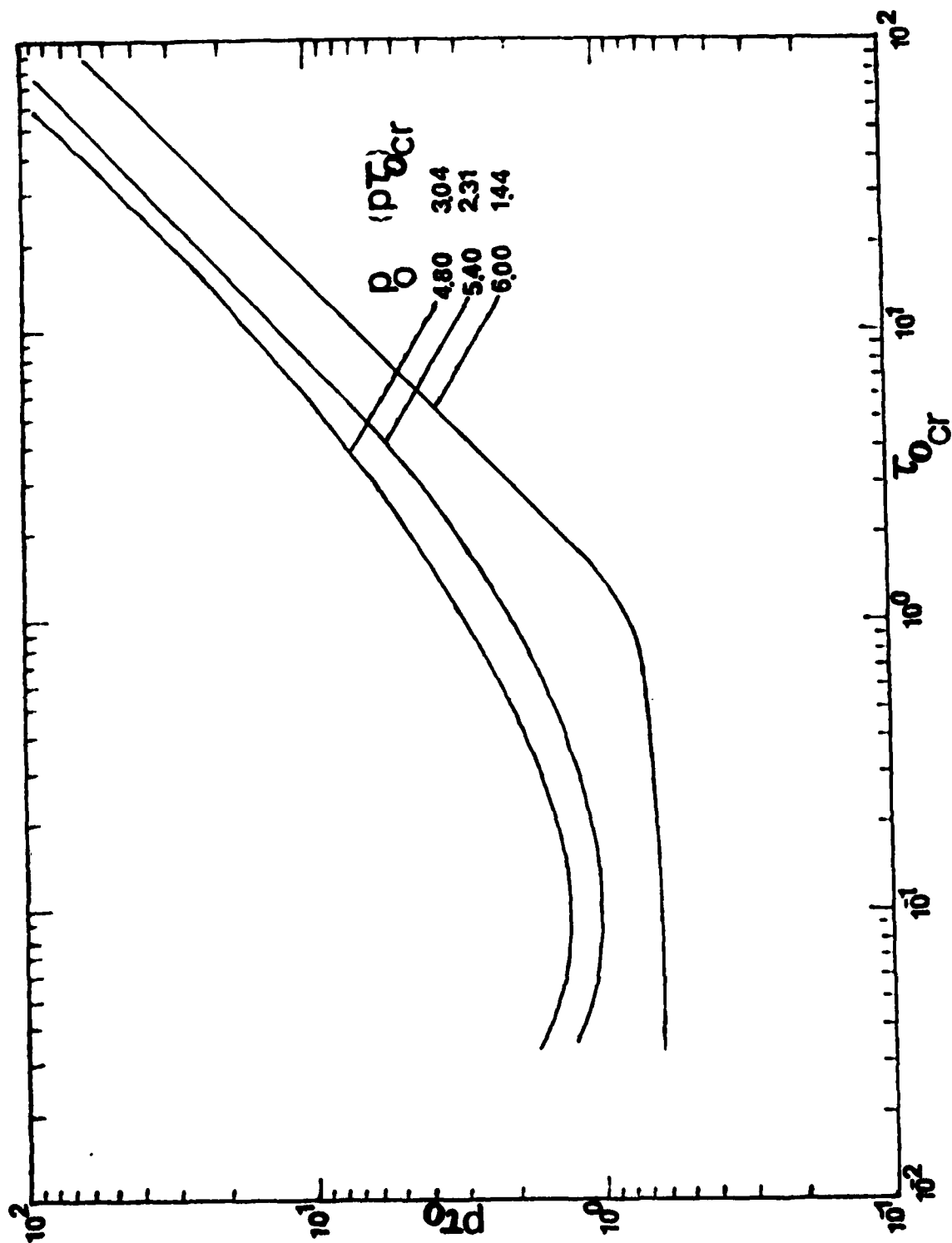


FIG. 6.19. Impulse, (p_0) , versus Critical Duration Time, τ_{0cr} , preloaded Model C, $\Lambda = 8.0$

SECTION VII
THE INFLUENCE OF SMALL DAMPING - CONSTANT LOAD OF FINITE DURATION

Statement of the Problem

In this section the effect of small damping on critical conditions and estimates for dynamic stability of the models are investigated. The problem of constant load for finite duration is considered here as stated in Section V, but small damping is introduced by a dashpot connected in parallel with a spring.

Since damping is small, the trajectory of the damped system could be thought of as a perturbation around the trajectory of the undamped one. This is the key assumption which helps find the estimates for the damped system as a sum of the corresponding estimates for the undamped system plus a product of the small damping coefficient, μ , times a quantity depending only on the model geometry.

General Approach

Damping forces F are introduced by a dashpot and are equal to

$$F = \mu \dot{L}$$

where μ is the damping coefficient and L the trajectory of the dashpot.

A nondimensionalization, $\bar{\mu}$, of the damping coefficient μ could be obtained by

$$\bar{\mu} = \frac{1}{\lambda k} \mu$$

where k is the elastic constant of the spring and λ a normalizing coefficient having dimension of time.

Furthermore the nondimensionalized dissipated energy, \bar{D} , is expressed by

$$\bar{D} = \bar{\mu} \int_L \dot{L} dL \quad (7.1)$$

where $\int_L \dot{L} dL$ stands for the nondimensionalized dissipated energy when $\bar{\mu} = 1$. The balance of energy is expressed by the equations

$$\bar{T}^P + \bar{U}_T^P + \bar{D} = 0 \text{ for } 0 < \tau < \tau_0 \quad (7.2)$$

$$\text{and } \bar{T}^0 + \bar{U}_T^0 + \bar{D} = C \text{ for } \tau_0 < \tau \quad (7.3)$$

where C is a constant. Eq. (7.2) characterizes the energy balance during the action of the load, p , and Eq. (7.3) after the release of P .

Moreover, the continuity and both kinetic and dissipated energies at the release of the load yields the constant coefficient C , equal to

$$C = \left[\bar{U}_T^0 - \bar{U}_T^P \right] \Big|_{\tau_0}$$

With this value of C , Eq. (7.3), the balance of energy after the action of the load P becomes

$$\bar{T}^0 + \bar{U}_T^0 + \bar{D} + \left[\bar{U}_T^P - \bar{U}_T^0 \right] \Big|_{\tau_0} = 0 \text{ for } \tau_0 < \tau \quad (7.4)$$

Since a system is called dynamically stable if it is not allowed to reach the zero-load unstable equilibrium point, L_u^0 , with the least potential energy, the total energy of the system, $\bar{E}^0 = \bar{U}_T^0 + \bar{T}^0$, with zero velocity (Kinetic Energy) at L_u^0 , must be less than the potential energy of the system at that point.

Consequently the balance of energy for $\tau > \tau_0$ expressed by Eq. (7.4) gives the critical condition

$$\bar{U}_T^0 \Big|_{L_U^0} = \bar{D} \Big|_{L_U^0} - \left[\bar{U}_T^P - \bar{U}_T^0 \right] \Big|_{\tau_0} \quad (7.5)$$

Furthermore the nondimensionalized damping coefficient $\bar{\mu}$ is very small ($\bar{\mu} \ll 1$) and the trajectory of the damped system could be thought of as a perturbation around the undamped one. The critical displacement, L_{cr}^P , the displacement which guarantees stability as long as the applied force is released before the system reaches it, may be expanded in a Taylor's series as,

$$L_{cr}^P = {}_0L_{cr}^P + \bar{\mu} {}_1L_{cr}^P + o(\bar{\mu}^2) \quad (7.6)$$

where ${}_0L_{cr}^P$ is the critical displacement for the same problem but without the influence of damping.

Use of Eq. (7.1) into Eq. (7.5) yields

$$\bar{U}_T^0 \Big|_{L_U^0} = -\bar{\mu} \int_0^{L_U^0} \dot{L} dL - \left[\bar{U}_T^P - \bar{U}_T^0 \right] \Big|_{L_{cr}^P} \quad (7.7)$$

Invoking the expression for L_{cr}^P from Eq. (7.6), the quantity $\left[\bar{U}_T^P - \bar{U}_T^0 \right] \Big|_{L_{cr}^P}$ may be expanded in Taylor's series also.

$$\left[\bar{U}_T^P - \bar{U}_T^0 \right] \Big|_{L_{cr}^P} = \left[\bar{U}_T^P - \bar{U}_T^0 \right] \Big|_{{}_0L_{cr}^P} + \bar{\mu} \sum_{i=1}^j \frac{\partial \left[\bar{U}_T^P - \bar{U}_T^0 \right]}{\partial L_i} \Big|_{{}_0L_{cr}^P} ({}_1L_{cr}^P) + o(\bar{\mu}^2) \quad (7.8)$$

where j stands for the degrees of freedom of the model.

Introducing Eq. (7.8) into Eq. (7.7) and separating terms of the same order of magnitude, yields two equations

$$\ddot{u}_T^0 \Big|_{L_u^0} - [\ddot{u}_T^P - \ddot{u}_T^0] \Big|_{L_{cr}^P} \quad (7.9)$$

and for one degree of freedom trajectory

$$L_{cr}^P = - \frac{\int_0^{L_u^0} \ddot{\phi} f(\phi) d\phi}{[\ddot{u}_T^P - \ddot{u}_T^0] \Big|_{L_{cr}^P}} \quad (7.10)$$

After evaluating L_{cr}^P , the critical time $t_{o_{cr}}$ for the release of the load P is found by the balance of energy equation (Eq. 7.2).

It is simply mentioned that Eq. (7.9) gives the displacement estimate L_{cr}^P for the undamped system and it is the same as that given in Section V.

On each model Eqs. (7.9) and (7.10) will be applied and the correction of the displacement, L_{cr}^P ($\bar{\mu} = 1$), will be found. Furthermore, corrections for the critical time, $\tau_{o_{cr}}$, will be computed also.

Model A - Geometrically Imperfect Model

Consider model A exhibited in Section II but under the influence of small damping. Damping is introduced by a dashpot connected with the spring as shown on Fig. 7-1.

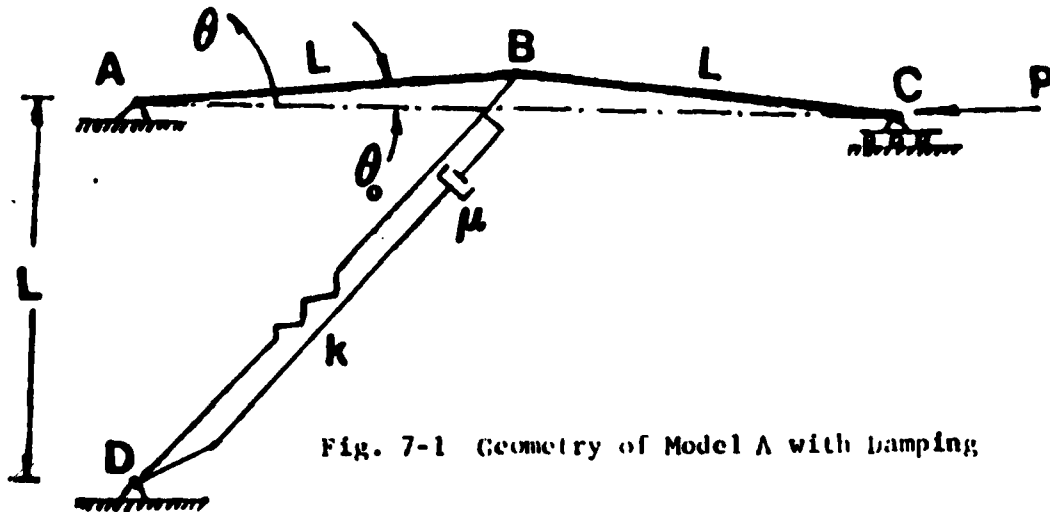


Fig. 7-1 Geometry of Model A with Damping

If μ is the damping coefficient, the nondimensionalized dissipated energy, \bar{D} , is expressed by

$$\bar{D} = \frac{D}{kL} = \bar{\mu} \int_{\theta_0}^{\theta} \dot{\varphi} \sin^2\left(\frac{\pi}{4} - \frac{\varphi}{2}\right) d\varphi \quad (7.11)$$

It is assumed that the velocity of the dashpot is equal to that of joint B, and that φ is the trajectory from θ_0 to θ .

Applying the nondimensionalization

$$\tau = \sqrt{\frac{2k}{m}} t, \quad \bar{\mu} = \frac{\sqrt{2}}{\sqrt{km}} \mu \text{ and } (\dot{}) = \frac{\partial}{\partial \tau} \quad (7.12)$$

and recalling that the unstable position, L_y^0 , on the zero load potential for the undamped system is given by $\theta = \frac{\pi}{2}$, the Eqs. (7.9) and (7.10) yield

$$\theta_{cr}^P = \arccos \left\{ \cos \theta_0 - \frac{(\sqrt{2} - \sqrt{1 + \sin \theta_0})^2}{P} \right\} \quad (7.13)$$

$$\text{and } I_{cr}^P = \int_{\theta_0}^{\frac{\pi}{2}} \dot{\varphi} \sin^2\left(\frac{\pi}{4} - \frac{\varphi}{2}\right) d\varphi / P \sin \theta_{cr}^P \quad (7.14)$$

The evaluation of the integral below is needed in Eq. (7.14)

$$I = \int_{\theta_0}^{\frac{\pi}{2}} \dot{\varphi} \sin^2\left(\frac{\pi}{4} - \frac{\varphi}{2}\right) d\varphi \quad (7.15)$$

Recalling the energy equation for the undamped system, Eqs. (5.1) and (5.2)

$$\dot{\varphi}^2 + [\sqrt{1 + \sin \varphi} - \sqrt{1 + \sin \theta_0}]^2 - P (\cos \theta_0 - \cos \theta) = 0 \quad \theta_0 < \varphi < \theta_{cr} \quad (7.16)$$

and

$$\dot{\varphi}_0^2 + [\sqrt{1+\sin\varphi_0} - \sqrt{1+\sin\theta_0}]^2 = p(\cos\theta_0 - \cos\theta_{cr}^P) - \theta_{cr}^P \varphi_0 < \frac{\pi}{2} \quad (7.17)$$

Hence the integral I becomes

$$I = \int_{\theta_0}^{\theta_{cr}^P} \sqrt{p(\cos\theta_0 - \cos\theta) - [\sqrt{1+\sin\varphi_0} - \sqrt{1+\sin\theta_0}]^2} \sin^2\left(\frac{\pi}{4} - \frac{\varphi_0}{2}\right) d\theta +$$

$$\int_{\theta_{cr}^P}^{\pi/2} \sqrt{p(\cos\theta_0 - \cos\theta_{cr}^P) - [\sqrt{1+\sin\varphi_0} - \sqrt{1+\sin\theta_0}]^2} \sin^2\left(\frac{\pi}{4} - \frac{\varphi_0}{2}\right) d\theta \quad (7.18)$$

The critical time $\tau_{o_{cr}}$ may be found by invoking Eq. (7.2) for $0 < \tau < \tau_{o_{cr}}$. Thus

$$\tau_{o_{cr}} = \int_{\theta_0}^{\theta_{cr}^P} \frac{d\theta}{\sqrt{p(\cos\theta_0 - \cos\theta) - [\sqrt{1+\sin\varphi_0} - \sqrt{1+\sin\theta_0}]^2} - \frac{\theta_0}{\mu} \int_{\theta_0}^{\theta_{cr}^P} \sin^2\left(\frac{\pi}{4} - \frac{\varphi_0}{2}\right) d\varphi} \quad (7.19)$$

Expanding $\tau_{o_{cr}}$ in power series of $\bar{\mu}$ we have

$$\tau_{o_{cr}} = \tau_{o_{cr}}^0 + \bar{\mu} \tau_{o_{cr}}^1 + O(\bar{\mu}^2) \quad (7.20)$$

where

$$\tau_{o_{cr}}^0 = \int_{\theta_0}^{\theta_{cr}^P} \frac{d\theta}{\sqrt{p(\cos\theta_0 - \cos\theta) - [\sqrt{1+\sin\varphi_0} - \sqrt{1+\sin\theta_0}]^2}} \quad (7.21)$$

is the critical time for the undamped system, and

$$\tau_{o_{cr}}^1 = \frac{\partial \tau_{o_{cr}}}{\partial \bar{\mu}} \Big|_{\bar{\mu}=0} = \frac{1}{2} \int_{\theta_0}^{\theta_{cr}^P} \frac{\left\{ \int_{\theta_0}^{\theta} \dot{\varphi} \sin^2\left(\frac{\pi}{4} - \frac{\varphi_0}{2}\right) d\varphi \right\} d\theta}{[p(\cos\theta_0 - \cos\theta) - (\sqrt{1+\sin\varphi_0} - \sqrt{1+\sin\theta_0})^2]^{3/2}} +$$

$$+ \frac{l_{cr}^{\theta^P}}{\sqrt{p(\cos\theta_o - \cos\theta_{cr}^P) - [\sqrt{1+\sin\theta_{cr}^P} - \sqrt{1+\sin\theta_o}]^2}} \quad (7.22)$$

Note that $l_{cr}^{\theta^P}$ is a function of parameters related to the undamped system only. The same holds true for l_o^{τ} .

The governing equations for finding critical conditions in the presence of small damping ($\bar{\mu} \ll 1$) are Eqs. (7.13), (7.14), (7.21) and (7.22). Note that Eq. (7.18) is employed in Eq. (7.14). These four equations relate the given small damping coefficient $\bar{\mu}$, the applied load p , and the time parameters θ_{cr}^P and $l_{cr}^{\theta^P}$. A critical condition is expressed in terms of a load level p and the corresponding time $\tau_{o_{cr}} = \tau_{o_{cr}} + \bar{\mu} l_{cr}^{\tau}$. Thus, a critical condition may be found by posing the problem as follows: for a given small damping coefficient $\bar{\mu}$ and load level p , find (through the simultaneous solution of the four governing equations) the corresponding critical time parameters, $\tau_{o_{cr}}$ and l_{cr}^{τ} , and position parameters, θ_{cr}^P and $l_{cr}^{\theta^P}$. Note that the range of p -values (assigned) must be greater than dynamic critical load for the case of a suddenly applied constant load of infinite duration, without damping. The computational procedure involves the following steps: (a) assign a p -value and compute θ_{cr}^P from Eq. (7.13), (b) Employ Eq. (7.18) in Eq. (7.14) and solve for $l_{cr}^{\theta^P}$, (c) From Eq. (7.21) solve for $\tau_{o_{cr}}$, and finally (d) Employ Eq. (7.22) and solve for l_{cr}^{τ} . A computer program is written to accomplish the solution and numerical results are generated for three values of the imperfection parameter δ_o (0.005, 0.010, and 0.020). These results are presented on Table 7.1.

Table 7.1. Critical Conditions for Constant Load of Finite Duration in the Presence of Damping; (Model A)

θ_o	P	$\alpha^T o_{cr}$	$1^T o_{cr}$
0.005	0.45	31.25	29.61
	0.50	19.55	11.15
	1.00	8.97	1.99
	3.00	3.42	.55
	5.00	2.63	0.35
	10.00	2.11	0.20
	50.00	0.63	0.06
0.010	0.41	33.23	78.53
	0.45	21.14	12.85
	0.50	12.32	7.30
	1.00	7.78	1.64
	5.00	2.00	.31
	10.00	1.24	.18
	50.00	0.42	.07
0.020	0.44	13.69	7.47
	0.55	9.98	3.62
	0.65	6.87	2.53
	1.00	5.85	1.30
	5.00	1.91	.27
	10.00	0.96	.16
	50.00	0.39	.06

Note that, since a critical condition corresponds to a set of $p, \tau_{o_{cr}}$ values, a small damping coefficient $\bar{\mu}$ has a stabilizing effect. This effect, though, is very small. For instance, at the high values of the load p (say for $\theta_o = 0.005$, $p = 10$) the corresponding value for $\tau_{o_{cr}}$ (if $\bar{\mu} = 0.04$) is $2.110 + 0.008 = 2.118$. Remember that the $p - \tau_{o_{cr}}$ curve for the undamped system (see Fig. 5) is very steep at the high p -value and virtually flat at the low values of p . On the other hand, when $p = 0.45$ (a value close to $p_{cr_o} = 0.432$) the corresponding critical time is $\tau_{o_{cr}} = 31.25 + 1.184 = 32.434$. Since the curve is very flat at this load p -value, one may conclude that the effect of small damping is virtually negligible.

Model B

Consider model B discussed in Section II, but under the influence of small damping. Damping is introduced by a dashpot connected with the spring on Fig. 7-2.

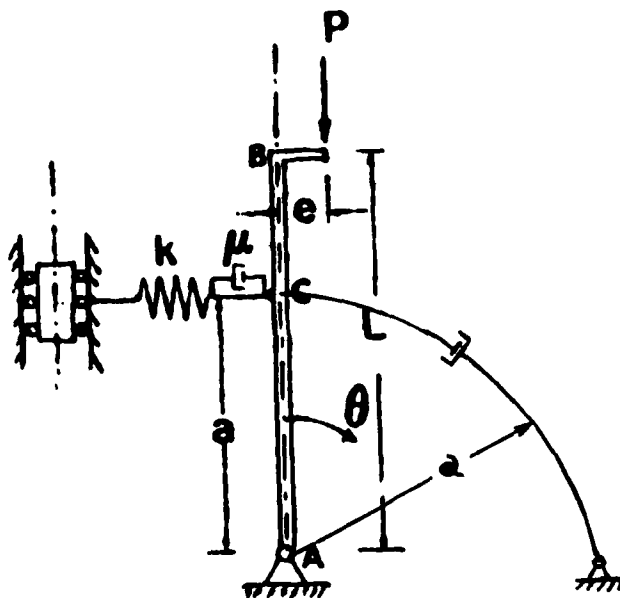


Fig. 7-2. Geometry of Model B with damping.

If μ is the damping coefficient, the nondimensionalized dissipated energy, \bar{D} , is expressed by

$$\bar{D} = \frac{D}{\frac{1}{2} k \alpha^2} = \frac{2\mu}{k} \int_0^{\theta} \dot{\phi} d\phi \quad (7.23)$$

It is assumed that the velocity of the dashpot is equal to that at joint C and ϕ is the trajectory from 0 to θ .

Applying the nondimensionalization

$$\tau = \frac{a}{L} \sqrt{\frac{k}{m}} t, \quad \bar{\mu} = \frac{2a}{L \sqrt{km}} \mu \text{ and } (\dot{}) = \frac{\partial}{\partial \tau} \quad (7.24)$$

and recalling that the unstable position, L_u^0 , for the "zero load" potential of the undamped system is given by $\theta_u^0 = \frac{\pi}{2}$, then Eqs. (7.9) and (7.10) yield

$$2p (1 - \cos \theta_{cr} + \bar{e} \sin \theta_{cr}) = 1 \quad (7.25)$$

and

$$I_{cr}^{\theta} = \frac{\int_0^{\frac{\pi}{2}} \dot{\phi} d\phi}{2p (\sin \theta_{cr} + \bar{e} \cos \theta_{cr})} \quad (7.26)$$

Thus for the evaluation of the integral

$$I = \int_0^{\frac{\pi}{2}} \dot{\phi} d\phi \quad (7.27)$$

the balance of energy expressions for the undamped system Eqs. (5.1) and (5.4) are recalled. Hence

$$\dot{\phi}^2 + \sin^2 \phi - 2p (1 - \cos \phi + \bar{e} \sin \phi) = 0 \quad \text{for } 0 < \phi < \theta_{cr} \quad (7.28)$$

and

$$\dot{\phi}^2 + \sin^2 \phi - 2p (1 - \cos \theta_{cr} + \bar{e} \sin \theta_{cr}) = 0 \quad \text{for } \theta_{cr} < \phi < \frac{\pi}{2} \quad (7.29)$$

Integral I becomes

$$I = \int_0^{\theta_{cr}^P} \sqrt{2p (1 - \cos_{\theta} \varphi + \bar{e} \sin_{\theta} \varphi) - \sin^2_{\theta} \varphi} d_{\theta} \varphi + \int_{\theta_{cr}}^{\frac{\pi}{2}} \sqrt{2p (1 - \cos_{\theta} \theta_{cr} + \bar{e} \sin_{\theta} \theta_{cr}) - \sin^2_{\theta} \varphi} d_{\theta} \varphi \quad (7.30)$$

The critical time, $\tau_{\theta_{cr}}$, may be found by invoking Eq. (7.2). Thus

$$\tau_{\theta_{cr}} = \int_0^{\theta_{cr}^P} \frac{d\theta}{\sqrt{2p (1 - \cos \theta + \bar{e} \sin \theta) - \sin^2 \theta - \bar{\mu} \int_0^{\theta} \dot{\varphi} d_{\theta} \varphi}} \quad (7.31)$$

Expanding $\tau_{\theta_{cr}}$ in power series of $\bar{\mu}$ ($\bar{\mu} \ll 1$) one obtains

$$\tau_{\theta_{cr}} = {}^0\tau_{\theta_{cr}} + \bar{\mu} {}^1\tau_{\theta_{cr}} + o(\mu^2) \quad (7.32)$$

where

$${}^0\tau_{\theta_{cr}} = \int_0^{\theta_{cr}^P} \frac{d\theta}{\sqrt{2p (1 - \cos \theta + \bar{e} \sin \theta) - \sin^2 \theta}} \quad (7.33)$$

is the critical time for the undamped system, and

$${}^1\tau_{\theta_{cr}} = \left. \frac{\partial \tau_{\theta_{cr}}}{\partial \bar{\mu}} \right|_{\bar{\mu}=0} = \frac{1}{2} \int_0^{\theta_{cr}^P} \frac{\int_0^{\theta} \dot{\varphi} d_{\theta} \varphi}{[2p(1 - \cos \theta + \bar{e} \sin \theta) - \sin^2 \theta]^{3/2}} d\theta + \frac{{}^1\theta_{cr}^P}{\sqrt{2p (1 - \cos_{\theta} \theta_{cr} + \bar{e} \sin_{\theta} \theta_{cr}) - \sin^2_{\theta} \theta_{cr}}} \quad (7.34)$$

Note that ${}^1\theta_{cr}^P$ is a function of parameters related to the undamped system parameters only. The same holds true for ${}^1\tau_{\theta_{cr}}$.

The governing equations for finding critical conditions in the presence of small damping ($\bar{\mu} \ll 1$) are Eqs. (7.25), (7.26), (7.33) and (7.34). Note that Eq. (7.30) is employed in Eq. (7.26). These four equations relate the given small damping coefficient $\bar{\mu}$, the applied load p , the time parameters $\tau_{o\ cr}$ and $\tau_{l\ cr}$, and the position parameters $\theta_{o\ cr}^P$ and $\theta_{l\ cr}^P$. A critical condition is expressed in terms of a load level p and the corresponding time $\tau_{o\ cr} = \tau_{o\ cr} + \bar{\mu} \tau_{l\ cr}$. Thus, a critical condition may be found by posing the problem as follows: for a given small damping coefficient $\bar{\mu}$ and load level p , find (through the simultaneous solution of the four governing equations) the corresponding critical time parameters, $\tau_{o\ cr}$ and $\tau_{l\ cr}$, and position parameters, $\theta_{o\ cr}^P$ and $\theta_{l\ cr}^P$. Note that the range of p -values (assigned) must be greater than dynamic critical load for the case of a suddenly applied constant load of infinite duration, without damping. The computational procedure involves the following steps: (a) assign a p -value and compute $\theta_{o\ cr}^P$ from Eq. (7.25), (b) employ Eq. (7.30) in Eq. (7.26) and solve for $\theta_{l\ cr}^P$, (c) from Eq. (7.33) solve for $\tau_{o\ cr}$, and finally (d) employ Eq. (7.34) and solve for $\tau_{l\ cr}$.

A computer program is written to accomplish the solution and numerical results are generated for three values of the eccentricity parameter \bar{e} (0.005, 0.010, and 0.020). These results are presented in Table 7.2.

Note that, since a critical condition corresponds to a set of p , $\tau_{o\ cr}$ values, a small damping coefficient $\bar{\mu}$ has a stabilizing effect. This effect, though, is very small. For instance, at the high values of the load p (say for $\bar{e} = 0.005$, $p = 10$) the corresponding value for $\tau_{o\ cr}$ (if $\bar{\mu} = 0.04$) is $0.16 + 0.0064 = 0.1664$. Remember that the p - $\tau_{o\ cr}$ curve for

the undamped system (see Fig. 5.3) is very steep at the high p -value and virtually flat at the low values of p . On the other hand, when $p = 0.95$ (a value close to $p_{cr_{\infty}} = 0.948$), the corresponding critical time is $\tau_{o_{cr}} = 1.93 + 0.055 = 1.985$. Since the curve is very flat at this load p -value, one may conclude that the effect of small damping is virtually negligible.

Table 7.2. Critical Conditions for Constant Load of Finite Duration in the Presence of Damping (Model B).

\bar{e}	P	$\sigma_{o_{cr}}^T$	$l_{o_{cr}}^T$
0.005	0.95	1.93	1.39
	1.20	1.28	1.04
	1.50	0.75	0.80
	5.00	0.23	0.27
	10.00	0.16	0.16
	100.00	0.029	0.04
0.01	1.15	1.22	10.04
	1.70	0.65	2.06
	5.00	0.27	0.33
	10.00	0.18	0.14
	20.00	0.11	0.07
	100.00	0.024	0.06
0.02	1.10	0.78	13.96
	1.50	0.46	2.90
	5.00	0.16	0.33
	10.00	0.092	0.14
	30.00	0.048	0.04
	75.00	0.022	0.02

Model C

In this article, the effect of small damping on a two-degree of freedom model (model C) is investigated. Damping is introduced through a dashpot connected with the extensional spring as is indicated on Fig. 4.2.

The damping coefficient is equal to μ .

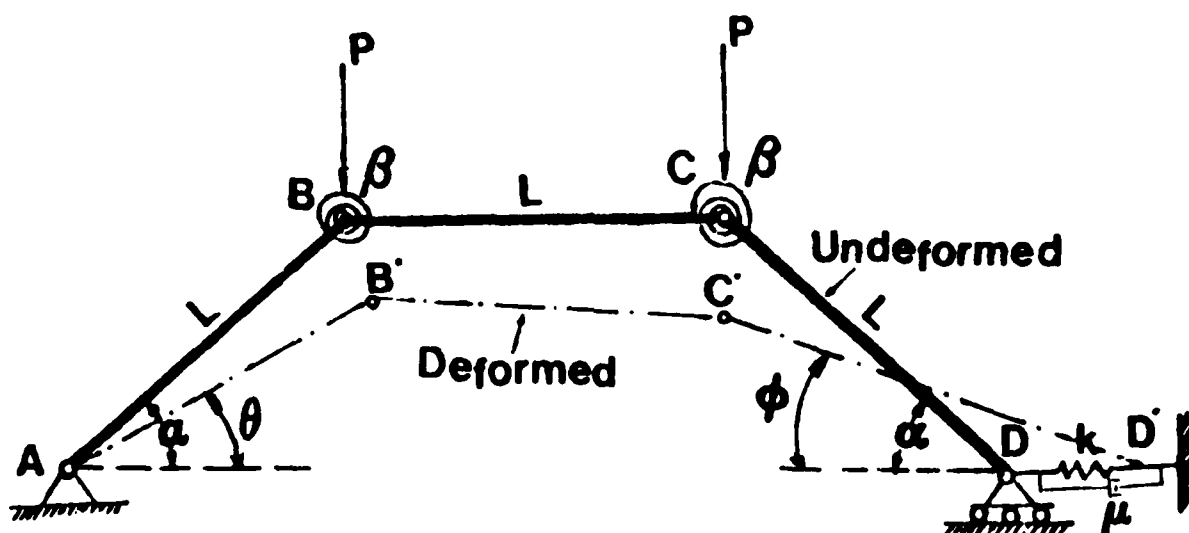


Fig. 7-3. Geometry of Model C with damping

Since the nondimensionalized extension of the spring is

$$w = \Lambda - r^2 - 3s^2 \quad (7.35)$$

the rate of change with respect to time is equal to

$$\frac{dw}{dt} = -2\dot{r}r - 3\dot{s}s \quad (7.36)$$

If $\bar{\mu} = \frac{1}{\left(\frac{Bk}{2m}\right)^{\frac{1}{2}} k} \mu$, the nondimensionalized damping coefficient and \bar{D} the nondimensionalized dissipated energy, then

$$\bar{D} = \bar{\mu} \int \frac{dw}{d\tau} dw \quad (7.37)$$

and with the right hand sides of the Eqs. (7.35) and (7.36), the nondimensionalize dissipated energy becomes

$$\bar{D} = \bar{\mu} \oint (2\dot{r}r + 6\dot{s}s) (2rdr + 6sds) \quad (7.38)$$

where \oint stands for the line integral along the trajectory of the system in the r - s plane. Furthermore, the lowest potential unstable equilibrium position of the "zero load" potential is the saddle point with

$$\bar{U}_T^0 = \frac{9}{2} (\Lambda - 1) \quad (7.39)$$

Recalling that for the undamped system the trajectory, which must be followed for maximizing the added energy when p is acting, lies on the r axis, and recalling Eq. (7.9), it is found that

$$r_{cr}^p = \frac{9}{4p} (\Lambda - 1) + \sqrt{\Lambda} \quad (7.40)$$

However, the trajectory that the system follows from the release of the load until it reaches the unstable saddle point ($r = \sqrt{\Lambda} - \frac{3}{2}$, $s = \pm (\sqrt{\Lambda} - \frac{7}{4})^{\frac{1}{2}}$) is not known. Since Eq. (7.38) gives the dissipated energy during this period of time as

$$\bar{D} = \bar{\mu} \int_{r_{cr}^p}^{\sqrt{\Lambda} - \frac{3}{2}} (2r + 6ss')^2 \frac{0}{r} dr ,$$

a lower bound for the absolute value of \bar{D} may be found, if one considers

the path, $s \equiv 0$ and $\sqrt{\Lambda} - \frac{3}{2} \leq r \leq \sqrt{\Lambda}$. Note that $r = \sqrt{\Lambda}$ is the starting point and $r = \sqrt{\Lambda} - \frac{3}{2}$ is the r -coordinate of the saddle point on the "zero load" potential.

Following the same steps as in the brachistochrone problem (see Appendix A), it is proven that the symmetric path $s \equiv 0$ is the minimizing path for \bar{D} min. Then from Eq. (7.10)

$$1r_{cr}^P = -\frac{1}{2p} \int_{\sqrt{\Lambda}}^{\sqrt{\Lambda} - \frac{3}{2}} 4\dot{r}^2 d\tau \quad (7.41)$$

where r_{cr}^P is the parameter shown in the equation

$$r_{cr}^P = {}_0r_{cr}^P + \bar{\mu} 1r_{cr}^P + o(\bar{\mu}^2) \quad (7.42)$$

Furthermore, recalling that the total energy for the undamped system along the r axis ($s \equiv 0$) is expressed by

$$\frac{1}{2} (\dot{r})^2 + (r - \sqrt{\Lambda})^2 + \frac{1}{2} (\Lambda - r^2)^2 - 2p(\sqrt{\Lambda} - r) = 0, \quad (7.43)$$

then

$$\dot{r} = -\sqrt{4p(\sqrt{\Lambda} - r) - (\Lambda - r^2)^2 - 2(r - \sqrt{\Lambda})^2} \quad (7.44)$$

Hence, Eq. (7.41) becomes

$$1r_{cr}^P = -\frac{2}{p} \int_{{}_0r_{cr}^P}^{{}_P r_{cr}^P} r^2 \sqrt{4p(\sqrt{\Lambda} - r) - (\Lambda - r^2)^2 - 2(r - \sqrt{\Lambda})^2} dr \\ - \frac{2}{p} \int_{{}_0r_{cr}^P}^{\sqrt{\Lambda} - \frac{3}{2}} r^2 \sqrt{4p(\sqrt{\Lambda} - {}_0r_{cr}^P) - (\Lambda - r^2)^2 - 2(r - \sqrt{\Lambda})^2} dr \quad (7.45)$$

In addition, the critical time τ_0 may be found by invoking Eq. (7.2), which

expresses the balance of energy for $0 < \tau < \tau_0$. Thus,

$$\tau_{0\text{cr}}^P = \int_{\sqrt{\Lambda}}^{r_{\text{cr}}^P} \frac{dr}{\sqrt{4p(\sqrt{\Lambda} - r) - (\Lambda - r^2)^2 - 2(r - \sqrt{\Lambda}) - 8\bar{\mu} \int_{\sqrt{\Lambda}}^{r_{\text{cr}}^P} x^2 dx}} \quad (7.46)$$

and expanding τ_0 in power series of $\bar{\mu}$ ($\bar{\mu} \ll 1$), one may write

$$\tau_{0\text{cr}} = {}_0\tau_{0\text{cr}} + \bar{\mu} {}_1\tau_{0\text{cr}} + O(\bar{\mu}^2) \quad (7.47)$$

where

$${}_0\tau_{0\text{cr}}^P = \tau_{0\text{cr}} \Big|_{\bar{\mu}=0} = \int_0^{r_{\text{cr}}^P} \frac{dr}{\sqrt{4p(\sqrt{\Lambda} - r) - (\Lambda - r^2)^2 - 2(r - \sqrt{\Lambda})^2}} \quad (7.48)$$

and

$$\begin{aligned} {}_1\tau_{0\text{cr}} &= \frac{\partial \tau_{0\text{cr}}}{\partial \bar{\mu}} \Big|_{\bar{\mu}=0} = \int_{\sqrt{\Lambda}}^{r_{\text{cr}}^P} \frac{8 \int_{\sqrt{\Lambda}}^r x^2 \sqrt{4p(\sqrt{\Lambda} - x) - (\Lambda - x^2)^2 - 2(x - \sqrt{\Lambda})^2} dx}{[4p(\sqrt{\Lambda} - r) - (\Lambda - r^2)^2 - 2(r - \sqrt{\Lambda})^2]^{3/2}} dr \\ &\quad - \frac{{}_1r_{\text{cr}}}{\sqrt{4p(\sqrt{\Lambda} - {}_0r_{\text{cr}}) - (\Lambda - {}_0r_{\text{cr}}^2)^2 - 2({}_0r_{\text{cr}} - \sqrt{\Lambda})^2}} \end{aligned} \quad (7.49)$$

Note that ${}_1r_{\text{cr}}^P$ is a function of the undamped system only. The same holds true for ${}_1\tau_{0\text{cr}}$.

The governing equations for finding critical conditions in the presence of small damping ($\bar{\mu} \ll 1$) are Eqs. (7.40), (7.45), (7.48) and (7.49).

These four equations relate the given small damping coefficient $\bar{\mu}$, the applied load p , the time parameters ${}_0\tau_{0\text{cr}}$ and ${}_1\tau_{0\text{cr}}$, and the position parameters ${}_0r_{\text{cr}}^P$ and ${}_1r_{\text{cr}}^P$. A critical condition is expressed in terms of a load level p and the corresponding time $\tau_{0\text{cr}} = {}_0\tau_{0\text{cr}} + \bar{\mu} {}_1\tau_{0\text{cr}}$. Thus, a

critical condition may be found by posing the problem as follows: for a given small damping coefficient $\bar{\mu}$ and load level p , find (through the simultaneous solution of the four governing equations) the corresponding critical time parameters, $\tau_{o_{cr}}$ and $\tau_{l_{cr}}$, and position parameters, $r_{o_{cr}}^p$ and $r_{l_{cr}}^p$. Note that the range of p -values (assigned) must be greater than dynamic critical load for the case of a suddenly applied constant load of infinite duration, without damping. The computational procedure involves the following steps: (a) assign a p -value and compute $r_{o_{cr}}^p$ from Eq. (7.40), (b) employ Eq. (7.45) and solve for $r_{l_{cr}}^p$ (c) From Eq. (7.48) solve for $\tau_{o_{cr}}$, and finally (d) employ Eq. (7.49) and solve for $\tau_{l_{cr}}$.

A computer program is written to accomplish the solution and numerical results are generated for three values of the parameter Λ ($\Lambda = 5.0, 6.0, 8.0$).

These results are presented on Table 7.3. Note that, since a critical condition corresponds to a set of $p, \tau_{o_{cr}}$ values, a small damping coefficient $\bar{\mu}$ has a stabilizing effect. This effect, though, is very small. For instance, at the high values of the load p (say for $\Lambda=5, p=10$) the corresponding value for $\tau_{o_{cr}}$ (if $\bar{\mu}=0.04$) is $0.32 + 0.029 = 0.349$. Remember that the $p-\tau_{o_{cr}}$ curve for the undamped system (see Fig. 5.5) is very steep at the high p -value and virtually flat at the low values of p . On the other hand, when $p=4.15$ (a value close to $p_{cr} = 3.71$) the corresponding critical time is $\tau_{o_{cr}} = 1.32 + 3.18 = 4.50$. Since the curve is very flat at this load p -value, one may conclude that the effect of small damping is virtually negligible.

**Table 7.3. Critical Conditions for Constant Load of Finite Duration
in the Presence of Damping (Model C)**

Λ	P	$\sigma_{\sigma_{cr}}^T$	$l_{\sigma_{cr}}^T$
5.0	4.15	1.32	79.66
	4.20	1.29	33.11
	4.30	1.13	16.50
	5.00	0.78	4.12
	8.00	0.39	1.10
	10.00	0.32	0.74
	30.00	0.11	0.10
	70.00	0.41	0.03
	100.00	0.29	0.02
6.0	5.25	1.70	131.11
	5.50	1.52	5.12
	7.00	0.60	2.94
	10.00	0.39	1.57
	12.00	0.34	0.78
	20.00	0.18	0.31
	30.00	0.13	0.16
	50.00	0.078	0.06
	80.00	0.042	0.03
8.0	7.75	0.71	56.31
	8.50	0.65	6.12
	9.00	0.55	4.34
	15.00	0.23	0.99
	20.00	0.21	0.68
	30.00	0.14	0.34
	50.00	0.089	0.11
	80.00	0.052	0.05
	150.00	0.018	0.01

REFERENCES

1. Bolotin, V. V., The Dynamic Stability of Elastic Systems, (Translated by V. I. Weingartner, et al.) Holden-Day, San Francisco, 1964.
2. Stoker, J. J., "On The Stability of Mechanical Systems", Communication on Pure and Applied Math., Vol. VIII, 1955, pp. 133-142.
3. Malin, J. G., Stability Theory of Motions, Oldenbourg, Munich, 1959.
4. Krasovskii, N. N., Stability of Motion, (translated by J. L. Brenner), Stanford University Press, Stanford, 1963.
5. Hahn, W., Theory and Application of Liapunov's Direct Method, Prentice-Hall, Inc., New Jersey, 1963.
6. LaSalle, J. and Lefschetz, S., Stability by Liapunov's Second Method with Applications, Academic Press, New York, 1961.
7. Seckel, E., Stability and Control of Airplanes and Helicopters, Academic Press, New York, 1964.
8. Lefschetz, S., Stability of Nonlinear Control Systems, Academic Press, New York, 1965.
9. Bolotin, V. V., Nonconservative Problems of the Theory of Elastic Stability, Moscow 1961; English Translation published by Pergamon Press, New York, 1963.
10. Herrmann, G., "Stability of Equilibrium of Elastic Systems Subjected to Nonconservative Forces", Applied Mechanics Reviews, Vol. 20, 1967, pp. 103-108.
11. Hsu, C. S., "Stability of Shallow Arches Against Snap-Through Under Tunewise Step Loads", J. Appl. Mech., Vol. 35, No. 1, 1968, pp. 31-39.
12. Hoff, N. J. and Bruce, V. G., "Dynamic Analysis of the Buckling of Laterally Loaded Falt Arches", J. Math. and Phys., Vol. 32, 1954, pp. 276-388.
13. Budiansky, B. and Roth, R. S., "Axisymmetric Dynamic Buckling of Clamped Shallow Spherical Shells", Collected Papers on Instability of Shell Structures, NASA TN D-1510, 1962.
14. Simitses, G. J., "On the Dynamic Buckling of Shallow Spherical Caps", J. Appl. Mech., Vol. 41, No. 1, 1974, pp. 299-300.
15. Budiansky, B. and Hutchinson, J. W., "Dynamic Buckling of Imperfection-Sensitive Structures", Proceedings of XI International Congress of Applied Mechanics, Munich, 1964.

16. Budiansky, B., "Dynamic Buckling of Elastic Structures: Criterion and Estimates", Dynamic Stability of Structures (Edited by G. Herrmann), Pergamon Press, 1967.
17. Hsu, C. S., "On Dynamic Stability of Elastic Bodies with Prescribed Initial Conditions", International J. of Eng. Sciences, Vol. 4, 1966, pp. 1-21.
18. Hsu, C. S., "The Effects of Various Parameters on the Dynamic Stability of a Shallow Arch", J. Appl. Mech., Vol. 34, No. 2, 1967, pp. 349-356.
19. Hsu, C. S., "Equilibrium Configurations of a Shallow Arch of Arbitrary Shape and Their Dynamic Stability Character", International J. Nonlinear Mechanics, Vol. 3, June 1968, pp. 113-136.
20. Hsu, C. S., Kuo, C. T. and Lee, S. S., "On the Final States of Shallow Arches on Elastic Foundations Subjected to Dynamic Loads", J. Appl. Mech., Vol. 35, No. 4, 1968, pp. 713-723.
21. Simites, G. J., "Dynamic Snap-Through Buckling of Low Arches and Shallow Spherical Caps", Ph.D. Dissertation, Department of Aeronautics and Astronautics, Stanford University, June 1965.
22. Hoff, N. J., "Dynamic Stability of Structures", Dynamic Stability of Structures (Edited by G. Herrmann), Pergamon Press, New York, 1967.
23. Simites, G. J., An Introduction to the ELASTIC STABILITY OF STRUCTURES, Prentice-Hall, Inc., Englewood Cliffs, New Jersey, 1976.
24. Kounadis, A. N., Giri, J., and Simites, G. J., "Nonlinear Stability Analysis of an Eccentrically Loaded Two-Bar Frame", J. Appl. Mech., Vol. 44, No. 4, December, 1977, pp. 701-706.
25. Simites, G. J., Kounadis, A. N. and Giri, J., "Nonlinear Buckling of Imperfection Sensitive Simple Frames", Stability of Structures Under Static and Dynamic Loads (Proceedings of the International Colloquium on Stability...) Published by ASCE, 1977, pp. 569-586.
26. Weinstock, R., Calculus of Variations, McGraw-Hill Book Company, Inc., New York, Toronto, London, 1952, pp. 36-38.
27. Apostol, T. M., Mathematical Analysis, Addison-Nesley Publishing Company, Inc. Massachusetts, Palo Alto, 1965, Theorem, 4-20.
28. Ince, L. E., Ordinary Differential Equations, Dover, New York, 1956, Theorem 3-3 pp. 71-72.
29. Gelfand, I. M., Fomin, S. V., Calculus of Variations, Prentice Hall, Inc. Englewood Cliffs, New Jersey, 1963, pp. 103-104.
30. Simites, G. J., "Dynamic Stability of Structural Elements Subjected to Step-Loads" Proceedings, Army Symposium on Solid Mechanics, 1980; Designing for Extremes: Environment, Loading, and Structural Behavior, South Yarmouth, Cape Cod, Massachusetts, Sept. 30-Oct. 2, 1980.

APPENDIX A. THE BRACHISTOCHRONE PROBLEM

Constant Load of Finite Duration-Model C.

The problem of dynamic stability of model C (Snap-through Model) subjected to constant load of Finite Duration and discussed in Section V, reduces to finding the brachistochrone path starting from point $(r, s) = (\sqrt{\Lambda}, 0)$ and reaching the vertical $r = r_{cr} = \sqrt{\Lambda} - \frac{9}{4p} (\Lambda - 1)$ (A.1) where p is the nondimensionalized load parameter and Λ is a geometric parameter of the model. Since, from physical considerations, the motion, in the interval $\sqrt{\Lambda - 3} \leq r \leq \sqrt{\Lambda}$ follows the steepest descent path, which is the symmetric path ($s \equiv 0$), the brachistochrone problem will be restated as follows: find the path that requires the smallest time, for the system to reach positions characterized by $r = r_{cr}$ and starting from $(r = \sqrt{\Lambda - 3}, s = 0)$ with $s' = 0$.

The total Potential Energy of the system is given by Eq. (2.13) as

$$\bar{U}_T^P = (r^2 + 9s^2 - 2\sqrt{\Lambda}r + \Lambda) + \frac{1}{2} (\Lambda - r^2 - 3s^2)^2 - 2p(\sqrt{\Lambda} - r) \quad (A.2)$$

Recalling Eq. (5.1).

$$\bar{U}_T^P + \bar{T}^P = 0 \text{ for } 0 \leq \tau \leq \tau_0 \quad (A.3)$$

where

$$\bar{T}^P = \frac{1}{2} (1 + s'^2) \left(\frac{dr}{d\tau} \right)^2 \quad (A.4)$$

and

$$()' = \frac{\partial}{\partial r} ,$$

then the brachistochrone problem reduces to extremizing the following integral

$$I = \int_{\sqrt{\Lambda-3}}^{r_{cr}} \left(- \sqrt{\frac{1+s'^2}{-2\bar{U}_T^P}} \right) dr = \int_{\sqrt{\Lambda-3}}^{r_{cr}} X(r, s, s') dr \quad (A.5)$$

by considering paths which start at $r = \sqrt{\Lambda - 3}$ and $s = 0$ with $s' = 0$ and reaching positions characterized by $r = r_{cr}$ (constant).

The Euler-Lagrange equation and the associated boundary conditions for this brachistochrone problem, Eq. (A.5), are (see reference [26])

$$\frac{\partial X}{\partial s} - \frac{d}{dr} \frac{\partial X}{\partial s'} = 0 \quad (\text{A.6})$$

$$\left. \frac{\partial X}{\partial s'} \right|_{r_{cr}} = 0 \rightarrow \left. s' \right|_{r_{cr}} = 0$$

Note also that $s = s' = 0$ at $r = \sqrt{\Lambda-3}$.

Since $X = -\sqrt{\frac{1+s'^2}{-2\bar{U}_T^P}}$, Eq. (A.6) yields

$$\begin{aligned} s'' + (s' + s'^3) \frac{r + 9ss' - \sqrt{\Lambda - (\Lambda - r^2 - 3s^2)}(r + 3ss') + p}{-\bar{U}_T^P} \\ - (1+s'^2)^2 \frac{9s - 3s(\Lambda - r^2 - 3s^2)}{\bar{U}_T^P} = 0 \end{aligned} \quad (\text{A.7})$$

One solution to Eq. (A.7), that satisfies the boundary conditions, is given by the path $s \equiv 0$. However, there is no guarantee that path $s \equiv 0$ is the unique extremal path of the variational problem. Suppose that the solution to Eq. (A.6) bifurcates at a point $(r = r_b, s = 0)$ where $r_{cr} \leq r_b \leq \sqrt{\Lambda-3}$. Obviously $s' = 0$ at that point.

However, considering a closed domain $D = [r, s, s']$, such that $s < \delta$ and $s' < \delta$ where δ is a very small positive number ($\delta \ll 1$) with the point $(r_b, 0, 0)$ lying in the interior of D and $\bar{U}_T^P < -w$ ($w > 0$ any proper positive number) everywhere on D , the function

$$\begin{aligned} f(r, s, s') = -(s' + s'^3) \frac{r + 9ss' - \sqrt{\Lambda - (\Lambda - r^2 - 3s^2)}(r + 3ss') + p}{\bar{U}_T^P} \\ - (1+s'^2)^2 \frac{9s - 3s(\Lambda - r^2 - 3s^2)}{\bar{U}_T^P} \end{aligned} \quad (\text{A.8})$$

is continuous and satisfies the following Lipschitz condition on D.

$$|f(r, \bar{s}, \bar{s}') - f(r, s, s')| < L_1 |\bar{s}' - s'| + L_2 |\bar{s} - s|$$

Since higher order terms in s and s' are cancelled out and L_1 and L_2 are equal to

$$L_1 = \max_{\bar{U}_T^P} \left| \frac{r - \sqrt{\Lambda - (\Lambda - r^2)} r + p}{\bar{U}_T^P} \right| = \max \Omega_1(r, s)$$

and

$$L_2 = \max_{\bar{U}_T^P} \left| \frac{9 - 3(\Lambda - r^2)}{\bar{U}_T^P} \right| = \max \Omega_2(r, s)$$

The existence of L_1 and L_2 is guaranteed by the continuity of the functions Ω_1 and Ω_2 on D. See reference [27].

Recalling the Uniqueness theorem (Picard-Lindelof) for a differential equation of second order, see reference [28], the initial value problem, composed by the differential Eq. (A.7) and the boundary conditions $s|_{r_b} = s'|_{r_b} = 0$, used as initial conditions in the mathematical sense, admits a unique continuous solution in the interior of D. Therefore, the solution to Eq. (A.7) which is initially symmetric does not bifurcate at any point on the r -axis. Consequently the symmetric solution is unique.

Since the total potential U_T^P is symmetric with respect to the r -axis, the extremal path, $s=0$, cannot be a minimax. Moreover, around any path there always exists another path yielding higher value for the time of motion [integral I expressed by Eq. (A.5)]. Thus, the extremal path $s=0$ cannot be a maximal path either. Therefore, $s=0$ is the brachistochrone path of the problem.

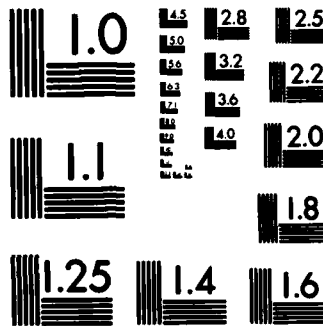
Note that path $s=0$ is not a fictitious path but a real one, since it satisfies the equations of motion.

$$\frac{d^2 r}{d\tau^2} - 2[r(\Lambda - 1 - r^2 - 3s^2) - p + \sqrt{\Lambda}] = 0$$

and

$$\frac{d^2 s}{dt^2} - 6s (\Lambda - 3 - r^2 - 3s^2) = 0$$

given in reference [30].



MICROCOPY RESOLUTION TEST CHART
NATIONAL BUREAU OF STANDARDS-1963-A